8-2023

TRANSIENT THERMAL PERFORMANCE ENHANCEMENT OF PHASE CHANGE MATERIALS THROUGH NOVEL PIN ARRANGEMENTS UNDER VARIED GRAVITY CONDITIONS

Junaid Khan
University of Tennessee, Knoxville, jkhan7@vols.utk.edu

To the Graduate Council:

I am submitting herewith a thesis written by Junaid Khan entitled "TRANSIENT THERMAL PERFORMANCE ENHANCEMENT OF PHASE CHANGE MATERIALS THROUGH NOVEL PIN ARRANGEMENTS UNDER VARIED GRAVITY CONDITIONS." I have examined the final electronic copy of this thesis for form and content and recommend that it be accepted in partial fulfillment of the requirements for the degree of Master of Science, with a major in Mechanical Engineering.

Prashant Singh, Major Professor

We have read this thesis and recommend its acceptance:

Wei Wang , Doug Aaron

Accepted for the Council:
Dixie L. Thompson

Vice Provost and Dean of the Graduate School

(Original signatures are on file with official student records.)

TRANSIENT THERMAL PERFORMANCE ENHANCEMENT OF PHASE CHANGE MATERIALS THROUGH NOVEL PIN ARRANGEMENTS UNDER VARIED GRAVITY CONDITIONS

A Thesis Presented for the

Master of Science

Degree

The University of Tennessee, Knoxville

Junaid Khan

August 2023

ACKNOWLEDGEMENTS

I shall forever be indebted to Dr. Prashant Singh for guiding me in my research and life in general. I also want to thank my Parents, wife and sisters for all the necessary support and motivation.

ABSTRACT

This thesis presents a comprehensive examination of encapsulation techniques and performance enhancement strategies for Phase Change Materials (PCMs) in the thermal management of spacecraft avionics. This research contributes to optimizing PCM applications in spacecraft through historical analysis, transient thermal performance enhancement, and computational studies.

The first chapter explains the significance of PCMs in passive thermal management since the beginning of space-age technology, it underlines the low thermal conductivity of PCMs and the necessity of incorporating materials with high thermal conductivity, such as metal foams, to improve heat transfer. It also discusses various advancements in PCM research for spacecraft thermal management applications like the shape-stabilized PCMs and also explains in details various encapsulations techniques for PCMs. This chapter also reflect upon the various efforts done by space agencies (NASA, ESA and ISRO) towards understanding the feasibility of phase change materials for spacecraft thermal management applications. It also examines the effect of various parameters such as direction of heat flow and orientation of PCM to obtain tailored heat transfer research which can be leveraged by phase change materials for effective thermal management of spacecraft avionics.

The subsequent chapter examines the transient thermal performance of a particular PCM, RT82, using novel pin arrangements. Through the strategic placement of fins, thermal conductivity and heat transfer surface area are enhanced. This study investigates numerically the melting characteristics under microgravity, terrestrial gravity, and hypergravity. This study focuses on the improvement in thermal performance brought about by fin integration under differing gravitational conditions.

The final chapter explores computational studies concentrating on the geometrical optimization of PCM encapsulation in Triplex Tube Heat Exchangers (TTHX) utilizing novel annular-fin configurations. This research examines the impact of fin shape, size, and positioning on the thermal characteristics of PCM. It identifies encapsulation geometries that facilitate vortex-like melting patterns, thereby accelerating PCM melting rates. In addition, it evaluates the heat transfer performance of these configurations under varying

gravity conditions, elucidating the physics underlying the enhancement of melting performance.

In conclusion, this thesis demonstrates that judicious encapsulation techniques and geometric optimisation significantly enhance the thermal management effectiveness of PCMs in spacecraft. This research paves the way for innovation in spacecraft thermal management systems employing PCMs by interweaving historical context with performance enhancement strategies and computational insights.

TABLE OF CONTENTS

NOMENCLATURE

Symbols

h_f	Heat of Fusion
$\dot{Q}_{pulse}$	Periodic Heat Dissipation Pulse
A_{rad}	Area of Radiator
Q_{pcm}	Heat stored by the PCM
$\dot{Q}_{rad}$	Heat rejected by the radiator per unit area
Q_{pcm}	Heat stored by the PCM
$\dot{Q}_{rad}$	Heat rejected by the radiator per unit area
Δt_{cycle}	Time taken for one ON/OFF cycle
K	Thermal Conductivity
m_{rad}	Mass of radiator
c_p	Specific Heat Capacity
C	Mushy-zone parameter
c_p	Specific heat capacity
g	Gravitational acceleration
h	Sensible enthalpy
ΔH	Latent heat content
S	Source term
T	Time
u	Velocity

Greek symbols

ε	Emissivity
σ	Stefan Boltzmann Constant
α	Thermal Diffusivity
ρ	Density
β	Heat pulse duty cycle
μ	Viscosity
γ	Liquid fraction

Abbreviations

PCM	Phase Change Materials
TES	Thermal Energy Storage
NASA	National Aeronautics and Space Administration,
ESA	European Space Agency,
LRV	Lunar Roving Vehicle,
ISRO	Indian Space Research Organisation,
LEO	Low Earth Orbit,
HSD	Heat Storage Device,
TMS	Thermal Management System,
LEO	Low Earth Orbit,
LLO	Low Lunar Orbit,
SS-PCM	Shape Stabilised PCM,
NSFC	Natural Science Foundation of China,
HVAC	Heat Ventilation & Air Conditioning,
SS-PCM	Shape Stabilised PCM,
TES	Thermal Energy Storage,
LWA	Light Weight Aggregate,
HSU	Heat Storage Unit,
LCOE	Levelized cost of energy,
PV	Photovoltaic

SUBSCRIPTS

l	Liquidus
ref	Reference
s	Solidus

LIST OF TABLES

LIST OF FIGURES

CHAPTER ONE

REVIEW OF PHASE CHANGE MATERIALS FOR SPACECRAFT AVIONICS THERMAL MANAGEMENT

Abstract: Phase Change Materials (PCMs) have played a significant role in the effective management of passive thermal cooling requirements of spacecraft. The demand for high levels of heat dissipation from the spacecraft's electrical components makes thermal control challenging. Latent Thermal Energy Storage and heat dissipation are the key components to quantify a constructive PCM cooling system. PCMs generally have a low thermal conductivity which can potentially inhibit their heat transfer characteristics. This necessitates their integration with certain high thermal conductivity materials such as metal foams. This chapter provides an account on the evolution of PCMs as the passive thermal management system of spacecraft avionics.

1. INTRODUCTION

PCMs release and absorb energy at phase transition temperatures [1]. This phase can change from solid to liquid, liquid to gas, and solid to a gaseous state. PCMs can be inorganic salt hydrates (e.g., $CaCl_2.6H_2O$), Organic Compounds (e.g., Paraffins), Eutectics of Organic Materials (e.g., 88% CH_3COOH + 12% $C_7H_6O_2$), Natural Organic Elements (e.g., Sulphur). Ablative Materials such as silicates and nanofibers which undergo solid to vapor phase transition can also be classified as PCM. PCMs are used as passive thermal management of spacecraft avionics since the early 1970s when it was used on the Lunar Roving Vehicle (LRV) by NASA for the first time in the Apollo 15 mission [2]. The integration of PCM allows for the radiators to be sized for average heat loads, rather than peak loads because they absorb the excess heat experienced by the radiators owing to their latent heat of fusion [3]. Thus, the integration of PCM for the thermal management of avionics provides a pathway to design spacecraft payload with reduced mass and volume. Fig. 1.1 illustrates the interaction between PCM and the avionic component in a typical thermal control module (TCM).

Despite having several desirable qualities, due to the low thermal conductivity of PCMs, their employment in the raw form is not practical. The low thermal conductivity of PCMs slows down the rate of heat transfer, which necessitates the inclusion of high thermal conductivity filler material in the PCM package to increase the effective thermal conductivity. Metallic foams, such as aluminum [5] and copper [6], are common filler materials for PCMs which can significantly enhance the effective thermal conductivity and as a result, improve the transient thermal performance. High porosity metal foams made from aluminum or copper are lightweight solution

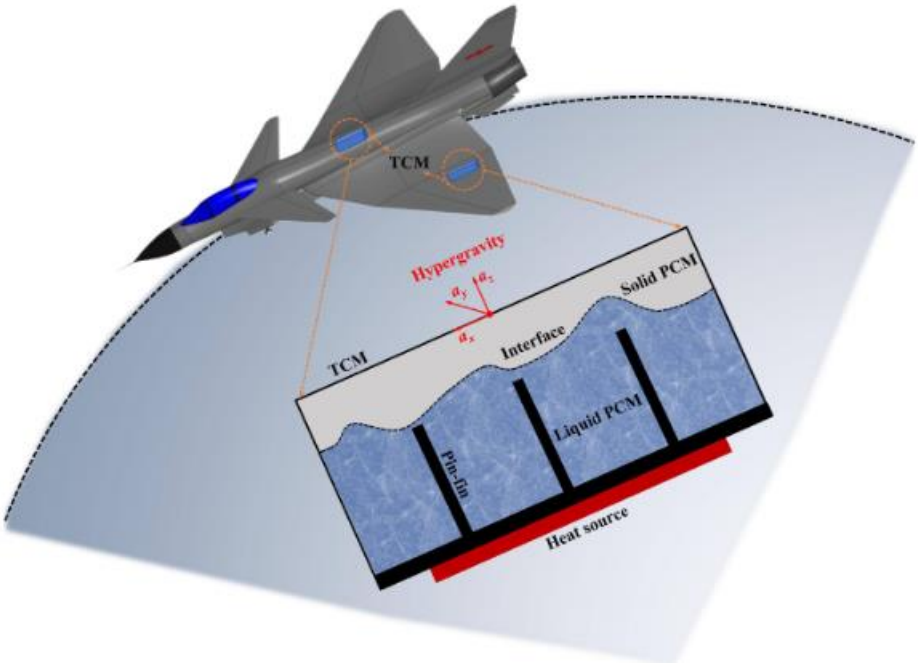

Fig. 1.1 PCM thermal-control system for a one-duty-cycle electronic component **[4]**

to the above problem, which offers high surface area-to-volume ratio and tortuous flow paths which promote thermal dispersion and flow mixing. Some other notable fillers include such as carbon fibers [7], Honeycomb [8], fins [9], and non-metallic foams such as Graphite foams [10].

Although PCMs offer several benefits in thermal management, there are some issues pertaining to avionics thermal management, such as, cyclic ratcheting, short-circuiting, and phase management of PCM as it transitions through various g-forces, which pose limitations on their employment in the spacecraft thermal management applications. These problems need to be identified and

evaluated and steps for mitigating such issues need to be taken for the widespread implementation of PCM technology for passive thermal management of avionics.

This chapter provides a comprehensive account of PCM's utilization in avionics thermal management. Fig. 1.2 shown below shows the organization of this review article and the topics covered.

2. FUNDAMENTALS OF PCM

2.1 WORKING PRINCIPLE

This section focuses on the design rationale involved in the development of thermal management systems (TMS) that utilise PCMs for spacecraft avionics, with a particular emphasis on radiator mass and size . Efficient operation of on-board electronics is contingent upon maintaining specific temperature ranges. The task of operating in space presents significant challenges due to extremely harsh and fluctuating conditions.

Radiators work as heat exchangers and play a crucial role in spacecraft thermal management by facilitating the dissipation of excess heat through radiation into the space. PCMs has the potential to for managing transient and sudden rise in heat generated from the electronic components. A proper design of PCMs in spacecraft TMS can result in the reduction of the size and weight of radiators required for heat dissipation [3]. The calculation of the duty cycle proposed by Busby and Mertesdorf [11] provides insight into the optimal utilisation of PCMs in design. Figure 1.3 depicts an example of a payload that generates heat in pulses (duty cycle, β) with a certain intensity, denoted as $\dot{Q}_{pulse}$.

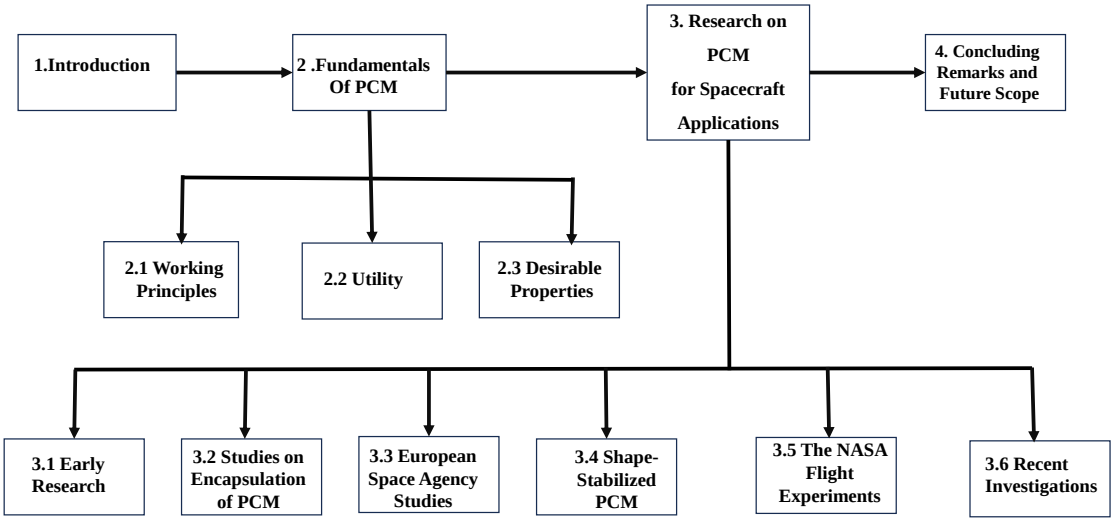

Fig. 1.2 Organization of the review article

$$M_{withoutpcm} = \frac{\dot{Q}_{pulse} m_{rad}}{\dot{Q_{rad}}} \quad (1)$$

In the first equation, $M_{withoutPCM}$ represents the mass of the radiator as determined by the mean thermal output, in addition to the mass of the phase change material setup.

$$M_{with,pcm} = \frac{\beta(\dot{Q}_{pulse} m_{rad})}{\dot{Q}_{rad}} + \frac{\beta(\Delta t_{cycle}(\dot{Q}_{pulse} - \beta \dot{Q}_{pulse})}{Q_{PCM}} \quad (2)$$

In Equation 2, the variable $M_{with,PCM}$ represents the combined mass of the radiator -PCM system. Upon equating Equations 1 and 2, one can ascertain the duty cycle (β') at which the preference for phase change materials (PCMs) over other alternatives is contingent on weight.

$$\beta' = \frac{m_{rad} Q_{PCM}}{\dot{Q_{rad}} \Delta T_{cycle}} \quad (3)$$

As depicted in Equation 3, there exists a threshold pertaining to the temporal extent of thermal pulses, beyond which the utilisation of phase change materials (PCMs) is rendered impractical, on account of the mass of the PCM and its corresponding packaging, which effectively annuls the benefits of a reduced radiator.

Additionally, the thermodynamic aspects need to be considered in the design of a PCM-based TMS (Fig. 1.4). A proper functioning radiator will operate very close to the PCM melting temperature at all times [13], ensuring continuous heat dissipation into the surrounding environment.

It can be inferred that the dimensions of the radiator are established based on the premise that the sole energy exchange that affects the system are the production and dissipation of heat. Given the absence of any solar or thermal radiation impacting the radiator surface and the presence of an absolute zero thermal radiation sink, one can express this phenomenon mathematically as follows:

$$\varepsilon A_{rad} \sigma T_{melt}^4 \triangle t_{cycle} = \dot{Q}_{pulse} \triangle t_{pulse} \quad (4)$$

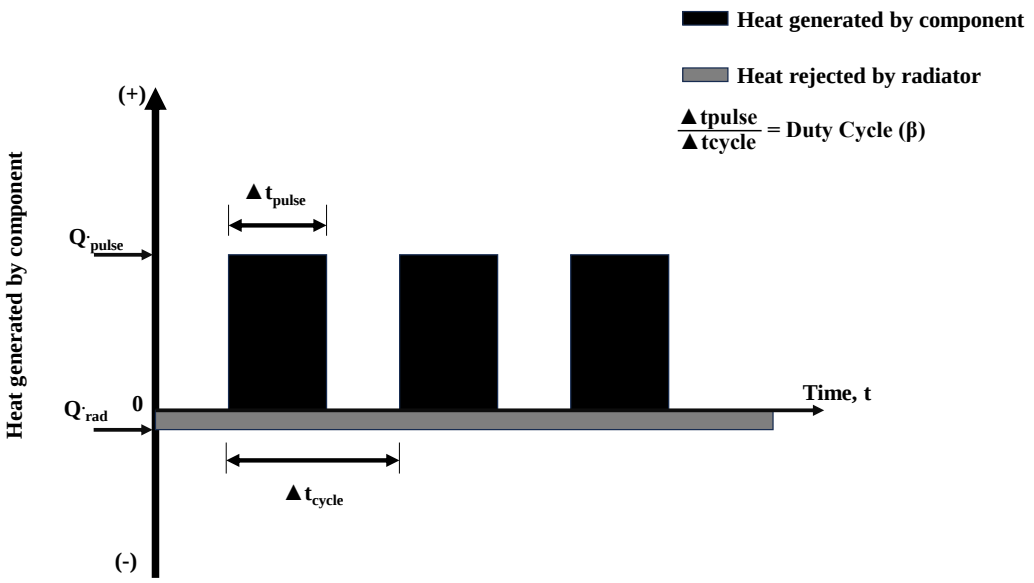

Fig. 1.3 Periodically operating component (Adapted from [12])

Assuming that T_{melt}, ε, Δt_{cycle}, Q_{pulse}, and Δt_{pulse} are all constants, one may ascertain the size of the radiator (A_{rad}) by employing Equation 5.

$$A_{rad} = \frac{\dot{Q}_{pulse} \triangle t_{pulse}}{\varepsilon \sigma T_{melt}^4 \triangle t_{cycle}} = \dot{Q}_{gen_{avg}} (\frac{1}{\varepsilon \sigma T_{melt}^4}) \quad (5)$$

The graphical representation in Fig. 1.3 depicts the maximum energy stored by a phase change material (PCM) during a cycle of activation and deactivation. The mass of the PCM required to store this energy as heat of fusion (h_f) can be determined using Equation 6.

$$M_{PCM} = \frac{E_{Max}}{h_f} \quad (6)$$

2.2 UTILITY OF PCMS

Atmospheric Re-entry

The utility of PCMs in spacecraft includes short-duty cycle applications in launch or re-entry vehicles, wherein large quantities of heat are absorbed by the coating of ablative materials such as silicates which prevents the overheating of re-entry capsules. The inherent ability of PCM to absorb large amounts of energy in a short amount of time is utilized here. These materials absorb upwards of 3,004 KJ/Kg at temperatures exceeding 1,600 degree Celsius.

Avionics

PCM is also used for cyclic ON/OFF applications where it undergoes a series of freeze and thaw cycles to prevent the spacecraft avionics from overheating [14], by dissipating heat from avionics to the radiator. This process is depicted in Fig. 1.5. At the phase transition temperature, PCM absorbs the heat as Latent Heat of Fusion. The PCM stores the heat energy generated when the component is ON. The PCM is then solidified when the component is OFF to prepare for the subsequent ON cycle by removing heat equivalent to "latent heat of fusion". The PCM can run (almost) isothermally because of the alternating melting and freezing. Therefore, a radiator with a

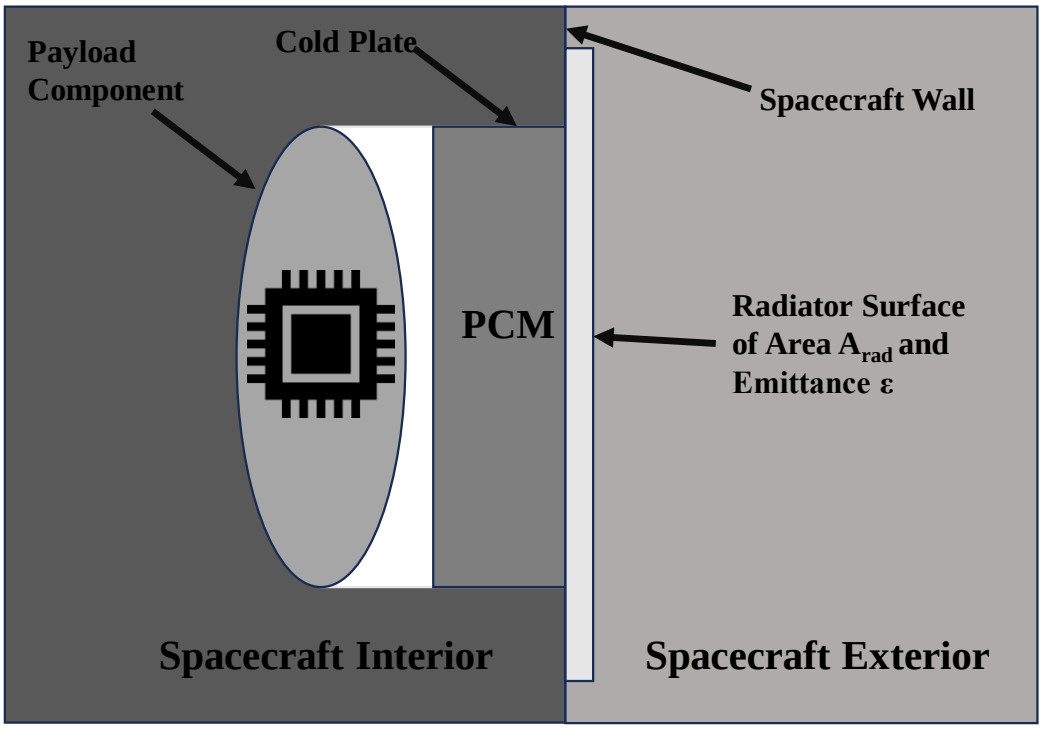

Fig. 1.4 PCM/Radiator Thermal control system (Adapted from [12])

smaller surface area can be used in conjunction with PCM. However, feasibility studies are often conducted to make decisions regarding these trade-offs.

Spacesuits

PCM also enables the astronaut space suits to remain nearly isothermal throughout scheduled spacewalks as these special suits are enwrapped by a layer of PCM that would absorb/ release heat as needed to maintain it at the appropriate temperature [15].

Extra-terrestrial Environment

PCM can maintain the isothermal conditions and thermal stability of a spacecraft in an extra-terrestrial environments. For instance, the variation in the temperature between night and day on the surface of Mars is nearly 170°F on a typical summer day. Similarly, PCM dampens the large temperature difference owing to its ability to charge and discharge [16]. Thus, this property of PCM to dampen out huge temperature variations during the 'diurnal thermal cycles' can play an instrumental role in survivability in extra-terrestrial environment.

Heat Sharing

Fig. 1.6 demonstrates the PCM's ability to share heat by allowing heat from one hot component to be routed to a "Central PCM" for later use in thermal control [17] . Typically, this heat is routed to a cold component that is at risk of running below the minimum temperature.

2.3 DESIRABLE THERMOPHYSICAL PROPERTIES OF PCM AND FILLER MATERIALS

PCM: PCM must have melting point within the operational range of temperature of the component to be protected. A high heat of fusion (typically of the order of 150KJ/kg for room temperature and 40KJ/kg for cryogenic applications) is desirable for efficient energy storage [18]. PCM should also be non-Corrosive and non-toxic. Volume change during melting is an important aspect that needs to be taken into consideration to ensure smooth reversible solid-to-liquid transition and vice versa because it can unnecessarily put a strain on the avionic components. Thus, a PCM must have a low coefficient of thermal expansion. A high flash point of the PCMs is desirable as it has lower risk of ignition during the operations. Similarly, the stability of PCM along with high thermal

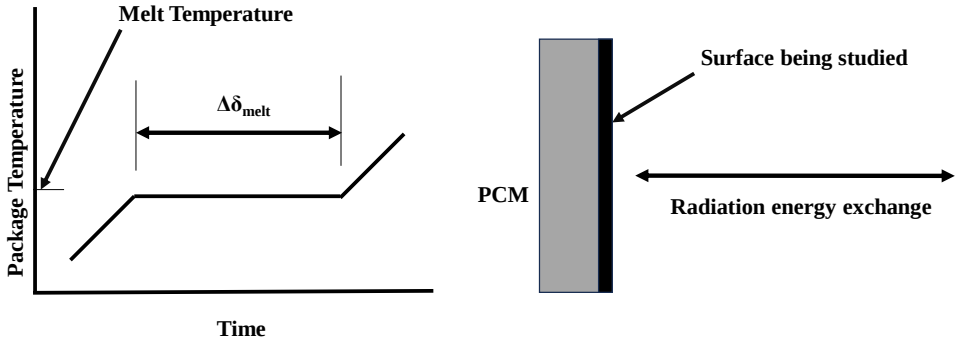

Fig. 1.5 PCM Storage for Radiometric Storage device (Adapted from [12])

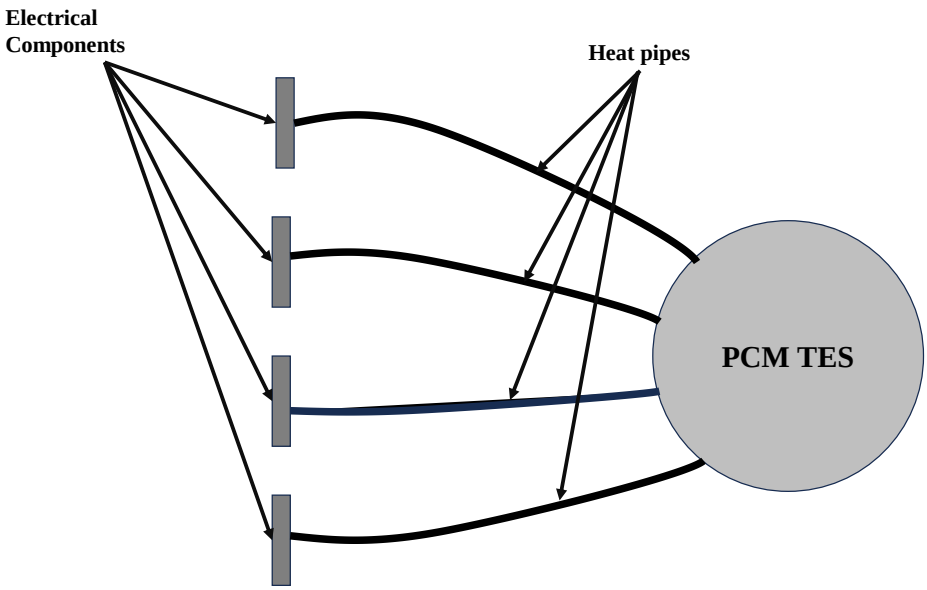

Fig. 1.6 Central PCM Thermal Storage System (Adapted from [12])

conductivity and specific heat capacity ensures an effective heat transfer with minimal contact resistances between the PCMs and the components. Based on the relevant literature [19],[20], [21], [22], the desirable thermophysical properties of a PCM for spacecraft applications can be effectively gauged. A higher value of latent heat of fusion, density, and specific heat is usually desired for effective heat storage and transfer characteristics.

Filler material:

As discussed in section 1, the integration of filler material with PCMs results in low thermal resistance paths, resulting in enhanced effective thermal conductivity and reduced temperature gradient which mitigates the avionic components from reaching their peak temperature. Filler materials for PCM integration has garnered attention of researchers and it has been observed that an iterative experimental procedure is typically followed to develop the filler material-PCM combinations [23].

The utilization of aluminium as a filler material has been popular recently, particularly in light of the emergence of organic phase change materials (PCMs) like paraffin wax. Historically, the utilization of aluminium in tandem with Phase Change Materials (PCMs) was restricted due to the fact that the primary components of PCMs were inorganic salts, such as lithium nitrate, which did not provide any discernible advantages when combined with aluminium. This observation is supported by historical precedents [24], [25]. The shift in paradigm towards organic phase change materials (PCMs) has resulted in the rise of aluminium as a prominent material due to its significant influence on the heat transfer characteristics [26].

Metallic foams, comprising of aluminium, titanium, and stainless steel, have also been used in the aerospace industry [19]. Despite its higher density, stainless steel exhibits remarkable elasticity, rendering it highly adaptable to variations in the volume of PCMs. The appeal of aluminium foams, in contrast, arises from its characteristic of having a low density, resistance to corrosion, superior strength-to-mass ratio, and high thermal conductivity. These attributes, taken together, establish it as a prime metallic filler for phase change materials (PCMs), as evidenced by sources [27], [28], and [29].

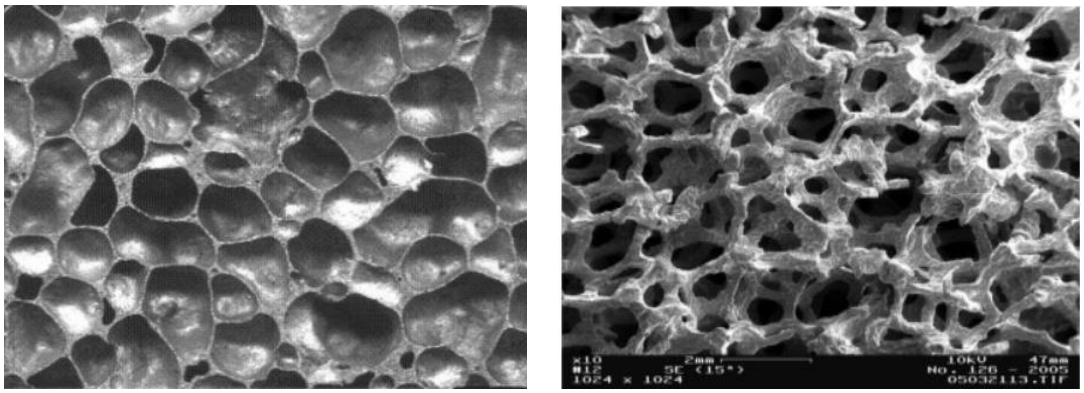

Fig. 1.7 Microstructure of (a) Open-celled Aluminium metal Foams and (b)Closed-Cell Aluminium metal Foams [30]

The metal foams have a cellular structure with interconnected ligaments and generally have many gas-filled pores (see Fig. 1.7). The metal foams can be machined, foamed, additively manufactured, or anodized. They can be diffused into PCM, or the latter can be permeated into them through their pores. The pores of the metallic foams can be sealed as is the case with closed-cell foam or they can form an interconnected network as can be observed in the case of open-celled foams [31]**.** They have high thermal conductivity, porosity, surface area-to-volume ratio, and mixing capability, and also have a high local heat transfer coefficient [32]**.** Moreover, they also facilitate a reduction in thermal variability and promote high thermal energy storage density. These qualities make them high-performing alternatives to fins delivering smaller, lighter, safer, and simpler systems and they can be applied across the full spectrum of thermal management schemes.

Since power electronics tend to favour compact designs with higher thermal outputs, metallic foams are adaptable to a variety of form factors. When phase transitions occur, the composite structure of PCMs embedded within metallic foams is adept at absorbing large peak thermal loads via latent heat. In this instance, the metal foam matrix is crucial in improving the thermal conductivity.

Although metal foams have a complex pore distribution, recent advances in computer tomography have improved the precision in thermal and flow transport. The bulk density to metal density ratio, which measures the relative density of metal foams, is essential for modifying the porous medium's thermal and flow properties [32]. Additionally, empirical investigations support the compatibility of metallic foams with organic PCMs, leading to improved thermal performance as a result of decreased supercooling, non-corrosive behaviour, and reduced phase segregation [33]. Metallic foams are essential for guaranteeing a consistent phase change process, catalysing phase change cycles without compromising heat storage capacity, and improving the thermal performance of avionic systems in spacecraft.

3. RESEARCH ON PHASE CHANGE MATERIALS FOR SPACECRAFT APPLICATIONS

This section reports research progress in the implementation of Phase Change Materials technology for passive thermal management of spacecraft from its nascent stages to its widespread

implementation over several decades. Moreover, this section also provides the prudential reasoning behind the choices of different filler materials used in space missions and the challenges faced for its effective implementation. A separate section on recent investigations (from 2016-present) is included to showcase ongoing efforts in this field.

3.1 EARLY RESEARCH

Early research on avionics was focused on determining the feasibility of the PCM system as a passive thermal management choice. Fixler (1966) [33] analytically evaluated the feasibility of PCM to damp the temperature fluctuations of onboard electronic systems and suggested an enhanced PCM core design (similar to the one as shown in Fig. 1.8) further emphasizing the need for better heat transfer characteristics. It was not until the early 1970s that space agencies initiated their full-fledged usage for passive cooling applications. The first implementation of this technology was performed by NASA on its Apollo 15 mission in 1971[34]**.**

Grodzka (1970) [24] conducted a detailed experimental study to establish the criterion of performance which were assumed from the PCM technology for spacecraft thermal control. Convection was identified as the major parameter affecting phase change. Complexity pertaining to the study of convection and phase change under zero gravity conditions were discussed in this study. These earlier studies mostly favored the implementation of non-paraffinic PCMs with a temperature range of 0-100°C. Kelliger et.al. (1972) [35] studied the feasibility of PCM for use as surface coating materials for passive and active thermal control of spacecrafts. By this period, the employed PCMs were hydrated salts like Lithium Nitrate with Zinc Hydroxyl crystal, Acetamide, and Myristic acid. The Soviet Space Agency [36] of the then USSR also used a similar PCM (Lithium Nitrate Trihydrate) for its Venera-8 (1972) mission launched toward Venus. Bain et.al. (1972) [37] further probed into the significance of gravity-influenced natural convection phenomenon in PCM modules intended for space explorations. The conduction-convection model used in the study which accounted for the effect of gravity in the melting phenomenon of PCM demonstrated good agreement between the numerical and experimental analysis enabling the velocity profile model to predict temperature profiles in the PCM design process. The alteration of melting interface profile effected by gravity variations was further belabored upon in this study.

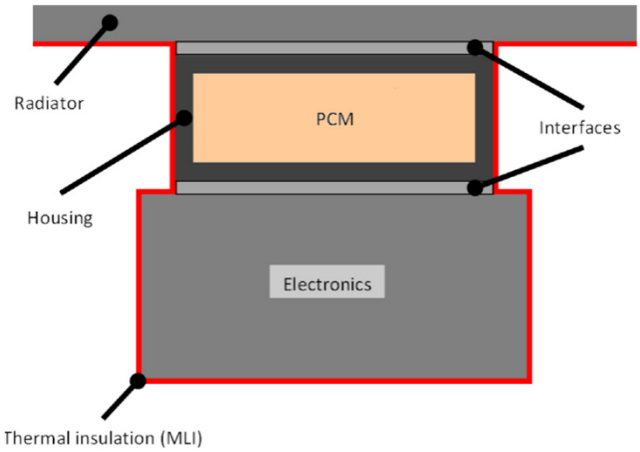

Fig. 1.8 Schematic Representation of PCM thermal control [33]

Abhat and M.Groll (1974) [38] evaluated PCM devices for thermal management applications in satellites. The importance of PCM device orientation for efficient thermal control under adverse gravity conditions was one of the main highlights of this study. This study suggested a restrictive geometry to encase the PCM device to solve the issue of PCM movement within a cellular honeycomb-shaped filler geometry. It was observed that minor fine-tuning resulted in enhanced thermal control performance of the PCM module.

Abhat (1976) [39] tested the time varying response of a honeycomb encapsulated phase change materials for utility in spacecraft applications. After following a lumped capacity model for heat transfer analysis involving low heat input at the honeycomb walls, the PCM prototype survived several space qualification procedures such as thermal soak and vibration testing performed on it. Olstad (1980) [40], while discussing the primary importance of thermal control for space explorations mentioned the work of Bledjian (1979) [21] where the influence of Biot number on phase change times and boundary temperatures was analyzed for spacecraft thermal control utility.

Murphy (1987) [41] demonstrated PCM's ability to regulate wide orbital heat flux alterations during short courses of time underlying their potential to mitigate catastrophic heat related damages. Crane & Dustin (1988) [42] investigated and tested fluoride salts and metallic PCMs for their latent storage properties. In a similar study, owing to the ease of integration and high degree of applicability of PCMs, they have also found utility in Lithium Bromide powered spacesuits wherein Son (1989) [43] on identifying the problem of high cell temperature as a potential safety hazard utilized solid-solid phase change properties of neopentyl glycol doped with an Aluminum matrix to lower the battery operational temperature.

While the experimental studies involving PCM in space research were yielding promising results, the computational evaluations were making equally significant progress in this area. The computational approach to solve the non-linear heat transfer problem by Phase Change receiver-storage system was formulated by Majumdar and Sharma (1989) [44]. In this study, a differential model was proposed to comprehend the motion of the solid-liquid interface wherein the position of the interface was plotted as a function of time for varying Stefan numbers. Sheffield and Wen (1990) [45] studied various computational models to simulate phase change material's

phenomenon and ultimately adopted the Finite Difference method for understanding the progress of the melting phenomenon.

3.2 STUDIES ON ENCAPSULATION OF PCM

The encapsulation of Phase Change Materials (PCMs) is a process whereby PCM is confined within capsules or containers to establish a structured and regulated system for the purpose of thermal energy storage [46] . The morphology of capsules can exhibit a broad spectrum of dimensional characteristics, spanning from the microscale to the macroscale. The utilisation of encapsulation techniques has been demonstrated to be a viable strategy for the efficient management of phase change processes, specifically those involving the melting and solidification of phase change materials (PCMs). Encapsulation of PCM assists to shield the PCM from external factors and provides an additional surface area to improve the heat transfer characteristics.

Torab (1989) [47] sought to enhance the latent heat storage provided by PCM in extraterrestrial environment by encapsulating them appropriately. It was argued that a minimalistic volume of encapsulated PCM could aid in increasing the density of energy which could be stored by the constrained PCM for an orbital time of 6000 seconds presumably with a spring duration of 600 seconds. A one-dimensional model based on the constant temperature approach was believed to account for the temperature distribution of fluid and PCM during the course of melting. However, the enhancement of latent heat storage due to integration of PCM inside a filler isn't always the case. The PCM-impregnated polymer micro composites investigated by Stark (1990) [48] indicated a counter-productive result wherein the encapsulation of PCM comprising of paraffin wax and high-density polyethylene wax infiltrated into an ordered PBZT polymer for the thermal management of military spacecrafts during elevated and intermittent high level burst combat modes. The transient variation of power level of such complicated systems is shown in Fig. 1.9**.**

Developing on the premise suggested by Colvin (1989) [50], and in a move to push for commercialization of PCM for aircrafts and spacecrafts regular usage, significant developments on PCM-based thermal management systems of avionics were made. Lauf and Hamby (1990) [51] studied a heat storage system to keep the engine operational during an eclipse where salt hydrates

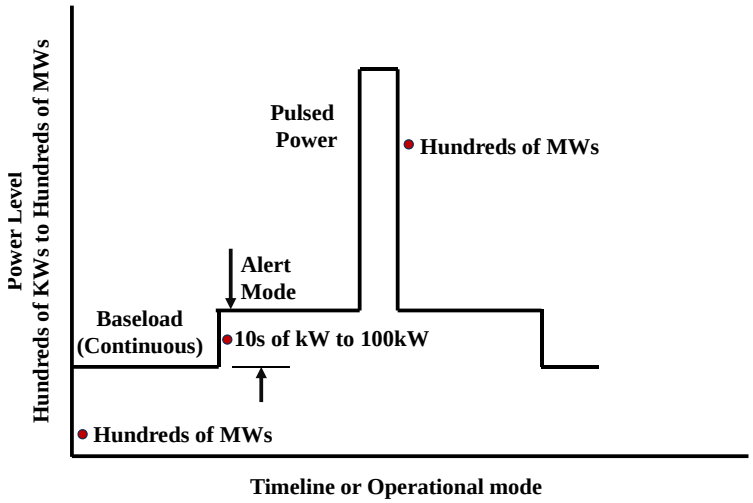

Fig. 1.9 Potential Mission Heat Rejection Load Profile (adapted from [49])

as PCM were eliminated despite their property to melt during insolation and freeze during an eclipse, with poor thermal conductivity being the major reason for their rejection. To account for

the chemical stability, enhanced thermal conductivity and minimalistic containment, modules constituting germanium-graphite composite were selected after extensive testing. The reduction in weight imparted by PCM to the test capsule was also earmarked as an important criterion for selecting the PCM. Each cycle consisted of one hour at 500˚C and two hours at 1,000˚C. The anomalous losses from the Germanium sample were the result of metal adhesion in the threaded closure.

A pioneering effort towards microencapsulation of PCM in a composite was documented by Mulligan et.al. (1996) [52] wherein an analytical system was modeled to demonstrate the benefits of incorporating 'Microencapsulated PCM suspension' as a working fluid to experimentally demonstrate this advanced method of source temperature control in radar and avionic components of spacecraft systems. Compact Heat rejection systems of the kind used in this earlier study employed smaller volumes of working fluid, thereby facilitating huge savings in terms of power, weight, and size requirements in spacecraft. A Newtonian behavior was assumed for the encapsulated PCM suspension assuming a spherical shape of the PCM particles and since the apparent viscosity of the suspension is three times that of water, a laminar flow was assumed in this study throughout the system. For spherical particles, Torquato [53] provided the following relationship:

$$K_s = K_w \left[\frac{1 + C_1\beta + C_2\beta^2}{1 + d_1\beta + d_2\beta^2} \right] \tag{7}$$

where,

$$\beta = \frac{K_{PCM} - K_w}{K_{PCM} + K_w} \tag{8}$$

In the above equations, C_1 and C_2 are constants, and K_w and K_{PCM} are the thermal conductivities of water and PCM. In this experimental work, octadecane, eicosane, heptadecane, and nonadecane

were encapsulated and pumped into a liquid-coupled heat exchanger loop to reduce system temperatures.

Several studies have shown the heat transfer potential of organic PCMs for spacecraft passive thermal management systems. Pal and Joshi (1998) [14] carried out a study on passive backup cooling capabilities of an organic Phase change material (n-triacontane) embedded in an Aluminum honeycomb substrate for avionics cooling. A honeycomb structure was chosen in this study along the lines of the research by Bledjian et al. (1979) [21]. It was concluded that the heat transfer was independent of the orientation since the effects of natural convection were completely negated rendering the heat transfer phenomenon for the PCM-Aluminum substrate system to be completely dominated by conduction. Moreover, this study also recommended against the single-cell model of melting since it did not account for the conjugate heat transfer phenomenon.

A similar contemporary exploration focused on the weight reduction of spacecraft by installing microencapsulated PCM heat sinks for sporadic thermal cooling requirements of avionics was pursued by Fossett et al. (1998) [54] with the inference that microencapsulated PCMs provide an excellent passive heat sink for heat dissipation of avionics of remotely located aircraft and missiles. The MicroPCMs tested were made of two brands namely Duocel and Lockhart [55]. A baseline was chosen in this study to offer a benchmark for MicroPCM^{TM} heat sink performance wherein the latter, when replaced with 270 grams of Aluminum took 10 times more time to reach the design temperature compared to the baseline which translates into very desirable results for effective thermal management of Avionics.

Around 2000s, the endeavors for interplanetary travel prompted Strauss and Daud (2000) [56] from NASA to develop non-volatile memory PCM comprising crystalline materials. The vision of this research was to enhance the spacecraft's potential to mitigate intense thermal radiation and relay valuable data. The impact of research and level of analysis increased manifold with the advent of advanced computational methods by the early 2000s. One such analysis was the idea of a hybrid heat sink put forward by Krishnan et.al. (2005) [57]. This involved the combination of a novel plate-fin heat sink with a phase change material and the development of easy-to-use guidelines to investigate the constant operation of time-varying encapsulated heat sinks under

transient cooling conditions. The governing energy conservation equation for the numerical model of the heat sink was given below [57]:

$$\rho\left(C_p + \Delta H \frac{\partial f_l}{\partial T}\right) = \nabla.(k\nabla T) \tag{9}$$

where f_l represents the fraction of the liquid.

The phase transition problem is described using the effective heat capacity, where Simpson et al. (2002) [58] provided the specifics of the mathematical model. In Ferziger & Perig (1996) [59], the computational domain was discretized into orthogonal finite volumes with a central differencing scheme utilized for approximating the spatial fluxes and a three-time levels scheme employed for temporal terms. According to Dantzig (1989) [60], the liquid fraction was smoothed since step-functions were difficult for numerical algorithms to oversee. Liquid fraction was calculated as follows:

$$f_l = \begin{cases} 0\,, & if\ T_p \le (T_{melt} + \varepsilon) \\ \dfrac{T_p - T_{melt} + \varepsilon}{2\varepsilon}\,, & if\ (T_{melt} - \varepsilon) \le T_P \le (T_{melt} + \varepsilon) \\ 1\,, & if\ T_p \ge (T_{melt} + \varepsilon) \end{cases}$$

Saha & Dutta (2008) [61] aimed to optimize the operation time of heat sinks for the recommended heat flux and critical chip temperature while validating the significance of melt convection in the design of heat sink with PCM. This study can be potentially implemented for the passive cooling technique for transient heat loads experienced by spacecraft avionics. This study focused on the geometric parameters of the fins such as their thickness and number which directly impact the design decision of the heat sink. An enthalpy-based CFD model was formulated in combination with a Genetic algorithm for optimization. The necessity of a systematic analysis of PCM-Thermal Conductivity Enhancer configuration was realized in this study which is deemed essential to probe into the effect of melt convection on the performance optimization of a Thermal Storage Unit (TSU) concerning its geometric parameters. The schematic diagram and the dependence of melt duration on various geometric parameters is also discussed in this study.

PCM transient thermal performance can also be enhanced by including pin-fins in the domain, e.g., a Triplex Tube Heat Exchanger (TTHX) which constitutes triple concentric tubes with the PCM RT-82 filled in its annulus, where fins are attached to the periphery of the tubes in different configurations as shown in Fig. 1.10. A popular example of the use of TTHX is the study by Mat et.al. (2013) [62] wherein the heat transfer phenomenon for melting of the PCM 'RT-82' was studied by providing heat to the encapsulation probe in different ways i.e., the internal heating, the external heating and the both sides heating method. The melting of PCM in this geometry was noticed to follow a Boussinesq pattern and the effect of natural convection dominated the heat transfer regime. The melting and solidification phenomenon of PCMs infused in this geometry during microgravity and hyper gravity conditions needs more investigations.

A 3D analysis of a Nano-encapsulated (NEPCM) slurry flowing within a manifold microchannel heat sink was performed by Kuravi et al. (2009) [63] while considering the wall fin effect and axial conduction in the expanding flow regime. The PCM slurries employed as the heat transfer fluid in these microchannels (see Fig. 1.11) are used in applications where large amount of heat was generated because they have an improved heat capacity during phase transition during melting. The objective of this study was to investigate how NEPCM slurry behaved in terms of heat transfer in a Manifold microchannel (MMC) heat sink and to compare it to a single-phase base fluid. In this work, attempts were made to achieve the maximum and minimum values of heat transfer enhancement and bulk mean temperature, respectively, by the melting range of PCM.

As a result, the inlet temperature was adjusted corresponding to the heat flux and concentration, which were both 100 W/cm^2. The fluid's bulk mean temperature rise and the Nusselt number as a function of non-dimensional inlet temperature for various melting ranges are studied in this research work [64]. This study concluded that it is preferable to maintain the input temperature of the microchannel close to the peak of the PCM melting curve for such PCM-microchannel configurations with a constrained PCM melting range. The purpose of this study was to lay the groundwork for future investigations into NEPCM slurry flow in MMC heat sinks. The resulting NEPCM slurry with polyalphaolefin (a coolant used in military avionics) also contributes to raising the Nusselt number and lowering the fluid's bulk mean temperature.

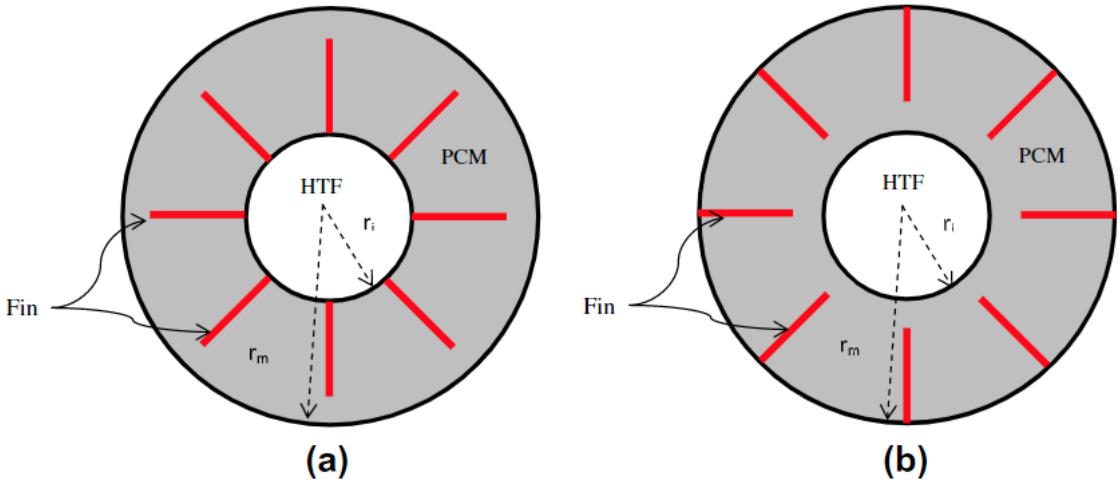

Fig. 1.10 Geometric Configurations in Mat et.al. (a) A Finned Tube and (b) An Internally Finned tube [62]

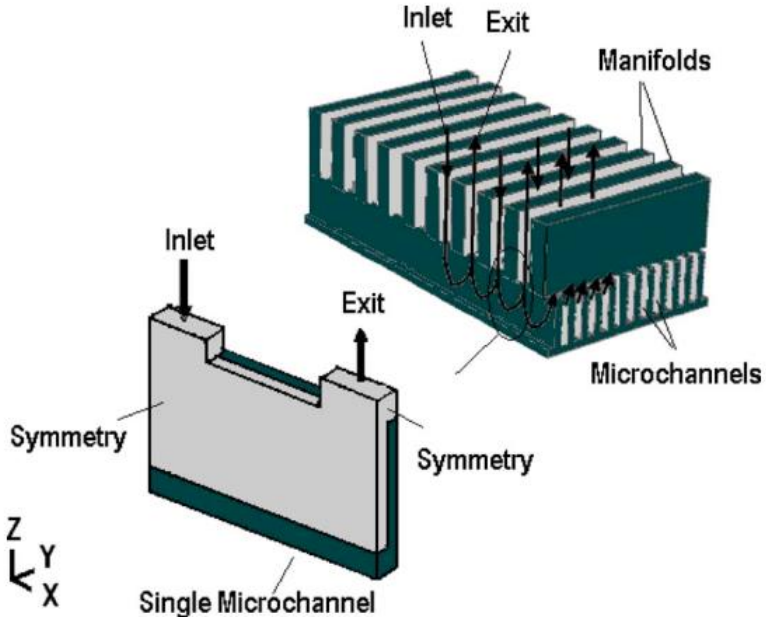

Fig 1.11 Manifold Microchannel (MMC) Heat sink [63]

Lou and Wang (2010) [65] investigated PCMs for heat shielding benefits in lunar orbiter spacecrafts wherein the PCM could absorb the additional heat during daytime and release during the colder night phase, thus maintaining optimum temperature. Due to their exceptional thermal conductivity and structural properties, carbon foams, which are known for their lightweight and highly porous nature, have garnered interest in numerous disciplines. These predominantly carbon-based open-celled structures have tremendous potential for applications requiring thermal management, such as in electronics. Their distinctive architecture combines high surface area, low density, and enhanced thermal conductivity, making them ideal for heat dissipation and insulation in compact electronic devices. Alshaer et al.'s (2015) [66] investigated the thermal management potential of carbon foams in electronic devices. The authors conducted a comprehensive experimental investigation of a hybrid composite system using carbon foam as the fundamental component. Specifically, they developed three distinct thermal management modules with pure carbon foam, a composite of carbon foam and Paraffin wax (RT65) as a phase change material (PCM), and an improved variant with multi-wall carbon nanotubes (MWCNTs) as a thermal conductivity enhancer. The infuser is shown in Fig. 1.12. Two types of Carbon foam were utilized: CF-20 with minimal thermal conductivity and KL1-250 with medium thermal conductivity. The addition of Paraffin wax to carbon foam caused a moderate delay in attaining steady-state temperatures, according to the researchers. The incorporation of MWCNTs resulted in an extraordinary delay and decrease in the temperature rise of the modules. In addition, the KL1-250 CF variant demonstrated superior control over high-power loads in comparison to the CF-20.

3.3 SOME EUROPEAN SPACE AGENCY (ESA) STUDIES ON PCM

Collette et.al. (2011) [67] critiqued the potential for phase change material composites to maintain temperature stability in terms of reduction in thermal strain on avionics and weight reduction of spacecraft. Evaluation of prospective PCMs typically in the melting range between -25˚C to 62˚C based on weight, power gains, temperature range, thermal conductivity, and design for typical spacecraft applications was also done in this study. Water, n-octadecane, RT27, and RT31 were selected as effective organic PCM, the properties of which can be shown in Table.1.1.

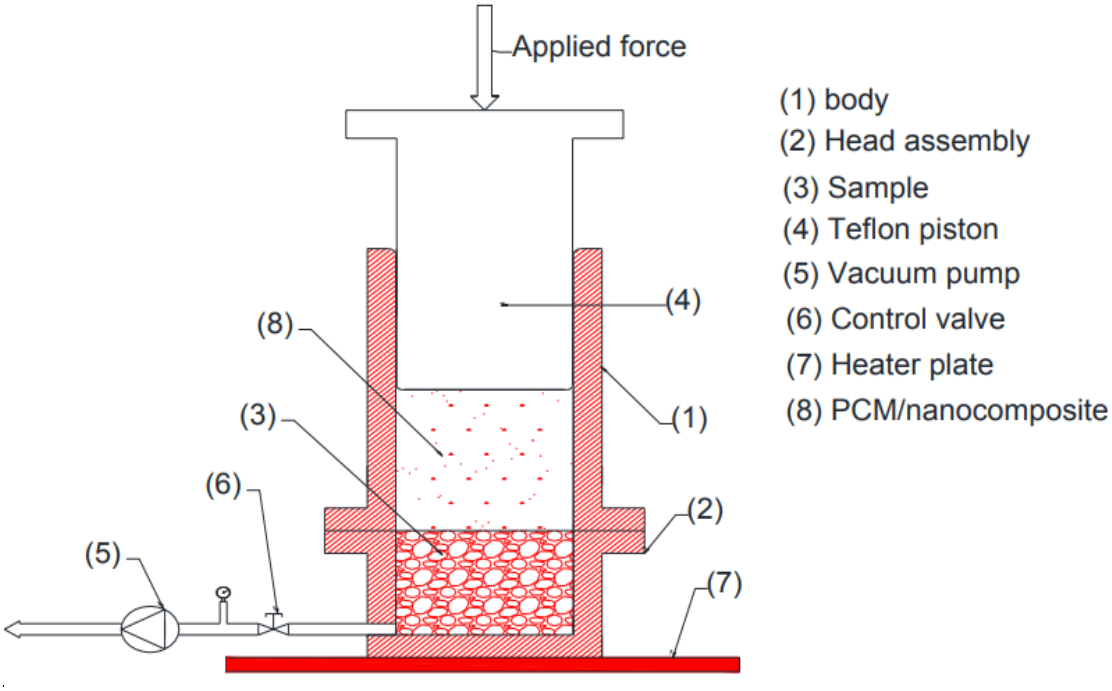

Fig. 1.12 Infuser configured for RT65/MWCNT with carbon foam [66]

In this study [67], the researchers rigorously evaluated a variety of materials to determine the most compatible combination with Phase Change Materials (PCMs). After determining the optimal filler to combine with PCMs, the team utilised numerical simulations to assess the efficacy of this composite under space conditions. To evaluate the efficacy of PCMs as passive thermal regulators, they simulated spacecraft in various orbits, such as the highly elliptical orbit of PROBA 3 and the low Earth orbit of SENTINEL-2. The outcomes, however, were varied. A significant obstacle was posed due to thermal ratcheting, which refers to the accumulated stress on spacecraft components caused by cyclical variations in temperature and pressure in space.

This phenomenon of net strain accumulation on a pressure vessel due to repeated cycles of loading and unloading is known as thermal ratcheting. In spacecraft, it occurs due to the transition between zones of different pressure, temperature, and g-forces which renders the spacecraft thermal management challenging. The PCMs tolerate this thermal ratcheting due to a narrow range of thermal cycles and hence they dampen out the peaks of such strain.

Another computational study of ESA focusing on the thermal control of launcher equipment by **Collette (2013)** [68] in an analogous manner at first, focus on the selection of appropriate PCM for the advanced thermal control of the launcher equipment bay by performing a feasibility study to choose the right PCM relevant to the thermal management demands of the mission. The study proceeded by evaluating various undesirable properties such as phase separation, subcooling, poor thermal conductivity, material compatibility, leakage, and volume change issues. The addition of chemicals to the original PCM to inhibit phase separation and integration of PCM with objects of larger thermal conductivity such as metal foams was proposed after due deliberation and analysis. Microencapsulation was proposed in this study to mitigate the leakage issue of PCM. A possible assembly of the PCM-HSD on Power and Propulsion Equipment (PPE) is shown in Fig.1.13.

Spreader plates and heat pipes were also considered for the heat dissipation issue but the weight gain due to their inclusion into the system was undesirable. An optimized approach was realized in this study and when the PCM-HSD design was evaluated, several desirable properties such as better heat transfer, lower mass, and ease of incorporating PCM were appreciated. However, it was also concluded that PCM without the filler material tends to short-circuit due to its poor thermal conductivity. A trade-off was reached to select n-docosane (with a mass of 1.78 kg and 33 mm

Table 1.1 Properties of RT27 and RT31 (Collette et.al.) [67]

	Density (kg/m^3)	**Specific heat (KJ/kg. K)**	**Thermal Conductivity (W/m. K)**	**Thermal Diffusivity (m^2/s)**	**Volume Change during melting (%)**
Rubitherm RT27 and RT31- solid	880	1800	0.2	1.3E-07	16
Rubitherm RT27 and RT31-liquid	760	2400	0.2	1.1E-07	16
n-octadecane -Solid State	865	1910	0.2	1.3E-07	11
n-octadecane -Liquid State	780	2220	0.148	8.5E-08	
Water- Liquid State	1000	4120	0.6	1.5E-07	-9

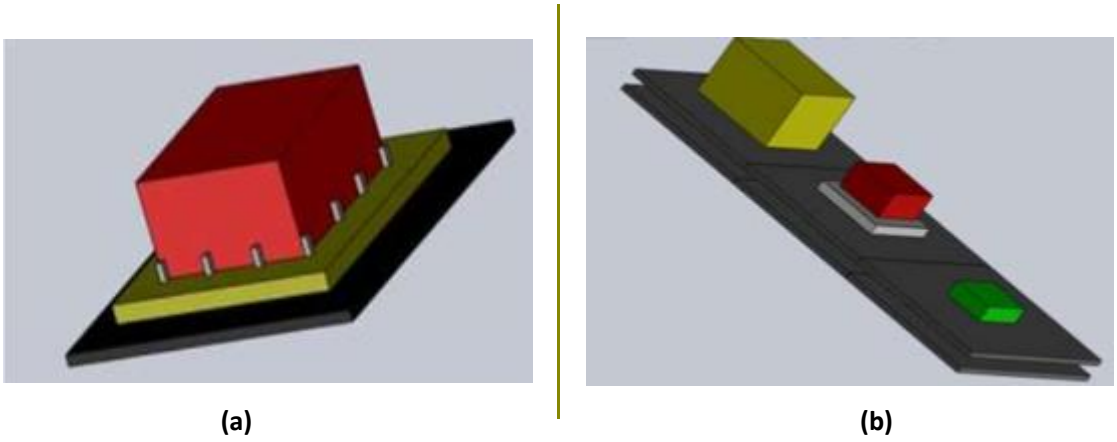

Fig. 1.13 (a) Assembly for Unit and PCM-HSD on PPE, (b) Doubled surface PCM-HSD [68]

thickness) as the PCM for the preliminary phase and this selection instead of Aluminium spreaders indicated a saving value upwards of € 375,000 owing to the reduced payload during launch.

Exomars Mission (2016) [69] is another example of a real space mission in which metal foam capacitors were incorporated with phase change materials (paraffin) to enhance the effective thermal conductivity. The capacitors installed on the surface platform capacitor of the EDM landing modulator of Exomars were the Miniature Intertial Measurement Unit (MIMU), CTPU (Central Terminal Processing Unit), and a transceiver , which stored 97 KJ, 216 KJ and 149 KJ of energy respectively and dissipated nearly 30-45W of energy with an operative design requirement of 40-45°C [70]**.**

Hexafly International Mission

Collette et al. (2019) [71] began an empirical investigation for the Hexafly International Project with the goal of evaluating an Experimental Flight Test Vehicle (EFTV) in a free flight scenario, paying special attention to velocities above Mach 7, in order to validate its potential prospects in terms of aerodynamic efficiency. Two heat accumulators that used PCMs were crucial to this investigation because their main goal was to prevent the high temperature levels inside crucial electronic components like telemetry systems, transmitters, and data collecting units from rising. In order to keep the operating temperature of the onboard avionics and gear under the established safety limits, n-octadecane was chosen as the PCM due to its passive cooling and thermal energy storage properties.

Additionally, from the start of the propulsion to the ejection sequence, it was ensured that the telemetry data was continuously transmitted to terrestrial stations. The PCM-based Heat Storage Device (PCM-HSD)'s (see Fig.1.14 and 1.15) admirable qualities, particularly its role in ensuring safety, enhancing stability, eliminating the need for moving components, and aiding in a significant mass reduction of the order of 14.3 tonnes, were the main highlights of this study.

3.4 SHAPE-STABILISED PCM (SS-PCM) FOR PROTECTION AGAINST SHORT-TERM HIGH-HEAT FLUX

Shape-Stabilized Phase Change Materials (SS-PCMs) is an advanced concept of thermal energy storage materials that combine the thermal energy storage capacities of conventional Phase Change Materials (PCMs) with improved structural integrity and shape retention during the phase transitions [72]. In essence, SS-PCMs are produced by impregnating or dispersing a PCM within a highly conductive, rigid matrix, which typically consists of polymers, fibres, or other supportive materials. Within the composite structure of Shape-Stabilized Phase Change Materials (SS-PCMs), the PCM is incorporated into a robust matrix, commonly comprised of highly conductive materials such as polymers, fibres, or mesoporous materials like carbon or silica. The rigid matrix functions as a frame of support that offers durability and preserves the morphological configuration of the phase change material throughout its cyclic phase changes, predominantly between solid and liquid phases. Thus, the shape-stabilized PCM (SS-PCM) serves to alleviate the necessity for external encapsulation, a technique frequently employed in traditional phase change materials (PCMs) to prevent leakage of PCM during phase transitions. Fundamentally, the rigid matrix present in SS-PCMs functions as an internal reinforcement system, guaranteeing the PCM's dimensional stability during its phase transitions, thus obviating the need for supplementary containment techniques.

Not only does the incorporation of the supportive matrix reduce PCM permeability during its liquid phase, but it also typically improves the composite material's thermal conductivity. This enhanced thermal conductivity is crucial, particularly for applications that require rapid thermal response and efficient heat transfer. In addition, the shape-stabilization effectively expands the range of potential applications by overcoming some of the limitations of conventional PCMs, such as material containment and handling difficulties.

Utilization of SS-PCMs is garnering considerable interest in the context of spacecraft avionics, where components are susceptible to thermal anomalies due to short-term high heat flux. This is primarily due to their ability to absorb and release thermal energy while maintaining structural integrity, thereby providing an effective means of protecting sensitive avionic components from transient thermal loads.

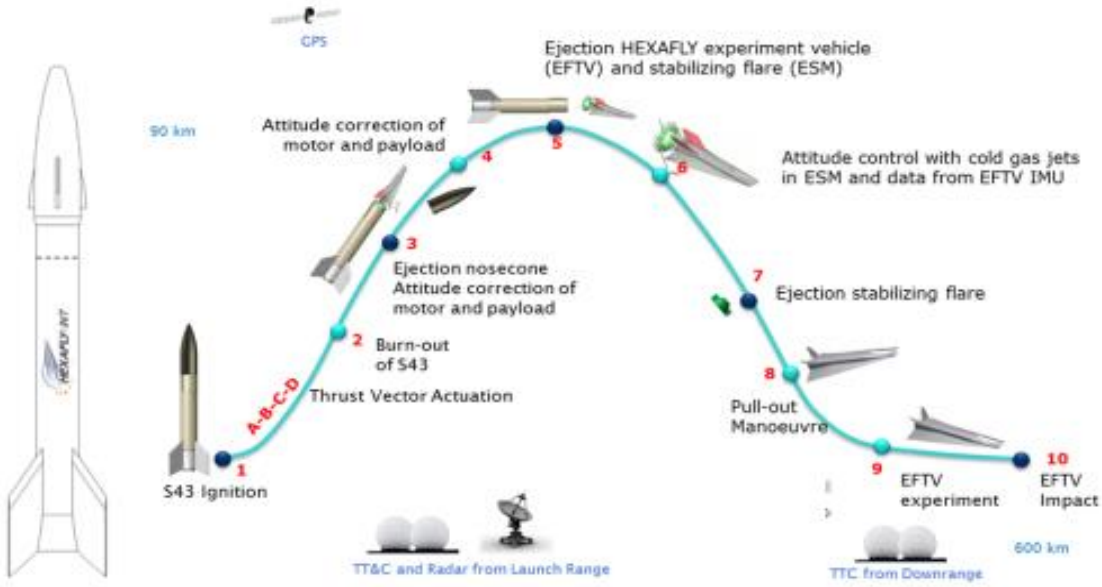

Fig 1.14 Hexafly-INT VBS-43 launch vehicle and Overall mission profile [71]

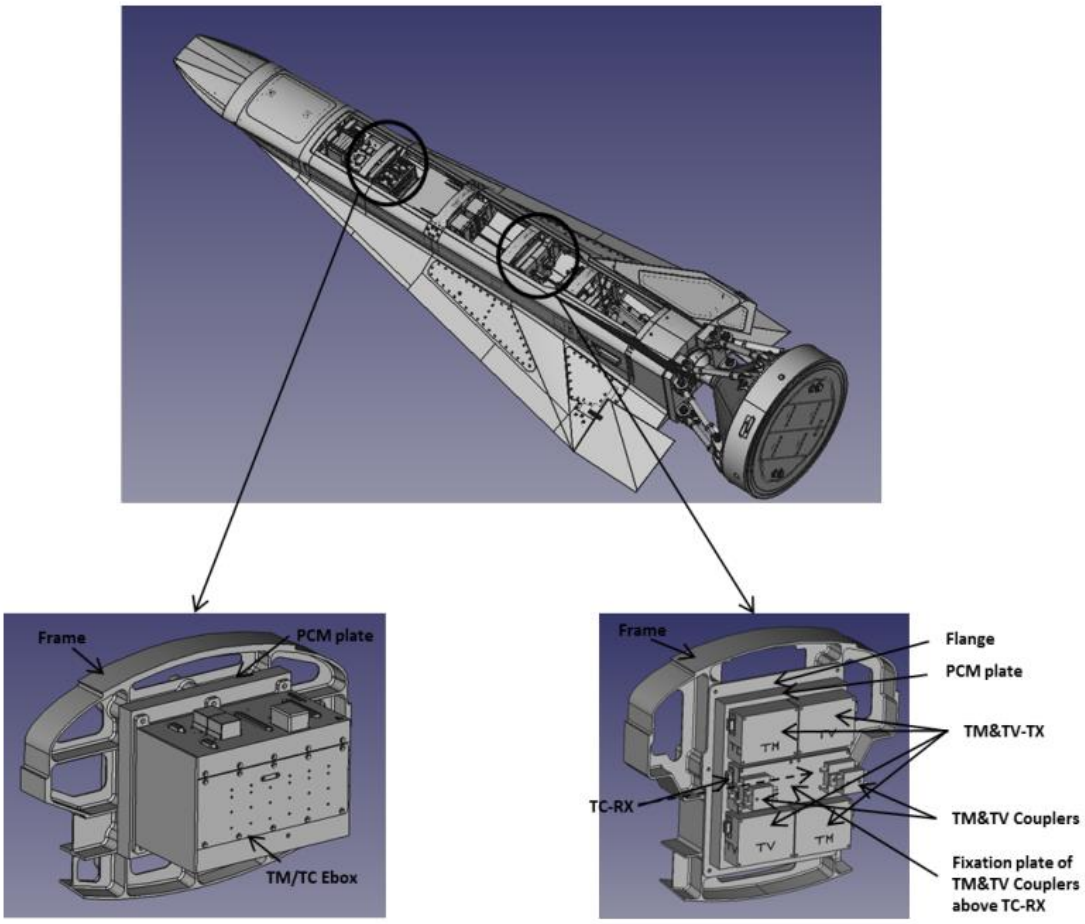

Fig. 1.15 Integration of the tested electronic units and PCM-HSD into the Experimental Flight test Vehicle (EFTV) [71]

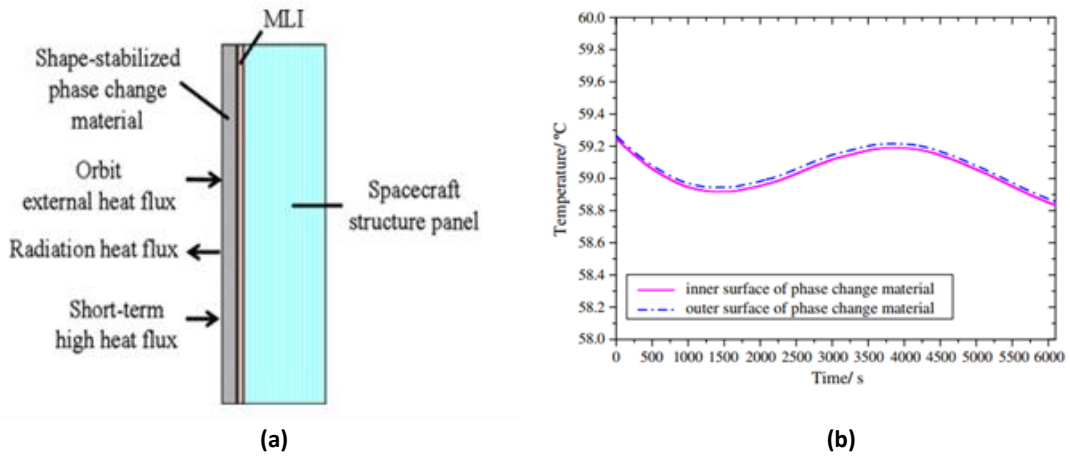

Fig. 1.16 Variation of PCM inside and outside temperature with Time [73]

Wu et al. (2013) studied the integration of SS-PCMs into spacecraft TMS [73]. High thermal conductivity SS-PCMs don't need to be packed densely into the module. To assess the viability of the SS-PCM system in comparison to traditional thermal control systems, the thermal response of SS-PCM towards high heat load was investigated in this study. Schematic for the thermal control and the variation of PCM temperature on the inside and outside surface is depicted in Fig.1.16 wherein a peak temperature of 59.3°C is reached.

It was concluded in this study that SS- PCM provides thermal protection to spacecraft from sudden bouts of high energy heat flux which cause anomalies in electronic equipment.

Xie et al. (2015) [74] investigated a novel composite material for thermal control applications that combines SS-PCM with an aluminium honeycomb structure. This innovative assembly seeks to capitalize on the thermal energy storage capabilities of SS-PCM while enhancing its thermal conductivity and structural strength through the incorporation of honeycomb aluminium. The thermal stability of the SS-PCM was confirmed and was found that it maintained its phase change temperature, latent heat, and thermal conductivity throughout multiple melting and solidification cycles, thereby establishing its dependability and safety. The incorporation of the aluminium honeycomb significantly improved the structural integrity, as evidenced by a 25.2% increase in stress tolerance limit (STL) in comparison to SS-PCM alone.

In addition, the thermal conductivity of the composite was found to be considerably increased to 2.08 W/m K, which is significant for ensuring efficient heat transfer. The effectiveness of the aluminium honeycomb structure in reducing the peak temperatures experienced by controlled objects, particularly under high heat loading, is one of the key findings of this study (see Fig.1.17). This capability is essential for assuring the safe operating temperature ranges of electronic devices, which can be extremely susceptible to thermal disturbances.

In conclusion, Xie et.al. [74] have made a seminal contribution through the creation and thorough evaluation of a composite material that combines SS-PCM with an aluminium honeycomb structure. This composite possesses exceptional thermal properties and mechanical toughness, making it ideally suited for thermal control applications.

Feng et al. (2021)[75] conducted an optimization study on SS-PCMs. In their investigation, a composite material was successfully produced by melting polyethylene glycol (PEG) into mesoporous carbon FDU-15. According to their findings, the PEG was effectively stabilised by the FDU-15 framework with a maximal loading of 75% wt%. Using a variety of analytical techniques, such as TEM, SEM, XRD, and FT-IR, in conjunction with molecular dynamic simulations, the researchers investigated the phase change and heat transfer mechanisms. According to their findings, the thermal conductivity of the composite was increased by more than 60% in comparison to unadulterated PEG. Fig. 1.18 shows the projection of localized heat flux with and without PEG.

In addition, this study sheds light on the significance of SS-PCMs' supporting materials. Specifically, the authors demonstrated that the FDU-15 carbon scaffold significantly outperformed other mesoporous carbons in terms of loading, crystallisation, and thermal transfer. This research by Feng et al.[75] contributes significantly to the field by not only developing a highly efficient SS-PCM but also elucidating the fundamental mechanisms governing its enhanced thermal properties. This study's findings may be useful in guiding the rational design of high-performance SS-PCMs for a variety of applications.

3.5 THE NASA FLIGHT EXPERIMENTS

A NASA-sponsored flight test was conducted in 2015 [76] to evaluate the viability of brazed aluminum paraffin wax composites as a passive heat sink in the environment of the International Space Station's permanent microgravity (ISS). This involved the incorporation of a phase management system to account for structural deformations that may occur due to high pressures. The PCM flight experiment wax prototype and finite element model mesh are shown in Fig.1.19(a& b), respectively. The PCM nodal model output shown in Fig.1.19 (c) demonstrates the way the coolant flow and sensible heat are incorporated into the model. The PCM unit is configured to serve the transportation, launch, environment, and pressure loads identified in the requirements.

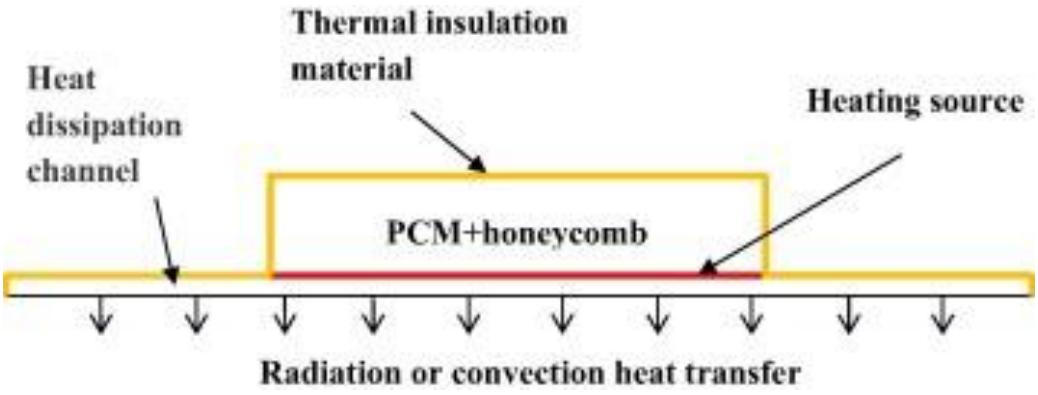

Fig. 1.17 Schematic of the PCM-thermal control device [74]

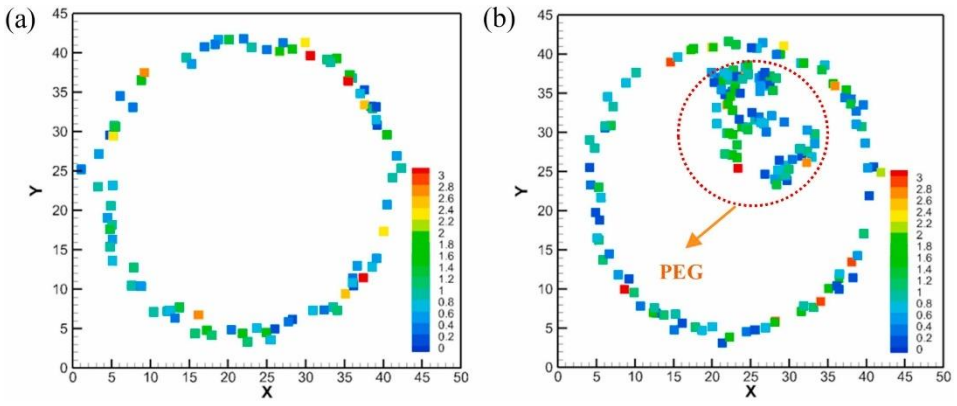

Fig. 1.18 Projection of localized heat flux of (a) FDU-15 and (b) PEG/FDU-15 on X–Y plane. [75]

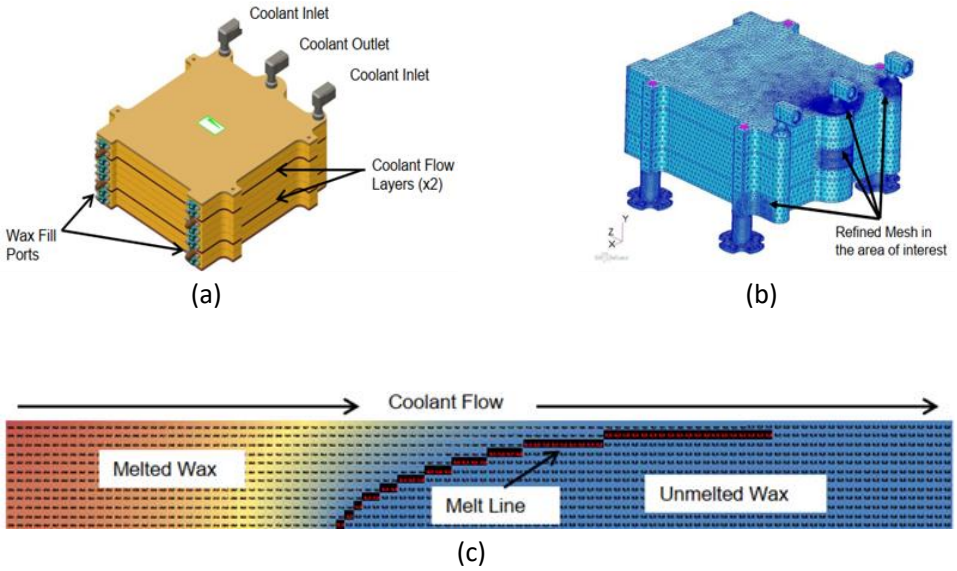

Fig. 1.19 (a) PCM Flight Experiment Flight prototype, (b) Finite Element Model mesh. (c) PCM nodal model output [76]

The test campaign comprised of three stages: laboratory, express rack, and ISS. It was found that the desired thermal performance goals were achieved, however, the pressure spikes on account of higher power and lower flow rate conditions rendered the thermal management concept partially effective with the issues such as short-circuiting, and dissolution being the prime contributors [77]**.** The results for the variation of pressure with time at laboratory conditions and conditions presented by the International Space Station is presented in Fig.1.20.

3.6 RECENT INVESTIGATIONS

3.6.1 PCM-BASED PACKING SYSTEM VERSUS FIN-BASED PACKING SYSTEM

Permanent Magnet Synchronous Motors (PMSMs) are electric motors that are constructed with permanent magnets and operate by synchronizing the rotation with the supply current frequency. PMSMs (as shown in Fig.1.21) are well-known for their efficiency, power density, and dependability. In the aviation industry, they have become a vital component for a variety of systems, especially electric propulsion.

Wang et al. (2016) [78] investigated the thermal management effects of a Phase Change Material (PCM)-based packing strategy in the context of onboard PMSMs in airplanes, where efficient thermal management is essential due to the confined space and the need for optimized performance. Their research sought to analyze and experimentally compare the efficacy of PCM-based packing systems versus Fin-based packing systems in mitigating the production of waste heat by PMSMs.

The focus of the study was on the capacity of PCM-packed systems to enhance heat durability during the continuous operation of the motors, as well as their ability to reduce the temperature peak in each cycle during intermittent operation. This study demonstrated through experimental analysis that PCM-based packing systems are superior to Fin-based packing systems in terms of thermal management for onboard PMSMs in airplanes.

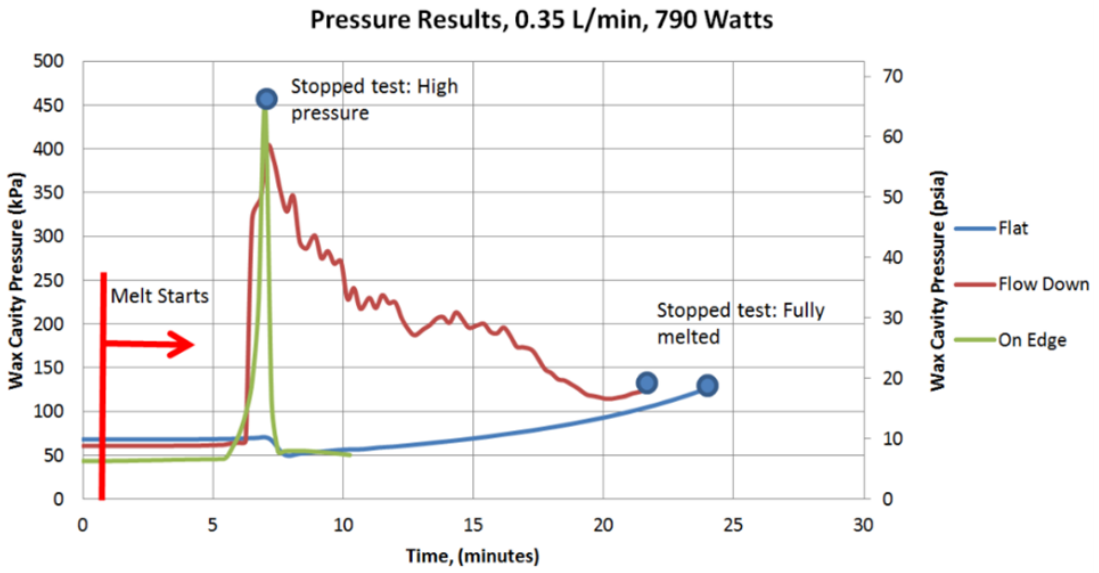

(a)

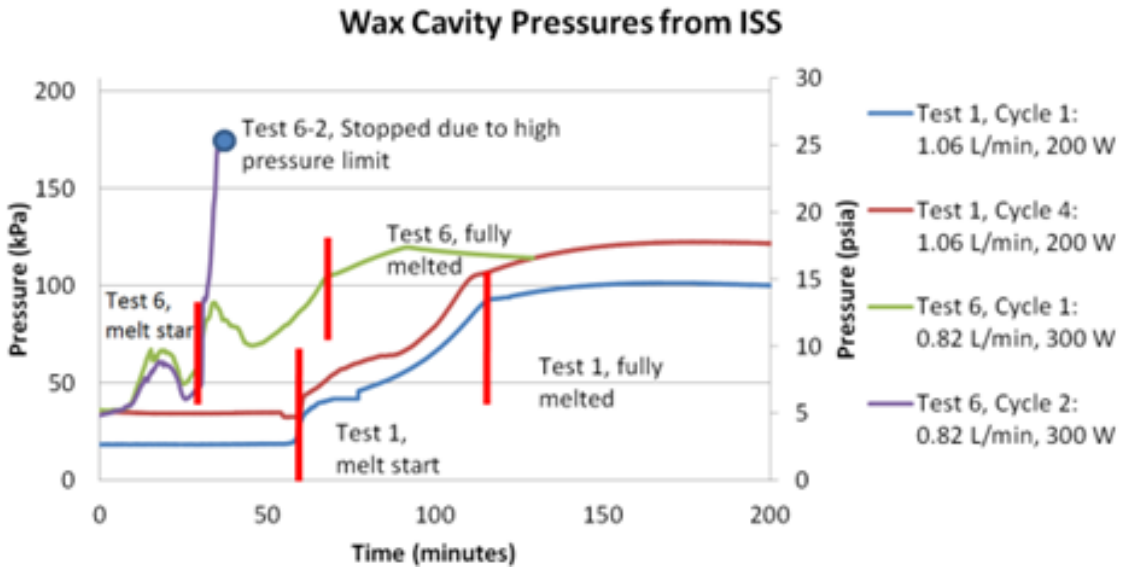

(b)

Fig. 1.20 (a) Wax cavity pressure measurements show different results for different orientations concerning gravity and (b) Pressure response of one wax cavity for two cycles of test points 1 and 6. [77]

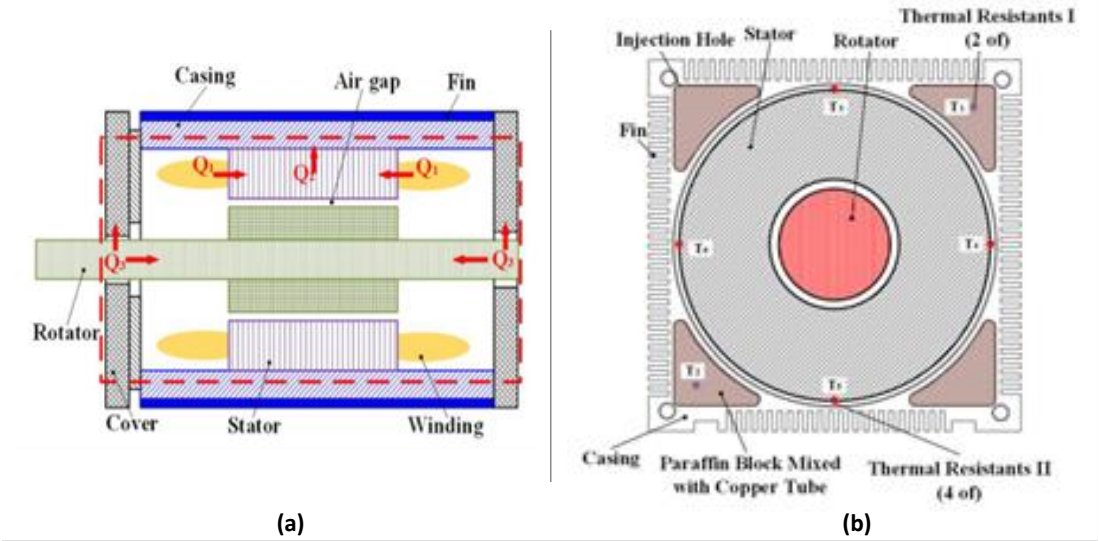

Fig. 1.21 (a) Structure Diagram of a Permanent Magnet Synchronous Motor (PMSM), (b) Schematic view of the PCM-based packing strategy of PMSM [78]

This finding is especially significant for the aviation industry because it suggests a more effective method of thermal management in PMSMs, which is crucial for the safety and performance of aircraft.

Without using any additional energy, the PCM packing technique (PPS) improved the PMSM system's economy and dependability. The PPS was demonstrated to significantly contribute to softening the temperature peak for each cycle during the intermittent heating mode.

3.6.2 Gallium-PCM heat sinks

Gallium has unique properties such as a low melting point and high thermal conductivity, is also a PCM candidate for TMS in space applications. Hartsfield et al. (2020) [79] examined the thermal properties of gallium in this capacity. The thermal storage and dissipation characteristics of heat sinks made from gallium and conventional phase change materials was studied.

Due to gallium's high density, thermal conductivity, and latent heat of fusion, the study found that using gallium could result in a 50-fold decrease in temperature during the phase change process. When subjected to transient heating, gallium can produce minimal thermal gradients, resulting in a nearly isothermal process.

A benefit of gallium highlighted in the study is its amenability to simplified computational modelling with lumped parameters, which is advantageous for predicting the behaviour of these systems without resorting to complex simulations. Gallium-based PCM devices are compact, due to substantial increase in density and higher mass-specific latent heat in comparison to conventional materials. In addition, the high thermal conductivity of gallium (2X greater than that of conventional PCMs) enables the construction of devices that are both simpler and more efficient. This high conductivity also contributes to a nearly uniform temperature distribution throughout the device, which is highly desirable for ensuring application reliability. Low volume, small temperature decreases, ease of manufacturing and design, and high energy storage make gallium-based PCMs an attractive option for systems requiring high thermal reliability. Fig. 1.22 indicate that investigations into the capabilities of gallium may pave the way for future research and development aimed at augmenting the efficiency of thermal management systems, particularly in aerospace applications.

3.6.3 Influence of Fin Configurations and gravity conditions (ISRO and NSFC, China)

Raj et al. (2020) [80] made a significant contribution to the field of thermal management for satellite avionics through their investigation of the influence of fin configurations within a thermal control module based on solid-solid phase change materials . Layered perovskite was utilized as the solid-solid PCM, while aluminium served as the heat absorber. The objective of the research was to optimize fin configurations, taking into account factors such as fin shape, fin thickness, base thickness, and the number of fins, under satellite orbital conditions. The horizontal axis numbers in Fig. 1.23 (a) depicts the heat sink configuration correspond to the experiment number in the L_{27} Taguchi and Fig.1.23 (b) illustrate the base temperatures corresponding to the heat sink configuration.

The authors analyzed the interaction of these factors on the thermal performance of the module by integrating Taguchi optimization with numerical simulations. Specifically, they focused on a scenario simulating an avionic component exposed to a constant heat flux of 10W under a duty cycle of 1200s "on" and 4800s "off". Compared to circular and triangular straight fin configurations, square straight fins demonstrated a superior ability to maintain lower base temperatures, attaining reductions of 1.3K and 0.5K, respectively. These findings were ascribed to the increased heat transfer surface area of square fins.

Nonetheless, the study also highlighted the benefits of tapered fins. These fins were approximately 0.6K more effective than their straight counterparts at lowering the base temperature, predominantly due to the increased volume near the base. In terms of both performance and efficiency, triangular fins, particularly when tapered, stood out, as they achieved 25% and 35% mass reductions compared to square and circular fins, respectively, at constant volume fractions. This could lead to cost savings without compromising thermal performance.

In conclusion, the study [80] is significant for the thermal management of satellite avionics because it sheds light on the optimization of fin configurations in Solid-solid PCM-based thermal control modules. The insights provided, particularly regarding the use of tapered triangular fins, are useful for the design and development of thermally efficient and cost-effective satellite system solutions.

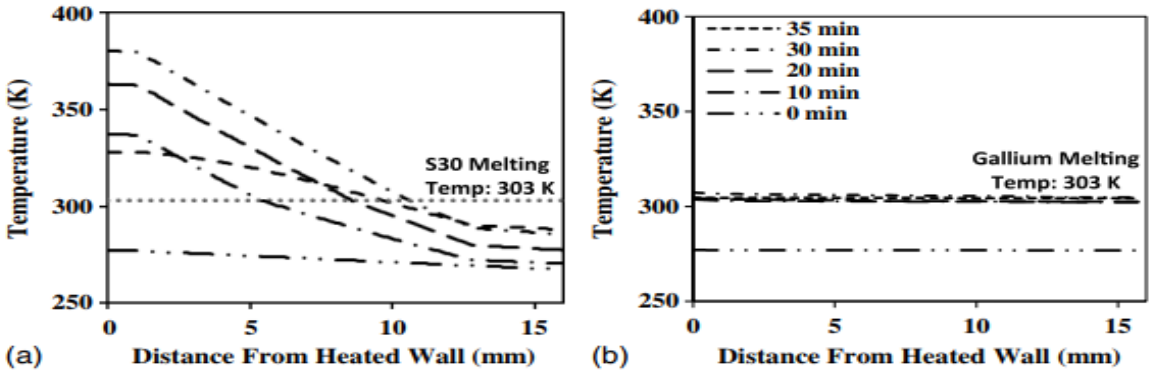

Fig. 1.22 Spatial distribution of Temperature v/s Distance from the heated wall in (a) S30 PCM heat sinks and (b) Gallium Heat sinks [79]

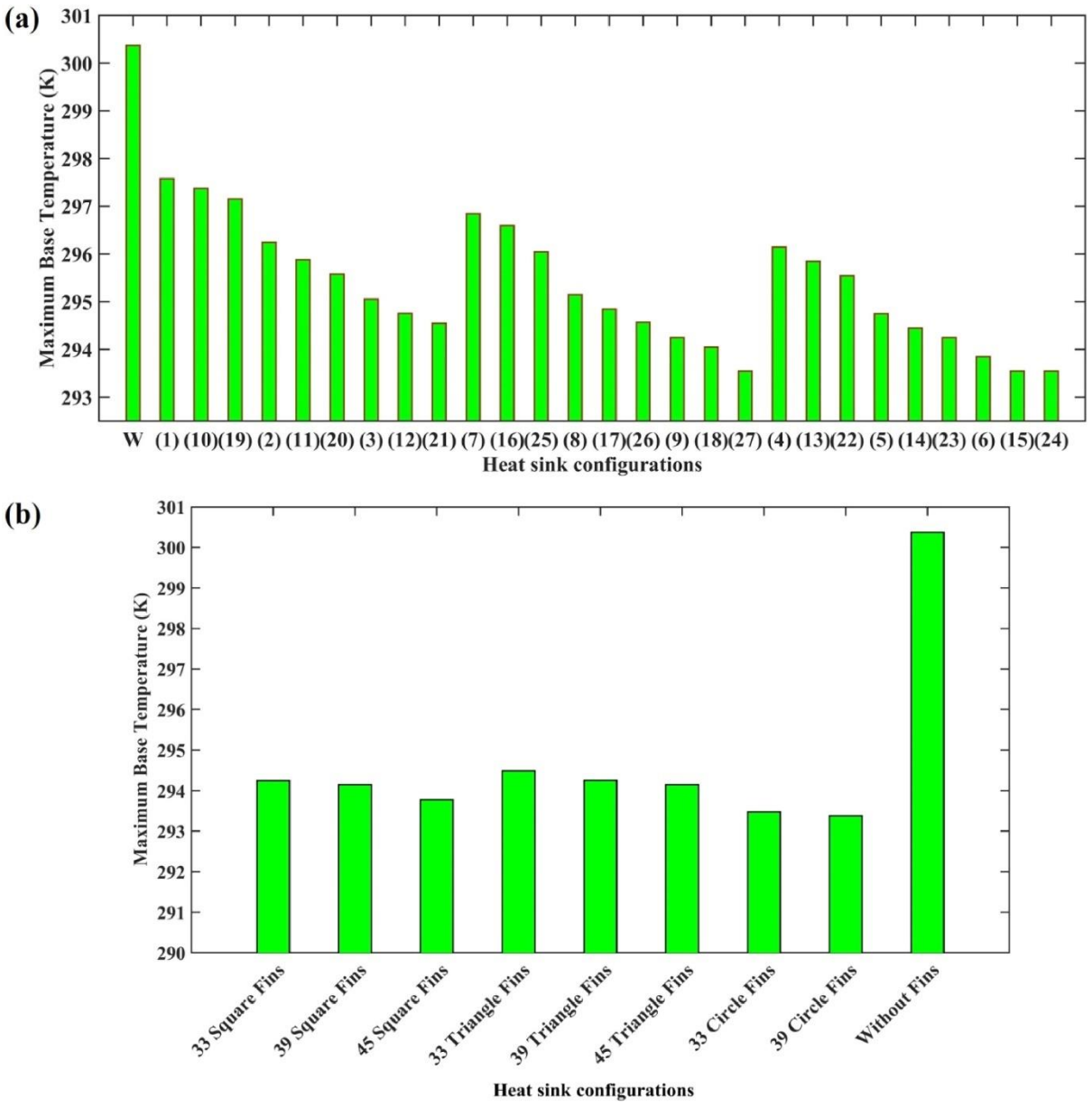

Fig. 1.23 Comparison of the thermal control module base temperature for solid state PCM (a) Normal configurations and (b) Tapered configurations. [80]

Kansara et al. (2021) [81] studied PCM-based thermal control module (TCM) in low gravity environments in an effort to comprehend the behavior of PCMs under the influence of gravity. This research is a timely response to the growing interest in Solid-Solid Phase Change Materials, which have shown promising properties such as minimal subcooling, limited volume expansion, and high thermal stability. Kansara et al. (2021) studied the effects of natural convection within the TCM using three different PCMs (hexadecane, acetic acid, and glycerol) for varied Grashof numbers. The authors captured the effects of natural convection during the melting cycle of PCM through a succession of simulations performed at different gravitational accelerations (see Fig. 1.24). It was found that natural convection had significant impact on the melting dynamics of hexadecane and acetic acid. This was evident from the fluctuating rate of average liquid fraction during the initial phases of melting. In contrast, natural convection had little effect on the melting of glycerol, as the rate of increase of the average liquid fraction remained nearly constant.

This distinction was attributable to glycerol's faster rate of heat propagation and minimal heat storage capacity. In addition, the study revealed that as gravitational acceleration decreased, the time required for the complete melting of the three materials increased. Acetic acid exhibited the minimum time for complete melting, while glycerol required the most time. The slight influence of gravity on the average Nusselt number for hexadecane and acetic acid demonstrates that the heat transfer mechanism at the beginning of the melting cycle is primarily controlled by conduction.

The temperature-time history presented by Kansara et al. (2021) [81] demonstrated an increase in the source temperature of TCM by approximately 21% (11 K) when the gravitational acceleration changed from g to g/80, with the largest temperature gradient observed in the upper portion of the melt front. The results provide invaluable insight into the influence of natural convection, gravitation, and material properties on the thermal performance of TCM.

Xu et al. (2021) [82] studied the melting heat transfer characteristics PCMs under hypergravity. The researchers examined n-docosane ($C_{22}H_{46}$) at varying levels of hypergravity (0-6g) and studied the melting heat transfer characteristics of PCM. This study reveals that hypergravity has a significant effect on the melting heat transfer characteristics of PCM. The authors conclude that increasing hypergravity accelerates melting and decreases the temperature of the heated wall.

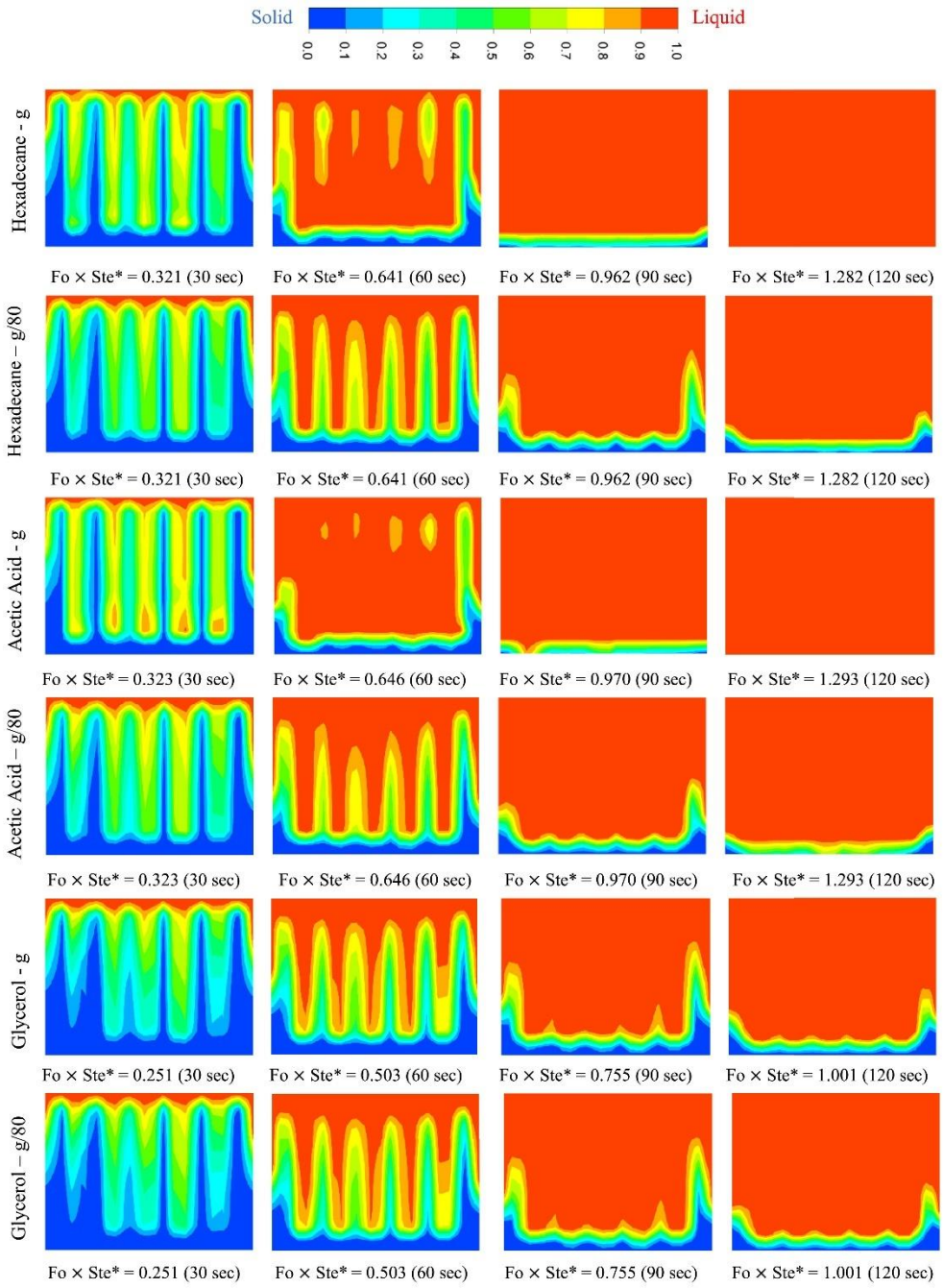

Fig. 1.24 Time evolution of flow field for (a) Hexadecane, (b) Acetic Acid, (c) Glycerol at g and g/80 for different times of 30 sec, 60 sec, 90 sec, and 120 sec. [81]

This is due to the hypergravity-induced enhancement of thermal convection within the liquid PCM. Specifically, the study found that under hypergravity, the time required for complete melting decreased by 20.6% and the heated wall temperature decreased by 21.0% compared to normal gravity conditions. However, the effect of hypergravity weakens with its increase, suggesting a saturation point beyond which hypergravity no longer substantially affects the melting characteristics.

In their experiments [82], the authors also investigated the melting characteristics at varying heat fluxes (2.5-7.5 kW/m^2) under constant hypergravity. The results indicate that an increase in heat flux accelerates the rate of melting and raises the temperature of the heated wall. In the presence of hypergravity, however, this effect is diminished.

For instance, when the heat flux was increased from 2.5 kW/m^2 to 7.5 kW/m^2 under a constant hypergravity of 4g, the rise in wall temperature was substantially less than under normal gravity conditions (see Fig.1.25). The authors hypothesize that the increased convection caused by hypergravity counteracts the increase in wall temperature caused by an increase in heat flux. This interaction between hypergravity and heat flux gives melting heat transfer characteristics a complex dynamic. The shift in liquid level induced by hypergravity can result in partial contact between the PCM and the heating wall. This can lead to overheating, which must be avoided to prevent damage to the PCM heat exchanger or other aviation equipment.

3.6.4 Influence of flow direction and orientation on PCM performance parameters

The flow direction of the heat transfer fluid is a crucial factor in determining the effectiveness of PCM-based heat sinks. Flow direction, which in some applications is characterized by the inclination angle, refers to the relative orientation of the flow of heat transfer fluid in relation to the PCM. It has a significant impact on the heat distribution within the PCM. The angle of inclination can impact the PCM's natural convection patterns, thermal stratification, and melting and solidification processes. In addition, the geometry of heat sinks, such as the presence of fins, can interact with the flow direction to produce complex thermal characteristics. To optimize the design and performance of PCM-based heat sinks, it is crucial to comprehend the interplay between flow direction and other geometrical and operational factors.

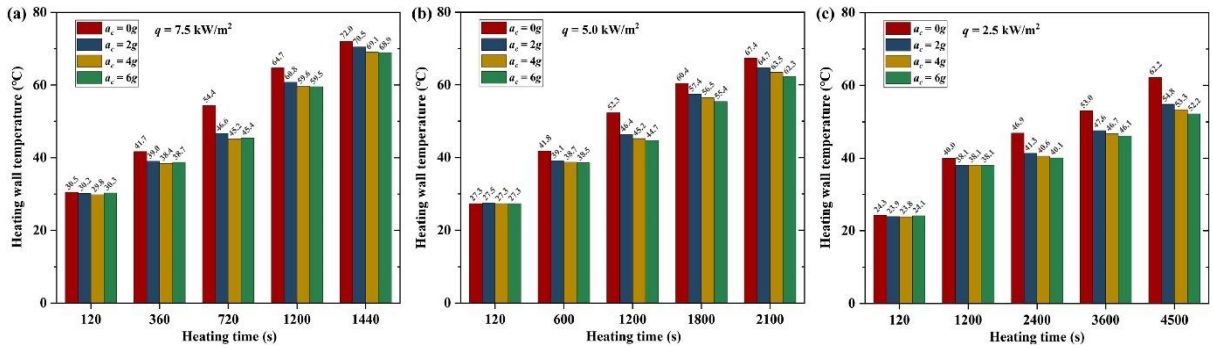

Fig. 1.25 Heating wall temperature for typical times at different heat flux [83]

Kothari et.al. (2021) [84] examined the role of the variation of heat flux on the thermal characteristics of PCM-based heat sinks which were finned as well as finless. The rate of melting of PCM at different inclination angles ranging from 0 to 90°, and heat flux is one of the key areas of focus in this study. The experimental setup and key results of this study are illustrated in Fig. 1.26-1.27. The inclination angle of the PCM-based heat sinks remarkably affects the thermal characteristics with an increase in the operating time observed on account of decreased angle of inclination. The number of fins holds a direct correlation with the 'Enhancement ratio'. An increase in the operating time varying between 40-65% and a decrease in melting time between 30-44% is observed in this study with a decrease in inclination angle.

These effects of the discussed key parameters are noticeably amplified in the case of finned PCM-based heat sinks as compared to finless heat sinks. It is also important to highlight the role of heat source orientation, which is an often-overlooked but crucial factor that governs the thermal performance of PCM-based Thermal Control Modules (TCMs). In situations where TCMs are utilized in environments with variable gravity, such as space, the orientation of the heat source with respect to the gravitational field becomes crucial. The orientation can substantially affect natural convection within the PCM, influencing the melting and solidification processes as a result. This, in turn, determines the rate at which thermal energy is absorbed or released, influencing the thermal performance as a whole. Depending on the orientation of a heat source, natural convection currents can be amplified or attenuated, particularly in environments with low gravity. Understanding these phenomena is crucial for the design of thermal management systems in spacecraft and other applications subjected to conditions of low gravity.

In an insightful study, Kansara and Singh (2021) [85] examined the effect of heat source orientation on the thermal performance of a phase change material (PCM)-based thermal control module (TCM) at varying levels of gravity. Two configurations were studied, 1) module was oriented against gravity (inverted case), 2) conventional orientation, referred to as the non-inverted case. Using hexadecane as the PCM, the study simulated a range of gravitational accelerations (g, g/2, g/10, g/20, g/40, and g/80) (see Fig. 1.28) and examined the melting and solidification processes using the enthalpy-porosity method. The authors reported a maximum variation of approximately 13.63 % between the inverted and non-inverted cases at normal gravity (g).

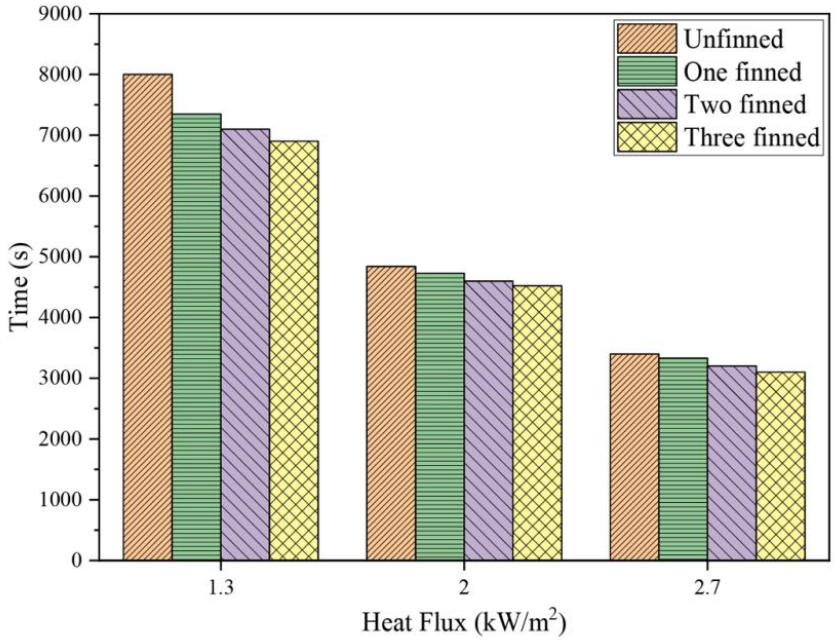

Fig. 1.26 Variation of Time (s) v/s Heat Flux (kW/m^2)- Kothari et.al. [84]

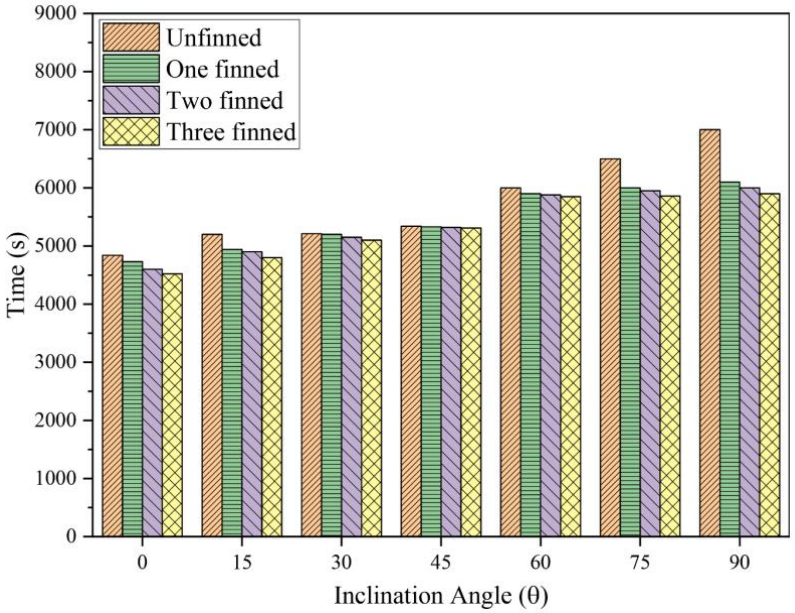

Fig. 1.27 Variation of time (s) v/s Inclination angle (degrees) (Kothari et.al.) [84]

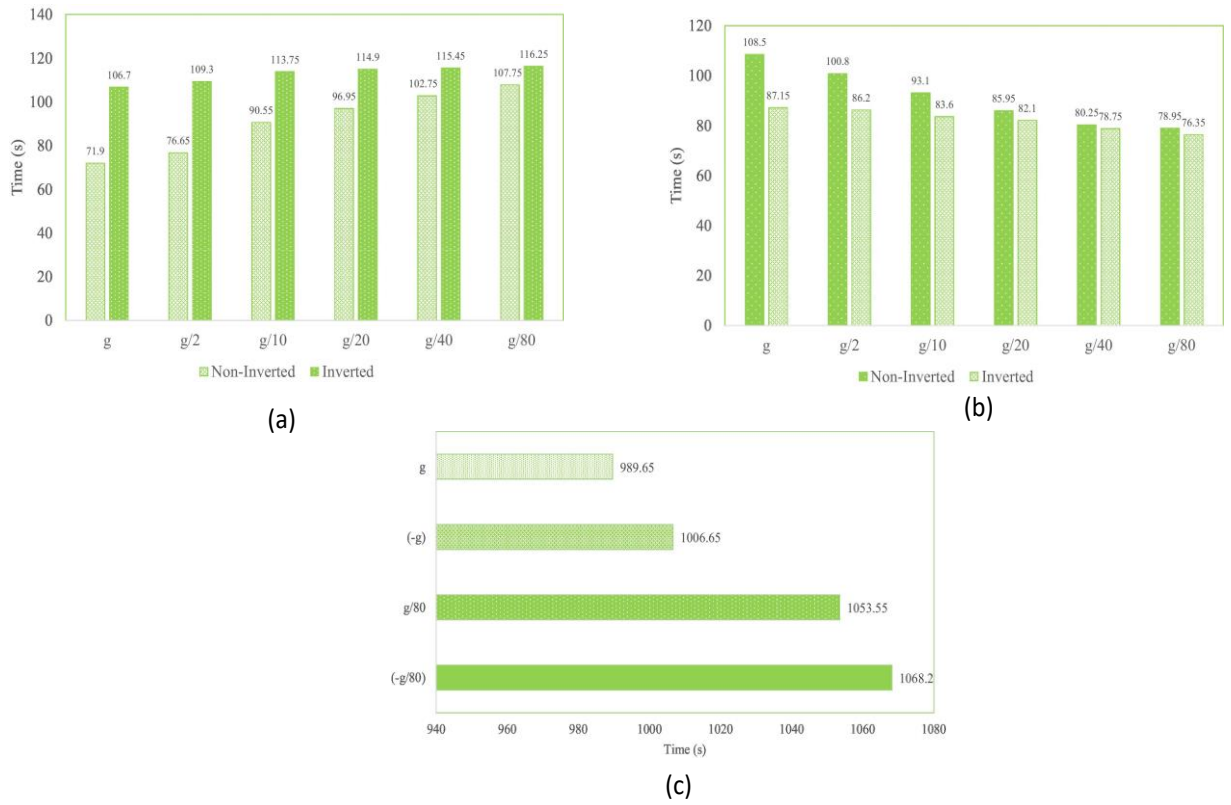

Fig 1.28(a) Allocation of Time Required for Inverted and Non-Inverted Cases to Reach a Set Point Liquid Fraction of 89% at Different Gravitational Accelerations

(b) Time Required for different Materials to Reach a Target Source Temperature of 355 K in the Presence of Various Gravitational Accelerations

(c) Comparative Analysis of the Time Required for PCM to Fully Solidify in Inverted and Non-Inverted States in earth gravity and reduced (g/80) gravity Conditions [85]

In exceedingly low gravity (g/80), this disparity shrunk to less than 2%. The study also revealed that reversing the direction of a heat source could elevate its temperature by up to 19.89% at normal gravity. This observation is essential for the design of PCM-based TCMs, particularly for applications in low-gravity environments where orientation relative to the gravitational field can have a significant effect on performance.

3.6.5 PV-PCM-Thermoelectric Energy Transmission in Space Conditions

A major ongoing investigation pertaining to 'PCM-Spacecraft' research is the study of He et.al. (2022) [86] wherein a photovoltaic thermoelectric coupling mechanism aids in achieving superior power generation efficiency under extraterrestrial environmental conditions. The composite photoelectric combined with a thermoelectric system as shown in Fig. 1.29 is evaluated for its periodic performance under space conditions and provides design reference to achieve the same. A 'Global Structural Parameter Optimization' was performed on the system and the various structural parameters were chosen to optimize the output from the system.

At the conclusion of this review article, Table 1.2 highlights the key properties of the PCM and filler material relating to the PCM-space research.

4. CONCLUDING REMARKS AND FUTURE SCOPE

This paper provides a comprehensive analysis of the research and development in the use of Phase Change Materials for thermal management of spacecraft avionics. The variety of explored topics reflects the multidimensionality and development of PCM technologies in space applications. Phase Change Materials, which are renowned for their ability to absorb and release thermal energy during phase transitions, are essential for stabilising temperature fluctuations within spacecraft. PCM research have witnessed significant refinement over time. Shape-Stabilized PCMs, which combine the thermal properties of PCMs with structural stability, represent a significant advancement among these materials.

In addition, the orientation and directionality of heat transfer have emerged as essential optimisation parameters for temperature control modules. By modifying the configuration and placement of PCMs, it is possible to obtain tailored responses that can be dynamically adapted to

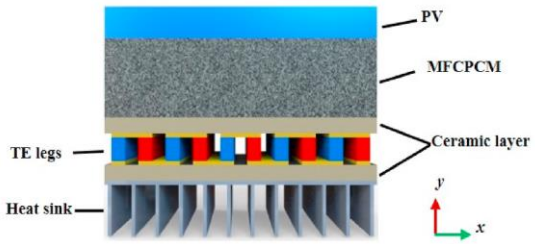

(a) PV-MFCPCM-TE system

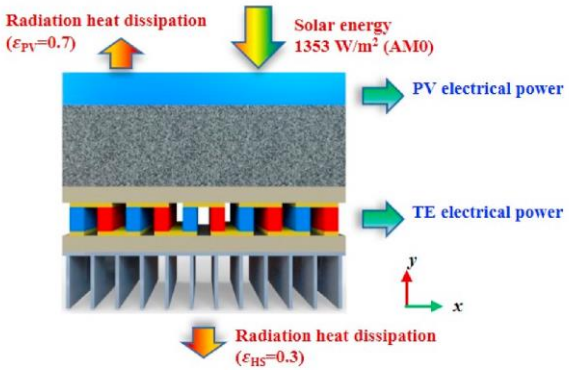

(b) Energy transmission and conversion during illumination period

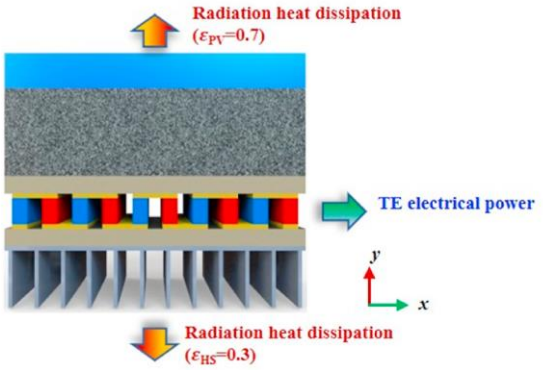

(c) Energy transmission and conversion during non-illumination period

Fig 1.29 (a) PV-MFCPCM-TE system, (b) Energy transmission and conversion during illumination period, and (c) Energy transmission and conversion during non-illumination period [86]

Table 1.2 Important Parameters of the Key Literature Survey Studies on PCM-Space Research

Authors/ Sponsoring Agency	**Type of Study**	**PCM**		**Filler Material**	
		Material	**Properties**	**Material**	**Properties**
Sol Z Fixler (1966) **(Grumman Aircraft Engineering Corporation)** **[33]**	Analytical	Technical Eicosane and Polyethylene Glycol (Carbowax 600)	**For Polyethylene Glycol,** ρ= 1120 kg/m^3, Melting Point = 20-25˚C, β=0.0075, Cp=2.26 KJ/Kg.K, ν=1.05 X 10-5 m^2/s, K= 0.16 W/m.K **For Eicosane,** ρ=750 Kg/m^3 , Melting point = 35˚C, β= 0.0003, Cp= 2.03 KJ/Kg.K, K= 0.23 W/m.K.	Aluminum Plates	N/A
Apollo-15 (1971) (NASA) **[34]**	Actual Mission	$LiNO_3$, Zinc Hydroxyl Nitrate Crystals, Myristic Acid,	N/A	N/A	N/A

Table 1.2 Important Parameters of the Key Literature Survey Studies on PCM-Space Research (Continued...)

Authors/ Sponsoring Agency	**Type of Study**	**PCM**		**Filler Material**	
		Material	**Properties**	**Material**	**Properties**
Venera 8 (1972) (USSR Space Mission) [36]	Actual Mission	Lithium Nitrate Trihydrate	N/A	N/A	N/A
Lauf and Hamby (1990) (NASA) [51]	Experimental	Germanium	T_{max}= 2000K; h_f= 370 KJ/Kg	Graphite Capsules	ρ= 1790 Kg/m3; Pore Size = 1.5 μm
JC Mulligan et.al. (1996) (NASA) [52]	Experimental and Analytical	n-Eicosane, n-Nonadecane, n-Octadecane, n-heptadecane	775<ρ<787 Kg/m^3; 2.09<c_p<2.14 KJ/Kg˚C; K=0.15 W/mK	N/A	N/A
D Pal and K Joshi (1998) (Motorola Inc) [14]	Experimental and Computational	RCM (n-tricontane)	k=0.23, ρ= 810, C_p=2050, μ=3.57 X 10^{30}	Aluminum	k=204 kg/m^3. ρ= 2707 Kg/m^3 ; C_p=896 KJ/kg.K μ=10^{30}

Table 1.2 Important Parameters of the Key Literature Survey Studies on PCM-Space Research (Continued...)

Authors/ Sponsoring Agency	**Type of Study**	**PCM**		**Filler Material**	
		Material	**Properties**	**Material**	**Properties**
Fossett et.al. (1998) **(US Airforce)** **[54]**	Experimental and Analytical	MicroPCM ™ 143	h_f = 221 KJ/Kg, ρ= 849 kg/m^3 K =0.147 W/mK, $c_{p,s}$ = 1800 J/Kg.K, $c_{p,l}$= 2720 J/Kg.K	Aluminum (Make: Lockhart and Duocel)	Weight=500 g
Saha and Dutta (2008) **(Academic Research)** **[87]**	Computational	Eicosane	K= 0.23 W/mK; c_p=2.050 KJ/Kg.K. ρ= 790 Kg/m^3 ; T_{melt} =35˚C ; h_f= 241 KJ/Kg	Aluminum	K=179.6 W/mK ; cp=0.96 KJ/Kg.K; ρ= 2712.9 Kg/m^3
Kuravi et.al. (2009) **(Office of Naval Research, USA)** **[64]**	Computational	Eicosane	K= 0.15-.025 W/mK. ρ= 778-856 Kg/m^3; c_p= 1.776-2.25 KJ/Kg.K	N/A	N/A

Table 1.2 Important Parameters of the Key Literature Survey Studies on PCM-Space Research (Continued...)

Authors/ Sponsoring Agency	**Type of Study**	**PCM**		**Filler Material**	
		Material	**Properties**	**Material**	**Properties**
JP Collette (2013) **(ESA)** **[67]**	Computational	Organic PCM, Fatty Acids, and Hydrated Salts	h_f = 180 KJ/kg Tm = 41-43°C $C_{p,s}$=1.95 KJ/kg.K $C_{p,l}$ = 2400 J/kg.K ρ_{solid}= 930 kg/m³ ρ_{liquid} = 873 kg/m³	N/A	N/A
Wu et.al. (2013) **(Beijing Institute of Space Longmarch Vehicle)** **[73]**	Analytical	n-onacosane	K= 1.76 W/mK. ρ = 826 Kg/m^3. c_p= 1.8 KJ/Kg˚K ;	Aluminum Foil	N/A

Table 1.2 Important Parameters of the Key Literature Survey Studies on PCM-Space Research (Continued...)

Authors/ Sponsoring Agency	**Type of Study**	**PCM**		**Filler Material**	
		Material	**Properties**	**Material**	**Properties**
Wang et.al. (2016) **(Beijing Institute of Space Systems Engineering) [89]**	Experimental	Paraffin Wax	K= 0.28-0.52 W/mK. c_p=2.6 KJ/kg.K ρ= 785-910 Kg/$m^{3.}$ h_f= 201.6 KJ/Kg	Aluminum	N/A
ExoMars Mission (2016) **(ESA/ Roscomos)** **[89]**	Actual Mission	Paraffin Wax	N/A	3 Aluminum foams namely MIMU, CTPU, and Transceiver	Energy = 97 - 216 KJ; Fusion Temperature = 37-43 ˚C; T_{Design} = 40-45 ˚C; Dissipation = 31-45 W
Collette et.al. (2019) **(ESA)** **[71]**	Experimental	n-Octadecane	h_f= 213 KJ/Kg; $T_{transition}$ =26-28˚C; Volume Change during Phase Change= 9.8%.	Filler Material	N/A

Table 1.2 Important Parameters of the Key Literature Survey Studies on PCM-Space Research (Continued...)

Authors/ Sponsoring Agency	**Type of Study**	**PCM**		**Filler Material**	
		Material	**Properties**	**Material**	**Properties**
Hartsfield et.al. (2020) **[79]**	Actual Mission	Gallium	T_{melt}= 302.8K; ρ= 5910 Kg/$m^{3;}$ h_f= 80.1 J/g; Latent Heat 473.3 J/ml. $c_p{}^{=}$ 0.37J/g.K; K= 29.4 W/mK; ρ = 774-865 Kg/m^3. α_{solid}=2.2x10^{-7} m^2/s. $c_{p,s}$=1.91 KJ/Kg˚K	N/A	N/A
Raj et.al. (2020) **(ISRO)** **[90]**	Computational and Analytical	SS-PCM [(1-$C_9H_{19}NH_3$) $2MnCl_4$]	K= 0.38 W/mK. h_f= 64.75-65.49 KJ/Kg; $T_{tranistion}$= 290.93 - 293.17 K; ρ=1050 Kg/m^3. c_p=1.91 KJ/Kg˚K ;	Aluminum Alloy	

Table 1.2 Important Parameters of the Key Literature Survey Studies on PCM-Space Research (Continued...)

Authors/ Sponsoring Agency	Type of Study	PCM		Filler Material	
		Material	Properties	Material	Properties
Kansara & Singh (2021) **(ISRO)** **[81]**	Computational	Hexadecane	K= 0.15 W/mK; c_p=2110 J/Kg.K. ρ= 835 Kg/m^3 ;T_{melt}.=289.85K; μ= 0.003454 Kg/m.s; Latent Heat= 237,100 J/Kg	Aluminum	K=202.4W/mK ; cp=871 J/Kg.K. ρ= 2719 Kg/m3
Kothari et.al. (2021) **(DST, India)** **[84]**	Experimental	Paraffin Wax	K= 0.2 W/mK; c_p=2.13-3.12 KJ/Kg.K; ρ= 775-900 Kg/m^3 ; T_{melt}=61.5˚C ; h_f= 202.4 KJ/Kg	Aluminum	K=218 W/mK ; cp=0.896 KJ/Kg.K; ρ= 2719 Kg/m3
Raj et.al. (2021) **(ISRO)** **[81]**	Experimental and Computational	Manganese based Organometallic layered perovskite SS-PCM	K=0.309 W/m.K; c_p=2.38 KJ/Kg.K; ρ= 1085 Kg/m^3. α = 1.2mm^2/s	Gallium-Indium Eutectic Metal Alloy	K= 0.309 W/m.K; cp=2.38 KJ/Kg.K; ρ=1085 Kg/m^3. α= 1.2mm^2/s

Table 1.2 Important Parameters of the Key Literature Survey Studies on PCM-Space Research (Continued...)

Authors/ Sponsoring Agency	**Type of Study**	**PCM**		**Filler Material**	
		Material	**Properties**	**Material**	**Properties**
Wu et.al. (2021) (Generic Technology Project, Equipment Pre-Research, China) **[91]**	Computational	RT80	K= 0.2W/m.K; c_p=2.1 KJ/Kg.K; ρ= 845 Kg/m^3 ; β= 0.001; μ= 0.002 kg/m.s. T_{melt} = 81˚C	Aluminum 6061	K=180 W/m.K; cp=0.963 KJ/Kg.K; ρ=2700 Kg/m^3
Xu et.al. (2021) **(National Natural Science Foundation & Aeronautic Science foundation, China)** **[83]**	Experimental	n-docosane	K= 0.15-0.22 W/m.K; c_p=1.813-1.9 KJ/Kg. K; ρ=770-794 Kg/$m^{3;}$ β= 0.001. μ= 0.003 kg/m.s; $T_{transition}$=42.8-45.4˚C	Aluminum	N/A

changing environmental conditions in space, as revealed by the studies. Indicative of the levels of control that can be exercised in managing heat dissipation, this provides an additional level of thermal regulation.

In addition to addressing the mechanical challenges, encapsulation techniques have also addressed the thermally conductive properties of PCMs. The review examines a variety of encapsulation techniques, such as the use of heat exchangers, metal foams, and heat sinks, which have been shown to be effective at enhancing the thermal performance of PCMs. These encapsulation techniques serve as a conduit for enhancing heat transfer as well as a structural support that reduces the mechanical stresses incurred during thermal cycling.

In addition, the review illuminates a number of studies that have investigated advanced encapsulation techniques, such as the use of 'Triplex Tube Heat Exhangers' Exchangers (TTHX) that exhibit a synergistic combination of high thermal conductivity and compactness, thus effectively bridging the gap between performance and space constraints.

Notable space agencies such as NASA, ESA, and ISRO have been at the forefront of these technological advancements. Their extensive research and development efforts have produced a wealth of information that informs the use of PCMs in space missions.

In conclusion, Phase Change Materials have developed into a technologically diverse and multifaceted field that continues to stretch the boundaries of thermal management research in spacecrafts. As demonstrated in this review, the culmination of research in material science, engineering, and thermodynamics provides an in-depth understanding that is essential for ongoing and future developments. As space missions become more ambitious and challenging, the historical and contemporary studies of PCMs will continue to play a crucial role in the development of innovative thermal management solutions for spacecraft avionics.

References

[1] N. Kumar and D. Banerjee, “Phase Change Materials,” in Handbook of Thermal Science and Engineering, Cham: Springer International Publishing, 2018, pp. 2213–2275. doi: 10.1007/978-3-319-26695-4_53.

[2] “43944200-Lunar-Rover-Operations-Handbook-07071971.pdf.” Accessed: Jan. 22, 2022. [Online]. Available: https://www.hq.nasa.gov/alsj/43944200-Lunar-Rover-Operations-Handbook-07071971.pdf

[3] “Spacecraft Thermal Control Handbook, Volume I: Fundamental Technologies,” The Aerospace Press. https://arc.aiaa.org/doi/abs/10.2514/4.989117 (accessed Jan. 27, 2022).

[4] Y. Xu, J. Wang, and T. Li, “Experimental study on the heat transfer performance of a phase change material based pin-fin heat sink for heat dissipation in airborne equipment under hypergravity,” J. Energy Storage, vol. 52, p. 104742, Aug. 2022, doi: 10.1016/j.est.2022.104742.

[5] S.-T. Hong and D. R. Herling, “Effects of Surface Area Density of Aluminum Foams on Thermal Conductivity of Aluminum Foam-Phase Change Material Composites,” Adv. Eng. Mater., vol. 9, no. 7, pp. 554–557, 2007, doi: 10.1002/adem.200700023.

[6] A. Diani and L. Rossetto, “Melting of PCMs Embedded in Copper Foams: An Experimental Study,” Mater. Basel Switz., vol. 14, no. 5, p. 1195, Mar. 2021, doi: 10.3390/ma14051195.

[7] N. C. Gallego and J. W. Klett, “Carbon Foams for Thermal Management,” Carbon, pp. 1461–1466, 2003.

[8] C. Y. Zhao, W. Lu, and Y. Tian, “Heat transfer enhancement for thermal energy storage using metal foams embedded within phase change materials (PCMs),” Sol. Energy, vol. 84, no. 8, pp. 1402–1412, Aug. 2010, doi: 10.1016/j.solener.2010.04.022.

[9] K. Y. Leong, S. Hasbi, and B. A. Gurunathan, “State of art review on the solidification and melting characteristics of phase change material in triplex-tube thermal energy storage,” J. Energy Storage, vol. 41, p. 102932, Sep. 2021, doi: 10.1016/j.est.2021.102932.

[10] R. O. James Klett and A. McMillan, “Heat Exchangers for Heavy Vehicles Utilizing High Thermal Conductivity Graphite Foams,” SAE International, Warrendale, PA (US), SAE/TPS-2000-01-2207, Jun. 2000. Accessed: Jan. 22, 2022. [Online]. Available:

https://www.osti.gov/biblio/770964-heat-exchangers-heavy-vehicles-utilizing-high-thermal-conductivity-graphite-foams

[11] M. BUSBY and S. MERTESDORF, “The benefit of phase change thermal storage for spacecraft thermal management,” in 22nd Thermophysics Conference, American Institute of Aeronautics and Astronautics. doi: 10.2514/6.1987-1482.

[12] NASA Technical Reports Server (NTRS), NASA Technical Reports Server (NTRS) 19720012306: Phase change materials handbook. 1971. Accessed: Feb. 01, 2022. [Online]. Available: http://archive.org/details/NASA_NTRS_Archive_19720012306

[13] W. R. Humphries and E. I. Griggs, “A design handbook for phase change thermal control and energy storage devices,” National Aeronautics and Space Administration, Huntsville, AL (USA). George C. Marshall Space Flight Center, N-78-15434; NASA-TP-1074; M-230, Nov. 1977. Accessed: Feb. 01, 2022. [Online]. Available: https://www.osti.gov/biblio/6899545-design-handbook-phase-change-thermal-control-energy-storage-devices

[14] D. Pal and Y. K. Joshi, “Thermal Management of an Avionics Module Using Solid-Liquid Phase-Change Materials,” J. Thermophys. Heat Transf., vol. 12, no. 2, pp. 256–262, Apr. 1998, doi: 10.2514/2.6329.

[15] S. Mondal, “Phase change materials for smart textiles – An overview,” Appl. Therm. Eng., vol. 28, no. 11, pp. 1536–1550, Aug. 2008, doi: 10.1016/j.applthermaleng.2007.08.009.

[16] H. Nazir et al., “Recent developments in phase change materials for energy storage applications: A review,” Int. J. Heat Mass Transf., vol. 129, pp. 491–523, Feb. 2019, doi: 10.1016/j.ijheatmasstransfer.2018.09.126.

[17] K. Faraj, M. Khaled, J. Faraj, F. Hachem, and C. Castelain, “Phase change material thermal energy storage systems for cooling applications in buildings: A review,” Renew. Sustain. Energy Rev., vol. 119, p. 109579, Mar. 2020, doi: 10.1016/j.rser.2019.109579.

[18] A. Sharma, R. Chauhan, M. Kallioğlu, V. Chinnasamy, and T. Singh, “A review of phase change materials (PCMs) for thermal storage in solar air heating systems,” Mater. Today Proc., vol. 44, Dec. 2020, doi: 10.1016/j.matpr.2020.10.560.

[19] “J. E Keville, ‘Development of Phase-Change Systems and Flight Experience on an Operational Satellite,’ Progress in Astronautics and Aeronautics, 56 (1977).”.

[20] E. W. Bentilla, L. E. Karre, and R. F. Sterrett, “Research and development study on thermal control by use of fusible materials Final report, Mar. 1964 - Mar. 1966,” NASA-CR-75041, Apr. 1966. Accessed: Feb. 01, 2022. [Online]. Available: https://ntrs.nasa.gov/citations/19660017401

[21] “L. Bledjian, J. R. Burden, and W. H. Hanna, ‘Development of a Low-Temperature Phase Change Thermal Capacitor,’ Progress in Astronautics and Aeronautics, 65 (1979).”.

[22] “P. G. Grodzka, E. Picklesimer, and L. E. Conner, ‘Cryogenic Temperature Control by Means of Energy Storage Materials’ AI.”

[23] J. Wang, H. Xie, Z. Xin, Y. Li, and L. Chen, “Enhancing thermal conductivity of palmitic acid based phase change materials with carbon nanotubes as fillers,” Sol. Energy, vol. 84, no. 2, pp. 339–344, Feb. 2010, doi: 10.1016/j.solener.2009.12.004.

[24] “P. G. Grodzka, ‘Space Thermal Control by Freezing and Melting, Second Interim Report,’ LMSC-HREC D 148619, NAS8-25183, Lockheed Missiles & Space Co., Huntsville, Ala. (May 1969).”.

[25] E. W. Bentilla, L. E. Karre, and R. F. Sterrett, “Research and development study on thermal control by use of fusible materials Final report, Mar. 1964 - Mar. 1966,” NASA-CR-75041, Apr. 1966. Accessed: Feb. 01, 2022. [Online]. Available: https://ntrs.nasa.gov/citations/19660017401

[26] K. Lafdi, O. Mesalhy, and S. Shaikh, “Experimental study on the influence of foam porosity and pore size on the melting of phase change materials,” J. Appl. Phys., vol. 102, no. 8, p. 083549, Oct. 2007, doi: 10.1063/1.2802183.

[27] R. P. Dambal and T. L. Rama Char, “Corrosion Prevention of Aluminum by Cathodic Protection” Corrosion Prevention and Control (February 1971).

[28] H. Y. Hunsicker, “Dimensional changes in heat treating aluminum alloys,” Metall. Trans. A, vol. 11, no. 5, pp. 759–773, May 1980, doi: 10.1007/BF02661205.

[29] K. R. Van Horn, Aluminum, Vol. I (American Society for Metals, Metals Park, Ohio, 1967).

[30] A. Kulshreshtha and S. K. Dhakad, “Preparation of metal foam by different methods: A review,” Mater. Today Proc., vol. 26, pp. 1784–1790, Jan. 2020, doi: 10.1016/j.matpr.2020.02.375.

[31] C. A. Bauer and R. A. Wirtz, “Thermal Characteristics of a Compact, Passive Thermal Energy Storage Device,” presented at the ASME 2000 International Mechanical Engineering Congress and Exposition, American Society of Mechanical Engineers Digital Collection, Nov. 2021, pp. 283–289. doi: 10.1115/IMECE2000-1395.

[32] H. F. Abbasov, “The Effective Thermal Conductivity of Composite Phase Change Materials with Open-Cellular Metal Foams,” Int. J. Thermophys., vol. 41, no. 12, p. 164, Oct. 2020, doi: 10.1007/s10765-020-02747-z.

[33] S. Z. FIXLER, “Satellite thermal control using phase-change materials.,” J. Spacecr. Rockets, vol. 3, no. 9, pp. 1362–1368, 1966, doi: 10.2514/3.28661.

[34] C. L. Mansfield, “Apollo 15,” NASA, Jan. 09, 2018. http://www.nasa.gov/mission_pages/apollo/missions/apollo15.html (accessed Feb. 22, 2022).

[35] W. C. Kelliher and P. R. Young, “Investigation of phase-change coatings for variable thermal control of spacecraft,” Art. no. NASA-TN-D-6756, Jun. 1972, Accessed: Dec. 04, 2022. [Online]. Available: https://ntrs.nasa.gov/citations/19720018274

[36] “NASA - NSSDCA - Spacecraft - Details.” https://nssdc.gsfc.nasa.gov/nmc/spacecraft/display.action?id=1972-021A (accessed Feb. 22, 2022).

[37] R. L. Bain, F. J. Stermole, and J. O. Golden, “The effect of gravity induced free convection upon the melting phenomena of a finite paraffin slab for thermal control,” NASA-CR-123954, Jan. 1972. Accessed: Dec. 16, 2022. [Online]. Available: https://ntrs.nasa.gov/citations/19730004403

[38] A. Abhat and M. Groll, “Investigation of phase change material /PCM/ devices for thermal control purposes in satellites,” in Thermophysics and Heat Transfer Conference, Boston,MA,U.S.A.: American Institute of Aeronautics and Astronautics, Jul. 1974. doi: 10.2514/6.1974-728.

[39] A. Abhat, “Experimental investigation and analysis of a honeycomb-packed phase change material device,” in 11th Thermophysics Conference, in Fluid Dynamics and Co-located Conferences. American Institute of Aeronautics and Astronautics, 1976. doi: 10.2514/6.1976-437.

[40] “Table of Contents,” in Heat Transfer, Thermal Control, and Heat Pipes, in Progress in Astronautics and Aeronautics. American Institute of Aeronautics and Astronautics, 1980, pp. i–xxiii. doi: 10.2514/5.9781600865442.0000.0000.

[41] “An Analysis of the Space Sector’s Surge Capacity. An Input-Output Approach.” Accessed: Dec. 18, 2022. [Online]. Available: https://apps.dtic.mil/sti/citations/ADA180260

[42] R. A. Crane and M. O. Dustin, Evaluation of alternative phase change materials for energy storage in solar dynamic applications. 1988, pp. 329–334. Accessed: Dec. 18, 2022. [Online]. Available: https://ui.adsabs.harvard.edu/abs/1988soen.proc..329C

[43] C. H. Son, “Solid-solid phase change materials as a space-suit battery thermal storage medium,” Columbia, SC (US); Univ. of South Carolina, Jan. 1989. Accessed: Dec. 18, 2022. [Online]. Available: https://www.osti.gov/biblio/7122035

[44] P. Majumdar and R. K. Sharma, “A moving boundary model for heat transfer in phase change material (for space power applications),” in Proceedings of the 24th Intersociety Energy Conversion Engineering Conference, Aug. 1989, pp. 2719–2733 vol.6. doi: 10.1109/IECEC.1989.74428.

[45] W. Sheffield and C. Wen, “PHASE CHANGE MATERIAL FOR SPACECRAFT THERMAL MANAGEMENT,” p. 72.

[46] “Encapsulation methods for phase change materials – A critical review - ScienceDirect.” https://www.sciencedirect.com/science/article/pii/S0017931022009279 (accessed Jun. 23, 2023).

[47] H. Torab, “Optimal design of thermal energy storage for space power,” Space Power, vol. 8, pp. 415–423, Jan. 1989.

[48] P. Stark, “PCM-Impregnated Polymer Microcomposites for Thermal Energy Storage,” SAE Trans., vol. 99, pp. 571–588, 1990.

[49] P. Stark, “PCM-Impregnated Polymer Microcomposites for Thermal Energy Storage,” SAE Trans., vol. 99, pp. 571–588, 1990.

[50] D. P. Colvin, “Microencapsulated Phase-Change Materials For Storage Of Heat,” MFS-27198, Jul. 1989. Accessed: Dec. 18, 2022. [Online]. Available: https://ntrs.nasa.gov/citations/19890000375

[51] R. J. Lauf and C. J. Hamby, “Metallic phase-change materials for solar dynamic energy storage systems,” Oak Ridge National Lab., TN (USA), ORNL/TM-11351, Dec. 1990. doi: 10.2172/6241485.

[52] J. C. Mulligan, D. P. Colvin, and Y. G. Bryant, “Microencapsulated phase-change material suspensions for heat transfer in spacecraft thermal systems,” J. Spacecr. Rockets, vol. 33, no. 2, pp. 278–284, Mar. 1996, doi: 10.2514/3.26753.

[53] J. B. Rittenhouse and J. B. Singletary, “Spacecraft materials experience.” Jan. 01, 1969. Accessed: Feb. 01, 2022. [Online]. Available: https://ntrs.nasa.gov/citations/19700011937

[54] A. J. Fossett, M. T. Maguire, A. A. Kudirka, F. E. Mills, and D. A. Brown, “Avionics Passive Cooling With Microencapsulated Phase Change Materials,” J. Electron. Packag., vol. 120, no. 3, pp. 238–242, Sep. 1998, doi: 10.1115/1.2792628.

[55] “Aluminum Foam | Duocel Open Cell Foam | Aluminium Foam,” https://ergaerospace.com/. https://ergaerospace.com/aluminum-foam-cell-structure-material/ (accessed Dec. 18, 2022).

[56] K. F. Strauss and T. Daud, “Overview of radiation tolerant unlimited write cycle non-volatile memory,” in 2000 IEEE Aerospace Conference. Proceedings (Cat. No.00TH8484), Mar. 2000, pp. 399–408 vol.5. doi: 10.1109/AERO.2000.878514.

[57] S. Krishnan, S. V. Garimella, and S. S. Kang, “A novel hybrid heat sink using phase change materials for transient thermal management of electronics,” IEEE Trans. Compon. Packag. Technol., vol. 28, no. 2, pp. 281–289, Jun. 2005, doi: 10.1109/TCAPT.2005.848534.

[58] J. E. Simpson, S. V. Garimella, and H. C. de Groh, “Experimental and Numerical Investigation of the Bridgman Growth of a Transparent Material,” J. Thermophys. Heat Transf., vol. 16, no. 3, Art. no. 3, 2002, doi: 10.2514/2.6709.

[59] J. H. Ferziger and M. Perić, “Solution of the Navier-Stokes Equations,” in Computational Methods for Fluid Dynamics, J. H. Ferziger and M. Perić, Eds., Berlin, Heidelberg: Springer, 1996, pp. 149–208. doi: 10.1007/978-3-642-97651-3_7.

[60] J. A. Dantzig, “Modelling liquid–solid phase changes with melt convection,” Int. J. Numer. Methods Eng., vol. 28, no. 8, Art. no. 8, 1989, doi: 10.1002/nme.1620280805.

[61] J. A. Dantzig, “Modelling liquid–solid phase changes with melt convection,” Int. J. Numer. Methods Eng., vol. 28, no. 8, pp. 1769–1785, 1989, doi: 10.1002/nme.1620280805.

[62] S. Mat, A. A. Al-Abidi, K. Sopian, M. Y. Sulaiman, and A. T. Mohammad, “Enhance heat transfer for PCM melting in triplex tube with internal–external fins,” Energy Convers. Manag., vol. 74, pp. 223–236, Oct. 2013, doi: 10.1016/j.enconman.2013.05.003.

[63] S. Kuravi, K. M. Kota, J. Du, and L. C. Chow, “Numerical Investigation of Flow and Heat Transfer Performance of Nano-Encapsulated Phase Change Material Slurry in Microchannels,” J. Heat Transf., vol. 131, no. 6, Art. no. 6, Mar. 2009, doi: 10.1115/1.3084123.

[64] S. Kuravi, K. M. Kota, J. Du, and L. C. Chow, “Numerical Investigation of Flow and Heat Transfer Performance of Nano-Encapsulated Phase Change Material Slurry in Microchannels,” J. Heat Transf., vol. 131, no. 6, Mar. 2009, doi: 10.1115/1.3084123.

[65] X. Luo and M. Wang, “Latest research development of spacecraft thermal control technology,” in 2010 2nd International Conference on Computer Engineering and Technology, Apr. 2010, pp. V5-499-V5-502. doi: 10.1109/ICCET.2010.5486160.

[66] W. G. Alshaer, S. A. Nada, M. A. Rady, E. P. Del Barrio, and A. Sommier, “Thermal management of electronic devices using carbon foam and PCM/nano-composite,” Int. J. Therm. Sci., vol. 89, pp. 79–86, Mar. 2015, doi: 10.1016/j.ijthermalsci.2014.10.012.

[67] P. ColletteJ, “Phase Change Material Device for Spacecraft Thermal Control.” https://www.semanticscholar.org/paper/Phase-Change-Material-Device-for-Spacecraft-Thermal-ColletteJ./852947fcac5a91c44d710b573808e0737d15ef41 (accessed Jan. 22, 2022).

[68] J.-P. Collette et al., “Advanced Thermal Control of Launcher Equipment Bay using Phase Change Material,” Sep. 2013, Accessed: Jan. 20, 2022. [Online]. Available: https://orbi.uliege.be/handle/2268/159131

[69] J. Vago et al., “ESA ExoMars program: The next step in exploring Mars,” Sol. Syst. Res., vol. 49, no. 7, pp. 518–528, Dec. 2015, doi: 10.1134/S0038094615070199.

[70] M. Gottero, V. Perotto, R. Martino, B. Leyda, and B. Ozmat, Phase-change thermal capacitors for ExoMars 2016 mission. 44th International Conference on Environmental Systems, 2014. Accessed: Jan. 14, 2022. [Online]. Available: https://ttu-ir.tdl.org/handle/2346/59519

[71] J.-P. Collette et al., “Phase Change Material Heat Accumulator for the HEXAFLY-INT Hypersonic glider,” in 49th International Conference on Environmental Systems, BOSTON, United States, Jul. 2019. Accessed: Feb. 01, 2022. [Online]. Available: https://hal.archives-ouvertes.fr/hal-02335121

[72] M. Gandhi et al., “A Review on Shape-Stabilized Phase Change Materials for Latent Energy Storage in Buildings,” Sustainability, vol. 12, no. 22, Art. no. 22, Jan. 2020, doi: 10.3390/su12229481.

[73] W. Wu, N. Liu, W. Cheng, and Y. Liu, “Study on the effect of shape-stabilized phase change materials on spacecraft thermal control in extreme thermal environment,” Energy Convers. Manag., vol. 69, pp. 174–180, May 2013, doi: 10.1016/j.enconman.2013.01.025.

[74] B. Xie, W. Cheng, and Z. Xu, “Studies on the effect of shape-stabilized PCM filled aluminum honeycomb composite material on thermal control,” Int. J. Heat Mass Transf., vol. 91, pp. 135–143, Dec. 2015, doi: 10.1016/j.ijheatmasstransfer.2015.07.108.

[75] D. Feng, P. Li, Y. Feng, Y. Yan, and X. Zhang, “Using mesoporous carbon to pack polyethylene glycol as a shape-stabilized phase change material with excellent energy storage capacity and thermal conductivity,” Microporous Mesoporous Mater., vol. 310, p. 110631, Jan. 2021, doi: 10.1016/j.micromeso.2020.110631.

[76] G. Quinn, J. J. Stieber, R. B. Sheth, and T. Ahlstrom, “Phase Change Material Heat Sink for an International Space Station Flight Experiment,” undefined, 2015, Accessed: Jan. 13, 2022. [Online]. Available: https://www.semanticscholar.org/paper/Phase-Change-Material-Heat-Sink-for-an-Space-Flight-Quinn-Stieber/b496376d9b84e5d2ce69e3ee10d2feea5b2efe8a

[77] G. Quinn, H. Le, T. Ahlstrom, and R. Sheth, “Phase Change Material Heat Sink Flight Experiment Results,” Jul. 2017, Accessed: Jan. 20, 2022. [Online]. Available: https://ttu-ir.tdl.org/handle/2346/72864

[78] J.-X. Wang, Y.-Z. Li, S.-N. Wang, H.-S. Zhang, X. Ning, and W. Guo, “Experimental investigation of the thermal control effects of phase change material based packaging strategy for on-board permanent magnet synchronous motors,” Energy Convers. Manag., vol. 123, pp. 232–242, Sep. 2016, doi: 10.1016/j.enconman.2016.06.045.

[79] C. R. Hartsfield, T. E. Shelton, B. O. Palmer, and R. O'Hara, "All-Metallic Phase Change Thermal Management Systems for Transient Spacecraft Loads," J. Aerosp. Eng., vol. 33, no. 4, p. 04020039, Jul. 2020, doi: 10.1061/(ASCE)AS.1943-5525.0001150.

[80] C. R. Raj, S. Suresh, R. R. Bhavsar, V. K. Singh, and K. A. Govind, "Influence of fin configurations in the heat transfer effectiveness of Solid solid PCM based thermal control module for satellite avionics: Numerical simulations," J. Energy Storage, vol. 29, p. 101332, Jun. 2020, doi: 10.1016/j.est.2020.101332.

[81] K. Kansara, V. K. Singh, R. Patel, R. R. Bhavsar, and A. P. Vora, "Numerical investigations of phase change material (PCM) based thermal control module (TCM) under the influence of low gravity environment," Int. J. Heat Mass Transf., vol. 167, p. 120811, Mar. 2021, doi: 10.1016/j.ijheatmasstransfer.2020.120811.

[82] Y. Xu, J. Wang, and Z. Yan, "Experimental investigation on melting heat transfer characteristics of a phase change material under hypergravity," Int. J. Heat Mass Transf., vol. 181, p. 122004, Dec. 2021, doi: 10.1016/j.ijheatmasstransfer.2021.122004.

[83] Y. Xu, J. Wang, and Z. Yan, "Experimental investigation on melting heat transfer characteristics of a phase change material under hypergravity," Int. J. Heat Mass Transf., vol. 181, p. 122004, Dec. 2021, doi: 10.1016/j.ijheatmasstransfer.2021.122004.

[84] R. Kothari, S. K. Sahu, S. I. Kundalwal, and S. P. Sahoo, "Experimental investigation of the effect of inclination angle on the performance of phase change material based finned heat sink," J. Energy Storage, vol. 37, p. 102462, May 2021, doi: 10.1016/j.est.2021.102462.

[85] K. Kansara and V. K. Singh, "Effect of heat source direction on the thermal performance of phase change material (PCM) based thermal control module (TCM) under the influence of low gravity environment," Int. Commun. Heat Mass Transf., vol. 128, p. 105615, Nov. 2021, doi: 10.1016/j.icheatmasstransfer.2021.105615.

[86] Y. He, Y. B. Tao, and H. Ye, "Periodic energy transmission and regulation of photovoltaic-phase change material-thermoelectric coupled system under space conditions," Energy, vol. 263, p. 125916, Jan. 2023, doi: 10.1016/j.energy.2022.125916.

[87] S. K. Saha and P. Dutta, "Role of Melt Convection on the Thermal Performance of Heat Sinks with Phase Change Material," in 2008 10th Electronics Packaging Technology Conference, Dec. 2008, pp. 539–544. doi: 10.1109/EPTC.2008.4763489.

[88] G. Quinn, J. J. Stieber, R. B. Sheth, and T. Ahlstrom, “Phase Change Material Heat Sink for an International Space Station Flight Experiment,” undefined, 2015, Accessed: Jan. 13, 2022. [Online]. Available: https://www.semanticscholar.org/paper/Phase-Change-Material-Heat-Sink-for-an-Space-Flight-Quinn-Stieber/b496376d9b84e5d2ce69e3ee10d2feea5b2efe8a

[89] Z. Wang, Z. Zhang, L. Jia, and L. Yang, “Paraffin and paraffin/aluminum foam composite phase change material heat storage experimental study based on thermal management of Li-ion battery,” Appl. Therm. Eng., vol. 78, pp. 428–436, Mar. 2015, doi: 10.1016/j.applthermaleng.2015.01.009.

[90] C. R. Raj, S. Suresh, R. R. Bhavsar, V. K. Singh, and K. A. Govind, “Influence of fin configurations in the heat transfer effectiveness of Solid solid PCM based thermal control module for satellite avionics: Numerical simulations,” J. Energy Storage, vol. 29, p. 101332, Jun. 2020, doi: 10.1016/j.est.2020.101332.

[91] B. Wu, P. Li, F. Zhang, and F. Tian, “A novel phase change material-based heat sink with an orthotropic plate to enhance the temperature field uniformity for avionics,” J. Mech. Sci. Technol., vol. 35, no. 5, pp. 2237–2246, May 2021, doi: 10.1007/s12206-021-0440-4.

CHAPTER TWO

TRANSIENT THERMAL PERFORMANCE ENHANCEMENT OF PHASE CHANGE MATERIAL (RT82) THROUGH NOVEL PIN ARRANGEMENTS UNDER VARIED GRAVITY CONDITIONS

This Chapter is based on my published work as the primary author in Numerical Heat Transfer, Part A: Applications – An International Journal of Computation and Methodology. Full citation below:

Junaid Khan, Inderjot Kaur, Youssef Aider, Heejin Cho, Seungdeog Choi & Prashant Singh (2023) Transient thermal performance enhancement of phase change material (RT82) through novel pin arrangements under varied gravity conditions, Numerical Heat Transfer, Part A: Applications, DOI: 10.1080/10407782.2023.2198738

Abstract: Phase change materials (PCMs) are an effective medium for thermal management of avionics because of their ability to absorb, store, and release high heat loads while operating within narrow temperature range in confined spaces. Despite hosting several benefits, PCM systems suffer from low thermal conductivity issue. Strategically placed fins in a volume filled with PCM has the potential to significantly improve the transient thermal performance of PCMs by improving the overall thermal conductivity and providing enhanced heat transfer surface area. Furthermore, avionics can be subjected to varying gravity conditions during flight that can have significant influence on the overall thermal performance of PCMs. This emphasizes the need to characterize the PCM performance under various gravity conditions that can impart different buoyancy induced effects in a confined system. To this end, numerical investigation to study the melting characteristics of PCM-fin configuration subjected to three different gravity conditions, i.e., (a) microgravity, (b) terrestrial gravity, and (c) hypergravity, is conducted. The influence of these three conditions on the performance of PCM-fin combination configuration is investigated and finally the temperature field, melt fraction, and melting time is reported. The performance of PCM-fin system is compared with the corresponding PCM-only configuration to highlight the benefits of adding fins under each investigated gravity condition.

Keywords: avionics; storage media; triplex tube heat exchanger

1. INTRODUCTION

PCMs are an effective thermal energy storage (TES) media because they can store large amount of heat at near-isothermal conditions due to inherent high latent heat of fusion. PCMs are currently employed in several engineering applications [1-4]. The present study is based on their application

in avionics thermal management [5]. Modern day electronic devices installed in aircrafts, artificial satellites, and spacecrafts are highly sophisticated which require efficient thermal management solutions to maintain the temperature within permissible limits. PCMs offer high energy storage density and the ability to absorb or release large heat loads while operating within narrow temperature range. The operating temperature can be decided based on the safe temperature levels the electronic components can withstand. The high latent heat of fusion enables the usage of PCMs in compact volumes, which is suitable for miniaturized modules and for constraints of payload mass/volume. The above discussed merits make PCMs very promising candidates for thermal management of avionics subjected to flexible duty cycles.

Several investigations have been conducted in the past to characterize the thermal performance of the PCMs. Joneidi et al. [6] experimentally investigated the effect of heat flux and inclination angle on the melting characteristics of RT35 filled in a rectangular enclosure. The total melting time decreased with increasing heat flux inputs and augmented with increasing heated side's inclination angle. Conduction was the dominant mode of heat transfer during early stages of melting process, whereas the convection mechanism became substantial when the PCM melted. Soodmand et al. [7] numerically analyzed the melting and solidification process of polyethylene glycol 1500 in rectangular, triangular, and cylindrical enclosures. Rectangular and triangular enclosures had the fastest melting due to the presence of sharp angles. Solidification was dominated by the conduction process whereas both conduction and convection had significant role during the melting process. Tan et al. [8] analyzed the buoyancy-driven convection for constrained melting of PCM in a spherical capsule. Buoyancy-driven convection grew stronger in later stages of melting resulting in faster melting in the top regions of the sphere as compared to the bottom zone.

The PCMs have been investigated both experimentally and numerically in various physical configurations such as cylindrical, spherical, triangular, and rectangular enclosures. The effect of the inclination angle on the melting and solidification processes has been analyzed as well. While the application of PCMs is promising, their wide-scale employment in real-world operations is significantly challenged by their low thermal conductivity which increases the charging and discharging time of the PCM system [9]. This drawback of the PCMs can be offset by using high thermal-conductivity filler materials such as metal-foams, carbon-fibers, nanoparticles, and pin-

fins. Amongst these filler materials, fins have gained significant attention in the past to augment heat transfer in several applications such as turbine blade cooling [10] and electronics cooling [11] because of their ability to provide high heat transfer, simple design, and ease of manufacturing. Recently, Zhao et al. [12] conducted experimental investigation to evaluate the benefits of using pin-fins in receiver tubes of parabolic trough solar air collectors. For the investigated range of the air flow rate, energy efficiency in the finned tube was higher than that of the corresponding smooth tube. Gong et al. [13] introduced pin-fin arrays in the absorber tube of the parabolic trough solar collector and reported the average Nusselt number increment of up to 9% at a representative geometrical parameter combination of pin-fin arrangement. Several other researchers have investigated the potential of using pin-fins in absorber tubes [14,15]. Kateshia and Lakhera [16] analyzed the performance of the solar still integrated with PCM reservoir and aluminum pin-fin inserts used for solar desalination of brackish water to generate freshwater. The total accumulated productivity, energy efficiency, and exergy efficiency was significantly improved as compared to the conventional solar still. Fins can have longitudinal, straight, annular, or tapered geometries and they are typically welded to the PCM-filled casing. The fins [17] accelerate heat transfer rate by enhancing surface area for heat transfer between the PCM and enclosure casing and they also improve the structural integrity of the PCM module. Ashraf et al. [18] optimized the passive cooling system with PCM using extruded circular and square finned surfaces arranged in staggered and inline fashion. The thermal performance of circular inline PCM-based heat sink was the best amongst the investigated configurations. Kamkari and Shokouhmand [19] performed a detailed experimental investigation of the melting characteristics of phase change material in an isothermally heated rectangular enclosure and also studied the influence of the fin inserts. The melting rate was reported to be higher above the fin-surfaces due to formation of vortex and chaotic motions in the liquid PCM. In a different study, Kamkari and Groulx [20] studied the influence of number of fins and inclination angle on the thermal performance of the finned PCM-filled rectangular enclosure. The maximum heat transfer rates were observed for the finned and unfinned configurations in horizontal orientation. The decrease in inclination angle led to uniform heat transfer rates.

Triplex-tube heat exchanger (TTHX) has gained significant attention recently where the annulus section accommodates the PCM, and the heat transfer fluid (HTF) passes through the

innermost and outermost tubes [21]. Fins can be attached to the walls of these tubes to further augment the overall heat transfer in TTHX. Leong et al. [22] provided a comprehensive review of the studies focused on PCM melting rates in TTHX geometries. Yao and Huang [23] examined the effects of longitudinal triangular fins, as opposed to the traditional rectangular fins, on the solidification time of an inorganic PCM and found that the novel triangular fins decreased the solidification time by ~ 31%. The solidification performance was the best when the fins were all connected to the outermost tube of the TTHX system. Zarei et al. [24] studied the effect of several fin parameters such as the fin number, dimensions, and angle of attachment, on the melting rate of PCM. Xu et al. [25] divided the triplex tube geometry into multiple sections and conducted comprehensive storage density evaluation to determine the melting performance of the TTHX geometry. Eslamnezhad and Rahimi [26] modified the standard TTHX model proposed by Al-Abidi et al. [27] by providing eccentricity to the center of the middle tube with respect to the other two tubes and fin orientation. Modified configurations decreased the melting time of the PCM. The geometrical parameters of TTHX have significant impact on the melting and solidification performance, and optimization of these parameters can potentially improve the efficiency of the heat exchanger.

Operating gravitational acceleration values also have significant influence on the melting characteristics of the PCM because of the buoyancy-induced effects in the molten PCM zone. Results obtained in laboratory tests conducted under the normal terrestrial gravity (1g) cannot be scaled directly to varying gravity conditions because of the considerable change in the thermal transport dynamics. Spacecrafts and launch vehicles are subjected to microgravity conditions (< 1 g) in space and hypergravity (>1g) during launch and re-entry. The transient thermal performance of PCMs should be evaluated for varying gravity conditions. The limited literature on this issue suggests that the melting rates of PCM are inhibited under microgravity and accelerated during hypergravity conditions.

Xu et al. [28] investigated the melting properties of n-docosane under hypergravity (2g, 4g, and 6g) with varying heat fluxes. Hypergravity strengthened the convection in the enclosure and led to accelerated melting with increasing hypergravity values at a fixed heat flux. Ding et al. [29] numerically investigated the melting behavior of PCM and metal foam combination configuration with hypergravity values in the range of 1g and 10g. Buoyancy-induced effects were

enhanced with increasing hypergravity value and consequently the heated wall temperature decreased. The velocity of the molten PCM showed increment of about 10 times as the hypergravity increased from 1g to 10g, however, the influence on the overall average liquid fraction trend with respect to time was not very profound. Kansara and Singh [30] studied the melting and solidification characteristics of hexadecane filled in a pin-fin based enclosure subjected to different microgravity conditions (0.5g, 0.1g, 0.05g, 0.025g, and 0.0125g) for two net heat flow directions – (a) in the direction of gravitational acceleration, and (b) opposite to the gravitational acceleration. The solidification process was reported to be not significantly impacted by the direction of net heat flow with respect to the gravity.

The discussion presented thus far highlights the advantages of using finned TTHX configuration in improving the overall heat transfer rates of the PCM. Very few studies address the influence of microgravity and hypergravity conditions for PCMs enclosed in such advanced heat exchanger designs. Further investigations are needed to gain thorough understanding of the behavior of TTHX with PCM packed in the middle tube under varying gravity values. To this end, PCM melting in triplex tube configurations is numerically investigated in this study under different gravity conditions (0.1g, 1g, and 1.5g), and the resulting temperature contours and streamlines are analyzed. Two configurations of the TTHX model are numerically investigated- (a) baseline (PCM without fin) configuration and, (b) finned (PCM + fin) configuration, under isothermal conditions imposed on the heated walls.

2. GEOMETRICAL DETAILS OF THE INVESTIGATED CONFIGURATIONS

The TTHX geometry investigated in the present study as shown in Fig.2.1 was adopted from Mat et al. [31]. The inner tube radius (r_i) was 25.4 mm with a thickness of 1.2 mm, middle (r_m) and outer tube radii (r_o) were 75 mm and 100 mm, respectively, with wall thicknesses of 2 mm each. Both baseline and finned TTHX had heat transfer fluid (HTF) passing through the inner and outer tubes whereas the annulus (middle tube) was packed with PCM RT-82 (Rubitherm GmbH). Equally spaced fins of length 42 mm and thickness 1mm were attached to both walls of the inner tube extending into the PCM annulus for the finned case (Fig. 2.1b). The tubes in both the heat exchangers were made of copper. The thermo-physical properties of the PCM material and copper are provided in Table 2.1.

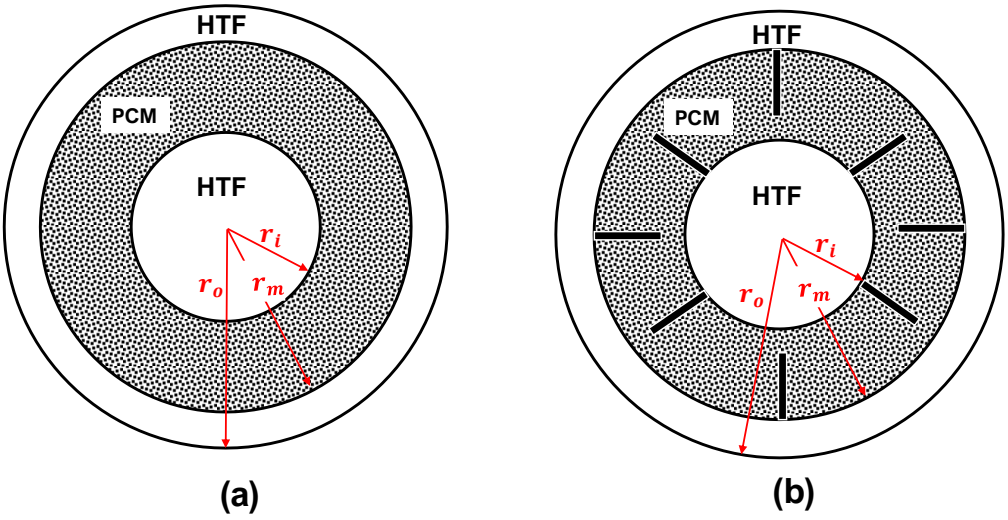

Fig.2.1. Physical configurations of the triplex tube heat exchanger (TTHX) model for (a) baseline configuration without fins and (b) finned configuration

Table 2.1. Thermo-physical properties of PCM and Copper

Property	**RT82**	**Copper**
Density of PCM, solid, $\boldsymbol{\rho_s}$ (kg/m^3)	950	8,978
Density of PCM, liquid, $\boldsymbol{\rho_l}$ (kg/m^3)	770	-
Specific heat capacity, $\boldsymbol{c_{p_l}}$, $\boldsymbol{c_{p_s}}$	2,000	381
Latent heat of fusion, L (J/kg)	176,000	-
Melting temperature, T_m (K)	343.15 –	-
Thermal conductivity, k (W/mK)	0.2	388
Thermal expansion coefficient, $\boldsymbol{\beta}$	0.001	-
Dynamic viscosity, μ (kg/ms)	0.035	-

3. GOVERNING EQUATIONS

The melting process of PCM was modeled as laminar, unsteady, and incompressible. Thermophysical properties such as specific heat capacity, thermal conductivity and viscosity were considered constant in the analysis. The buoyancy-induced effects due to density variations were modelled by invoking the Boussinesq approximation.

The continuity, momentum and energy transport equations are given as:

$$\nabla.(\rho\vec{u}) = 0 \qquad (1)$$

$$\rho\frac{\partial\vec{u}}{\partial t} + \rho(\vec{u}.\nabla)\vec{u} = -\nabla p + \mu\nabla^2\vec{u} + \rho\vec{g}\beta(T - T_l) - S\vec{u} \qquad (2)$$

$$\frac{\partial}{\partial t}(\rho H) + \nabla.(\rho\vec{u}H) = \nabla.(k\nabla T) \qquad (3)$$

where, ρ is the density of the PCM, u is the field velocity, μ is the dynamic viscosity, g is the gravitational acceleration, k is the thermal conductivity.

Enthalpy H can be expressed as follows:

$$H = h + \Delta H \qquad (4)$$

where h is the sensible enthalpy given as:

$$h = h_{ref} + \int_{T_{ref}}^{T} c_p dT \qquad (5)$$

In Eq. 5, h_{ref} is the reference enthalpy at the reference temperature T_{ref}, and c_p is the specific heat, ΔH is the latent heat content that changes between 0 (solid) and L (liquid), which is the latent heat of the PCM. The liquid fraction, γ, that is generated during the phase change between solid

and liquid state when the temperature 'T' lies between T_l and T_s (i.e., $T_l > T > T_s$) is given as:

$$\gamma = \frac{\Delta H}{L} \tag{6}$$

where the value of γ varies as:

$$\gamma = \begin{cases} 0\,, & if\ T < T_s \\ 1, & if\ T > T_l \\ \dfrac{(T - T_s)}{(T_l - T_s)}, & if\ T_l > T > T_s \end{cases} \tag{7}$$

In Eq. 7, T_s and T_l represent the solidus and liquidus temperatures, respectively. The temperature below which the PCM remains solid is referred to as solidus temperature, whereas the temperature beyond which the PCM remains entirely as liquid is defined as liquidus temperature.

The source term in the momentum equation 'S' is defined as:

$$S = \frac{C(1-\gamma)^2}{\gamma^3 + \varepsilon} \tag{8}$$

where the mushy zone constant C reflects the mushy zone morphology and determines how steeply the velocity is reduced to zero when the material solidifies. Typically, the value of 'C' is a large number varying between 10^4 and 10^7, however, based on study by Mat et al. [31] where the authors studied similar configuration with RT82, C = 10^5 was considered in the present study. The constant ε has a small positive value and is introduced for numerical stability.

4. COMPUTATIONAL DOMAIN, NUMERICAL MODELING, MESH GENERATION, INITIAL AND BOUNDARY CONDITIONS

The numerical simulations were conducted using commercial finite volume-based solver ANSYS FLUENT (2022 R1). Phase-change was modeled through an enthalpy-porosity formulation in which the liquid-solid front is not tracked explicitly but is treated as porous zone with porosity

equal to the liquid fraction. Fig.2.2a shows the schematic of the two-dimensional computational domain simulated in the present study. Since the gravity was acting in the radial direction, the buoyancy-induced effects were assumed to be independent of the axial location. Therefore, two-dimensional domain shown in Fig.2.2 was adopted for the simulations in the current study. Only half of the channel was simulated due to symmetry of the tube at the mid-plane parallel to the gravity direction. Thickness of the wall was taken into consideration when modelling the computational domain. Assuming that the heat transfer fluid (HTF) flowing in the inner and outer tube of the TTHX was maintained at constant temperature, isothermal boundary conditions ($T_W = T_{HTF}$) were imposed on the inner and outer walls of the PCM annulus. Fig.2.2b shows the mesh generated in the finned configuration. The mesh was predominantly composed of the quadrilateral elements with refinements near the heated and the interface walls.

During melting, the initial temperature of the PCM and solid was 300.15 K and the heated wall temperature ($T_W = T_{HTF}$) was maintained at 363.15 K. These conditions were similar to the one adopted by Mat et al. [31] in their experimental and numerical investigation. Coupled boundary condition was imposed on the interface walls in which temperature and heat flux continuity was maintained. Mat et al. [31] performed simulations on finned TTHX with normal terrestrial gravity acceleration (1g) and reported that the results were independent of the adopted grid size and time step when the number of elements were 17,956 and time step was 0.5s.

Based on the reported values in [31], 18,292 elements and 0.5s time step size was adopted in the present study which provided good agreement with the results reported in [31] as discussed in the next section. The liquidus temperature of 355.15K was chosen as the operating temperature for Boussinesq equation and the density was equal to the liquid density. The baseline and finned configurations were simulated under different gravity conditions, viz. 0.1g, 1g and 1.5g. The pressure-velocity coupling was solved using the SIMPLE algorithm and PRESTO scheme was used for pressure interpolation. The convergence criteria for continuity, velocities, and energy was based on residuals reaching a value ~ 10^{-3}, 10^{-5}, and 10^{-7}, respectively.

5. RESULTS AND DISCUSSION

This section discusses the melting behavior of PCM in the baseline and finned configurations

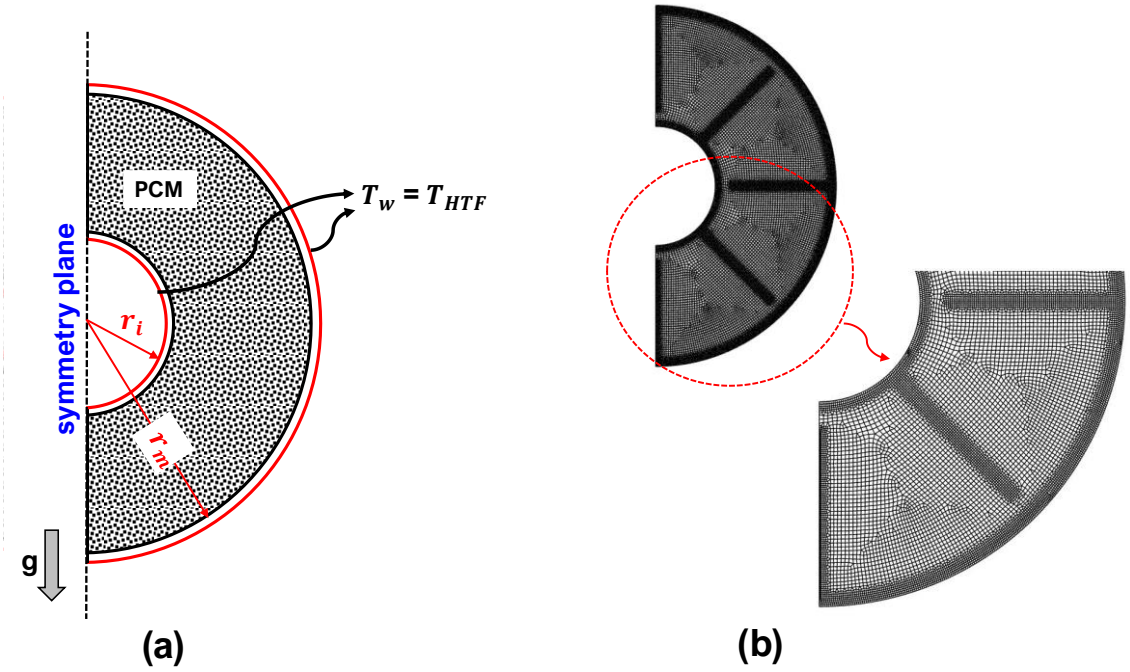

Fig.2.2 (a) Schematic of the 2D computational domain for TTHX configuration simulated in the present study (boundary conditions shown for melting process), and (b) structured mesh generated with refinements near the walls

subjected to 0.1g, 1g, and 1.5g gravity conditions. The contours demonstrating the temporal evolution of temperature and liquid fraction field are presented and thoroughly discussed. Buoyancy-induced motion in the molten PCM is highlighted and its role in the thermal transport is presented. Finally, the liquid fraction temporal evolution is presented to facilitate a discussion on the advantage of the finned configuration with respect to the baseline case.

Computational Model Validation: Averaged Liquid Fraction Temporal Evolution

The temporal variation of liquid fraction for the baseline and finned configurations subjected to gravitational acceleration of 1g is presented against the results reported by Mat et al. [31] in Fig.2.3. The trends obtained in the present study for both the configurations agreed well with that presented in [31] which established the fidelity of the current numerical set-up.

Average Temperature Validation

The variation of average temperature during the melting process of RT-82 at the acceleration of 1g was validated with the trends of Mat et al. [31] as shown in Fig.2.4. Moreover, the local temperature field at different time stamps was also validated against [31] and the results are shown in Fig.2.5 and Fig.2.6 for the baseline and finned TTHX configurations, respectively. After establishing the accuracy of the current numerical set-up by obtaining good qualitative and quantitative agreement with previous study of Mat et al. [31], further simulations for microgravity and hypergravity conditions were conducted.

5.1 TEMPERATURE CONTOURS

Baseline configuration

The progression of the temperature contours for the melting of PCM in baseline configuration with respect to reference time (T_{ref}) under different gravity values is shown in Fig.2.7. In Fig.2.7, T_{ref} was the time taken to completely melt the PCM at terrestrial gravity conditions (1g). Also shown are the streamlines at four reference time stamps corresponding to 25%, 50%, 75%, and 100% of T_{ref}, to present the motion of melted PCM. Initially, the melting

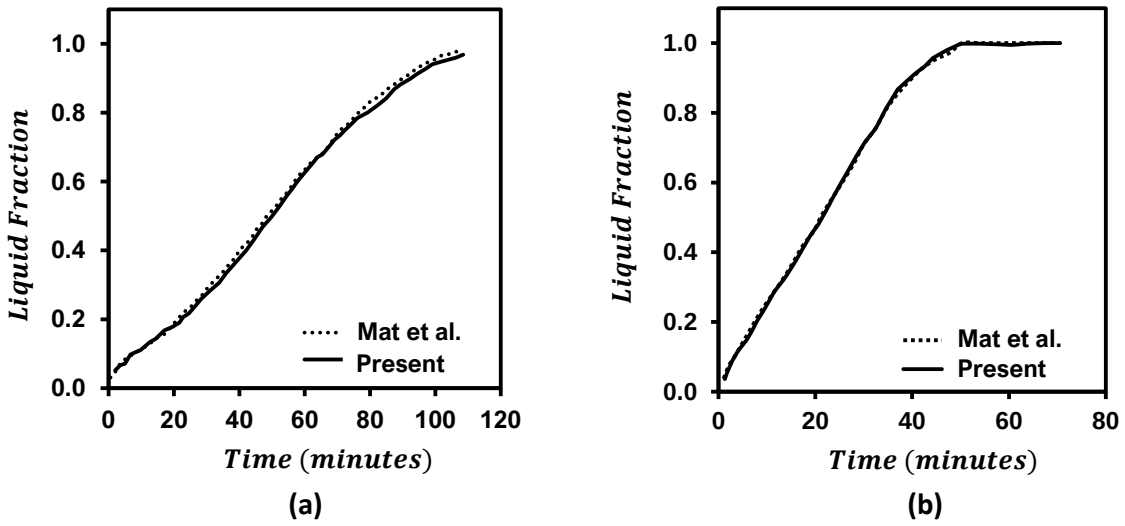

Fig.2.3 Validation of liquid fraction versus time results with Mat et al. [31] under 1g gravity condition for (a) baseline configuration and (b) finned configuration

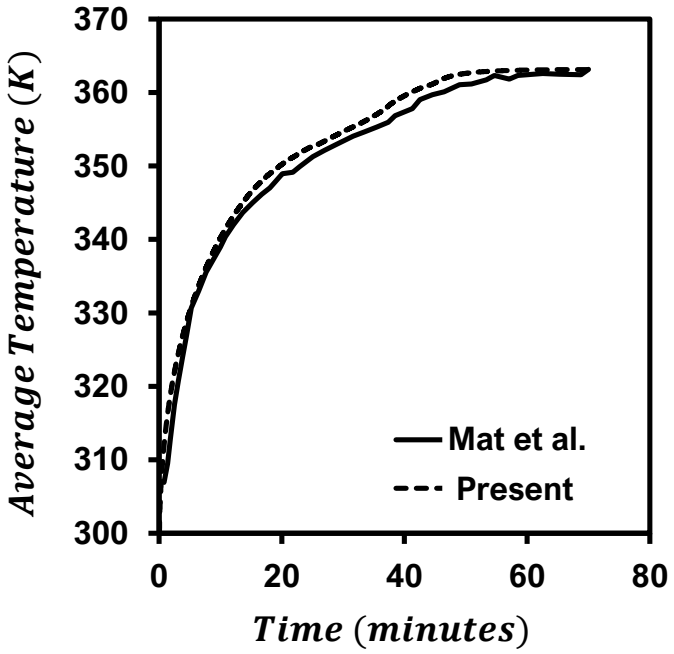

Fig.2.4 Validation of average temperature versus time results with Mat et al. [31] under 1g gravity condition for finned configuration

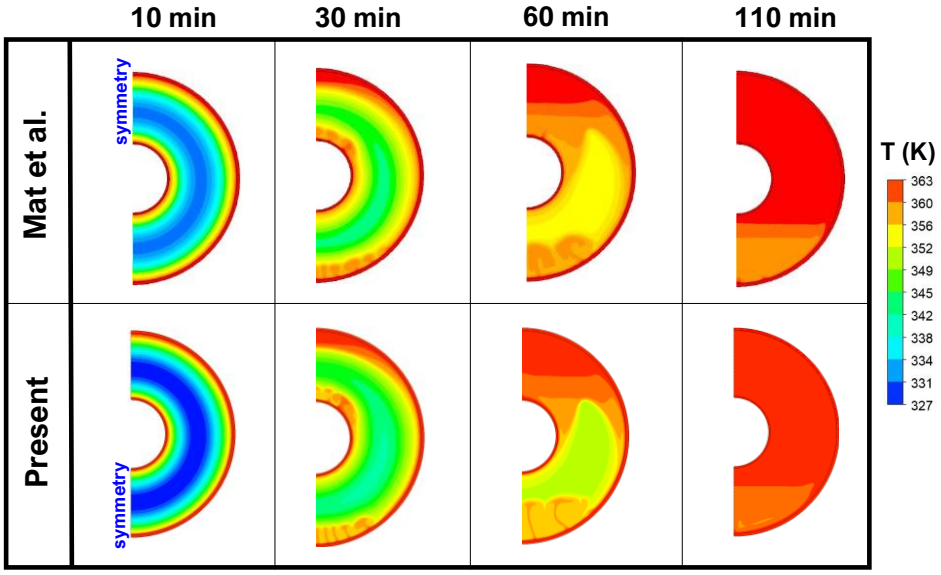

Fig.2.5 Validation of local temperature field with Mat et al. [31] under 1g gravity condition for the baseline configuration

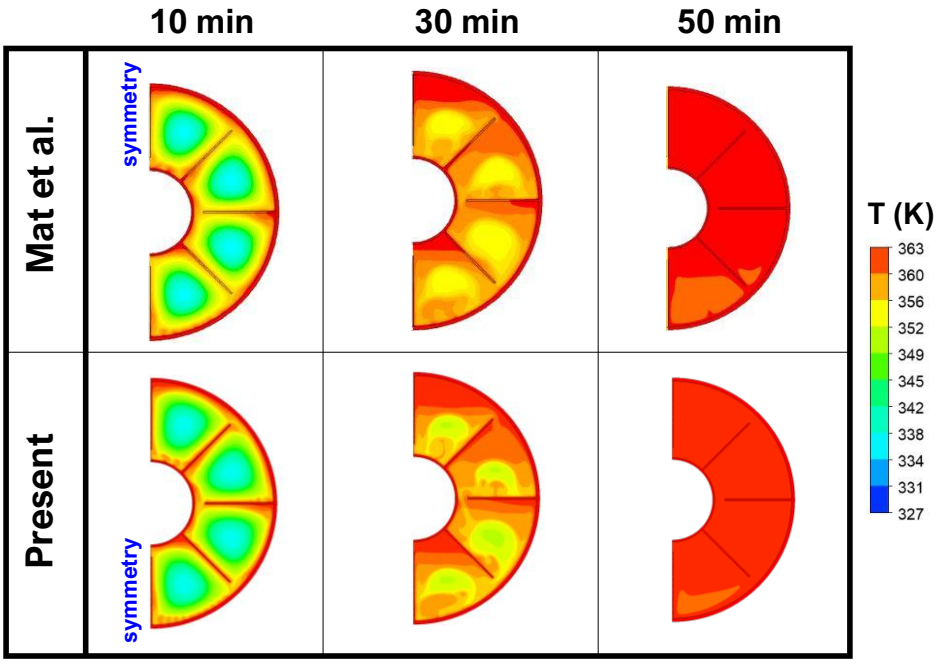

Fig.2.6 Validation of local temperature field with Mat et al. [31] under 1g gravity condition for the finned configuration

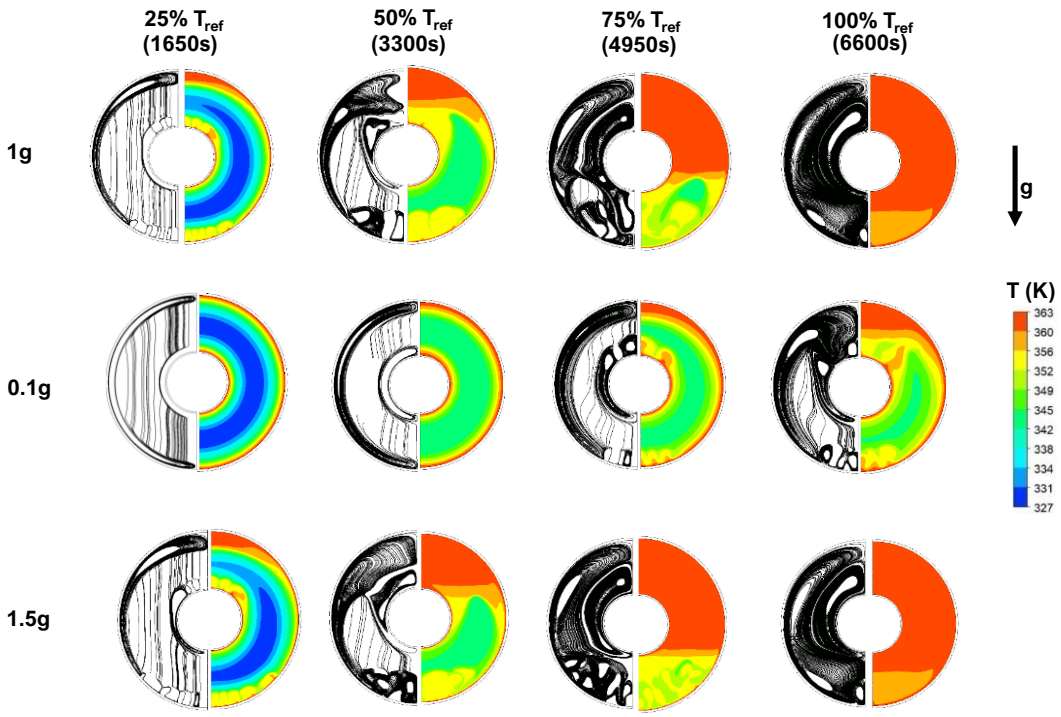

Fig.2.7 Progress of temperature contours and streamlines at various stages of melting under varying gravity conditions for the baseline configuration

occurred due to heat transfer between the heated tube walls and PCM in solid state and it was mainly conduction dominated.

Thin layers of liquid PCM were formed near the inner and outer casing walls due to conduction. Continuous single elongated convection cells conforming the inner and outer walls were observed for microgravity at 25% and 50% of the T_{ref} but discrete pockets of fluids were visible at the 75% of T_{ref} on the upper surface of the inner tube. For higher gravity value of 1.5g, discrete chaotic streamlines were visible even at 50% of T_{ref} suggesting stronger buoyant forces as compared to microgravity condition. As the melting progressed, the streamlines in the annulus further intensified engulfing the upper region of the TTHX geometry in all three configurations. The upper half of TTHX demonstrated higher PCM temperature at 75% of T_{ref} under 1g and 1.5g conditions. The streamlines showed the formation of small convection cells in lower regions of the geometry at 50% and 75% of T_{ref}, especially for 1g and 1.5g gravity conditions which finally merged into larger convection pockets as the process progressed towards complete melting of the PCM.

Finned configuration

Fig.2.8 shows the progressive temperature contours for the finned configuration under different gravity values for 25%, 50%, 75% and 100% value of T_{ref}, which was the time taken to completely melt PCM at terrestrial gravity conditions (1g). Fins directly attached on the TTHX inhibited the liquid PCM from rising to the upper part of the geometry freely and restricted the flow within the respective unit cells formed between two adjacent fins. However, the clearance present between the fin tips and the enclosure walls offered limited passage for melted PCM to flow across different cells. Since the addition of fins divided the geometry into multiple unit cell geometries, the streamlines showed a pattern of wrapping around the fins in each unit cell. The intensity of the formation of convection cells was minimized under microgravity and maximized under hypergravity as it can be observed at 50% and 75% stages of melting with respect to T_{ref}, especially

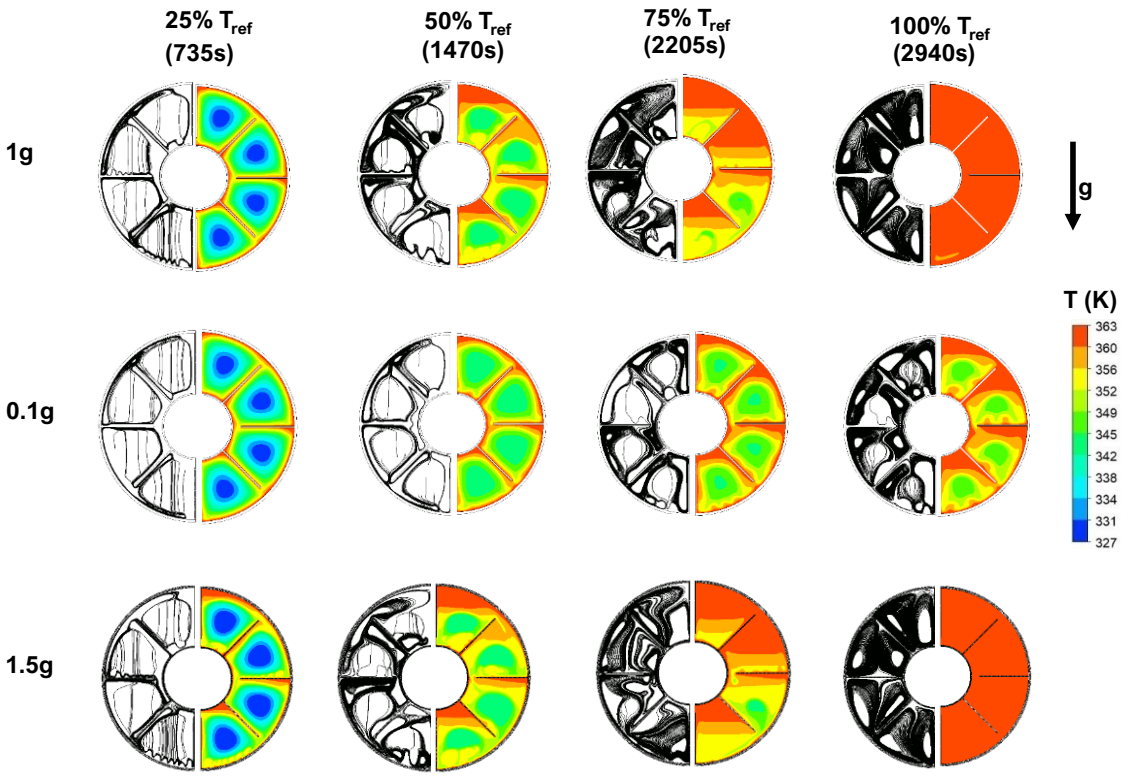

Fig.2.8 Progress of temperature contours and streamlines at various stages of melting under varying gravity conditions for the finned configuration configurations due to natural convection under all gravity conditions.

near the outer walls of the upper half. Addition of fins promoted the formation of numerous convection cells in various zones of the PCM, thereby fostering the melting at multiple locations and causing a decrease in melting time of the PCM relative to the baseline case.

5.2 LIQUID FRACTION CONTOURS

Baseline configuration

Fig.2.9 illustrates the progress of liquid fraction contours of the baseline geometry under different gravity conditions. The time taken to completely melt RT-82 in baseline TTHX configuration at '1g' gravity condition was taken as the reference time (T_{ref}) which was 6600s (110 min). As stated earlier, the heat transfer was initiated between the heated tube walls and the solid PCM by conduction due to which liquid PCM was observed to be aligned along the walls of inner and outer tubes. The thickness of the melt zone in the upper region was the highest under hypergravity (1.5g), followed by terrestrial gravity conditions. On the other hand, PCM melt zone showed uniform growth along the periphery walls of the enclosure until 50% of the T_{ref} under microgravity conditions. The liquid fraction proportion increased significantly in the upper half of the TTHX. Well-defined convection cells were observed under hypergravity at 75% value of T_{ref} wherein only 15% of the un-melted PCM remained at this stage. For microgravity, nearly 35% of the un-melted PCM remained at 100% of T_{ref}. This suggests that the buoyancy-driven flows strengthen under hypergravity conditions and lead to faster melting of the phase-change material.

Finned configuration

The progression of liquid fraction contours for the finned configuration at various stages of reference time under varying gravity conditions is shown in Fig.2.10. The reference time (T_{ref}) for the finned TTHX geometry was 2940s (49 minutes). A thin liquid layer appeared at the interface between the fins and solid PCM on account of enhanced conduction facilitated by increased surface contact by the fins. Melting occurred within the unit cells in a vortex-like pattern. Augmented natural convection heat transfer for hypergravity condition resulted in 60% of the melting at 50% of T_{ref}. However, due to the absence of strong buoyant forces at microgravity, 21% PCM by volume still remained un-melted at 100% of T_{ref}. Lower local temperature zones in Fig.2.8 were characterized by the lower liquid fraction values in each unit cell of the finned TTHX configuration

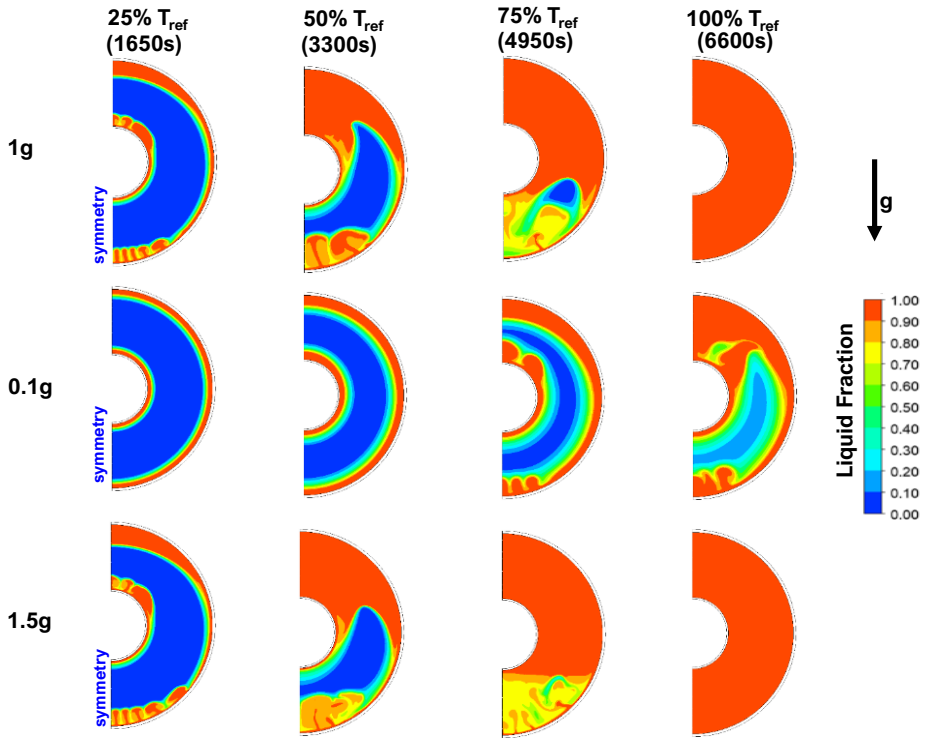

Fig.2.9 Progress of liquid fraction contours at various stages of melting under varying gravity conditions for the baseline configuration

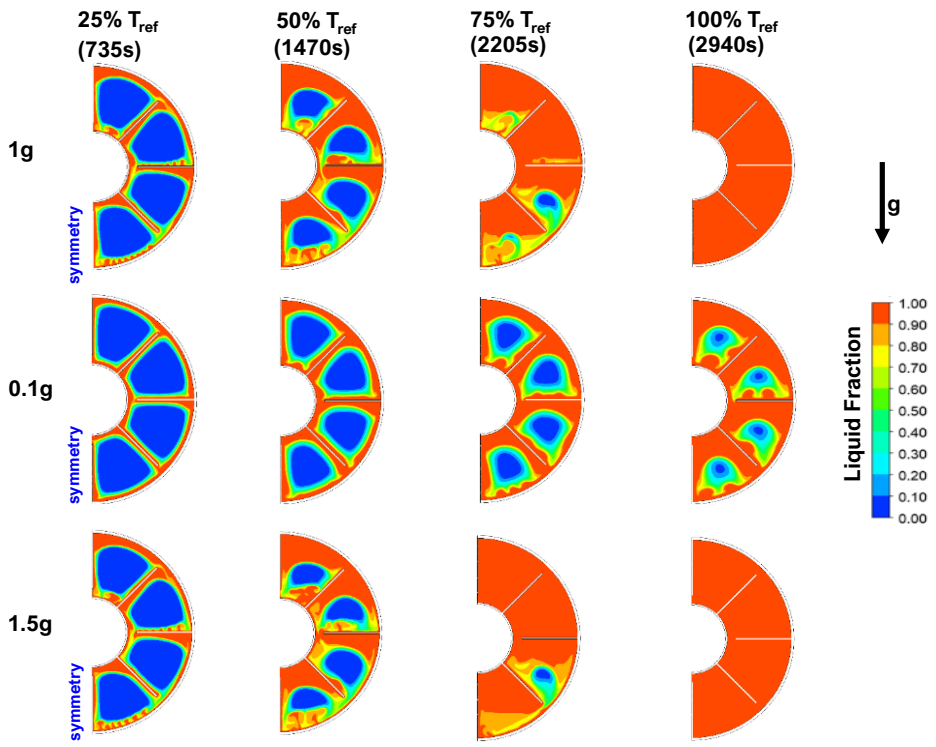

Fig.2.10. Progress of liquid fraction contours at various stages of melting under varying gravity conditions for the finned configuration

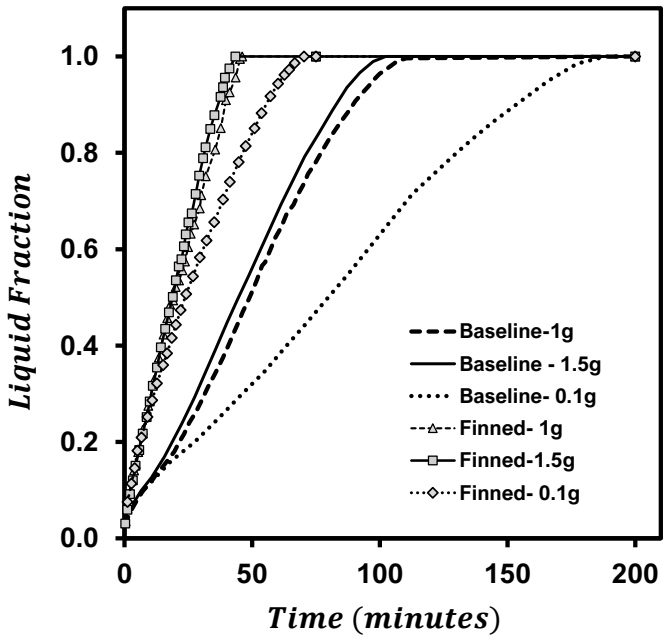

Fig.2.11. Liquid fraction versus time variation for baseline and finned configurations of TTHX under varying gravity conditions during melting

in Fig.2.10.

5.3 COMPARISON OF LIQUID FRACTION VERSUS TIME TRENDS UNDER DIFFERENT GRAVITY CONDITIONS DURING MELTING OF RT-82

The temporal evolution of PCM liquid fraction at different gravity conditions is shown in Fig.2.11. For the baseline configuration, the melt times under 0.1g, 1g and 1.5g conditions were 188 minutes, 110 minutes, and 102 minutes, respectively. For the finned TTHX configuration, the melt times were 70 minutes, 49 minutes, and 43 minutes under 0.1g, 1g and 1.5g conditions, respectively.

The melting times of the finned TTHX were lower than the corresponding baseline configuration for all the investigated cases. For each configuration, however, the reduction in melting time for change of gravity from 0.1g to 1g was much more substantial than that from 1g to 1.5g. The melting time required by PCM at hypergravity (1.5g) condition was approximately 7% and 46% lower than the melting time at earth gravity (1g) and microgravity (0.1g) conditions, respectively, for baseline case. Because of buoyancy-induced convection in multiple unit cells formed by the fins, the melting time required at hypergravity (1.5g) condition was approximately 12% and 39% lower than the melting time at earth gravity (1g) and microgravity (0.1g) conditions, respectively, in finned configuration.

6. CONCLUSIONS

In the present study, the melting characteristics of phase-change material (PCM) RT-82 were numerically investigated in triplex tube heat exchanger (TTHX) subjected to three different gravitational accelerations, viz 0.1g, 1g and 1.5g. Two different TTHX configurations with isothermal conditions imposed on the heated walls were tested- (a) baseline case without fins, and (b) finned case with fins in the PCM section. Following conclusions were drawn based on the results obtained in the current study:

1. Initial melting of the PCM was dominated by heat conduction but later stages of melting were significantly impacted by the buoyancy-induced fluid motion.

2. Convection was helpful in accelerating the melting due to which the total melting times were

lower for hypergravity (1.5g) and earth gravity (1g) conditions in comparison to the microgravity conditions. For baseline configuration, the melting time required by PCM at hypergravity (1.5g) condition was approximately 7% and 46% lower than the melting time at earth gravity (1g) and microgravity (0.1g) conditions, respectively.

3. Finned TTHX supported the emergence and development of convection cells at multiple locations along with providing enhanced surface area for heat conduction, leading to the faster melting of PCM in comparison to the baseline case. For finned configuration, the melting time required by PCM at hypergravity (1.5g) condition was approximately 12% and 39% lower than the melting time at earth gravity (1g) and microgravity (0.1g) conditions, respectively.

ACKNOWLEDGEMENTS

The financial support from National Aeronautics and Space Administration (NASA) through Pass Through Entity/Prime Award No. NNH21ZHA001C, Sub-award No. 22-09-28 is greatly appreciated.

References

[1] M.R. Yazdani, A. Laitinen, V. Helaakoski, L.K. Farnas, K. Kukko, K. Saari, and V. Vuorinen, “Efficient storage and recovery of waste heat by phase change material embedded within additively manufactured grid heat exchangers,” Int. J. Heat Mass Transf., vol. 181, p. 121846, Dec 2021. DOI: 10.1016/j.ijheatmasstransfer.2021.121846.

[2] M.J. Huang, P.C. Eames, and B. Norton, “Thermal regulation of building-integrated photovoltaics using phase change materials,” Int. J. Heat Mass Transf., vol. 47, no. 12-13, pp. 2715-2733, Jun 2004. DOI: 10.1016/j.ijheatmasstransfer.2003.11.015.

[3] Y.B. Seong and J.H. Lim, “Energy saving potentials of phase change materials applied to lightweight building envelopes,” Energies, vol. 6, no. 10, pp. 5219-5230, Oct 2013. DOI: 10.3390/en6105219.

[4] Z. Chen, X. Li, J. Zhang, L. Ouyang, Y. Wang, and Y. Jiang, “Simulation and analysis of heat dissipation performance of power battery based on phase change material enhanced heat transfer variable fin structure,” Numer. Heat Transfer, Part A: Appl., vol. 80, no. 11, pp. 535-555, Dec 2021. DOI: 10.1080/10407782.2021.1959834.

[5] A.J. Fossett, M.T. Maguire, A.A. Kudirka, F.E. Mills, and D.A. Brown, “Avionics passive cooling with microencapsulated phase change materials,” J. Electron. Packag., vol. 120, no. 3, pp. 238-242, Sep 1998. DOI: 10.1115/1.2792628.

[6] M.H. Joneidi, M.J. Hosseini, A.A. Ranjbar, and R. Bahrampoury, “Experimental investigation of phase change in a cavity for varying heat flux and inclination angles,” Exp. Therm. Fluid Sci., vol. 88, pp. 594-607, Nov 2017. DOI: 10.1016/j.expthermflusci.2017.07.017.

[7] A.M. Soodmand, S. Nejatbakhsh, H. Pourpasha, H. Aghdasinia, and S.Z. Heris, “ Simulation of melting and solidification process of polyethylene glycol 1500 as a PCM in rectangular,

triangular, and cylindrical enclosures," Alex. Eng. J., vol. 61, no. 11, pp. 8431-8456, Nov 2022. DOI: 10.1016/j.aej.2022.02.011.

[8] F.L. Tan, S.F. Hosseinizadeh, J.M. Khodadadi, and L. Fan, "Experimental and computational study of constrained melting of phase change materials (PCM) inside a spherical capsule," Int. J. Heat Mass Transf., vol. 52, no. 15-16, pp. 3464-3472, Jul 2009. DOI: 10.1016/j.ijheatmasstransfer.2009.02.043.

[9] K. Lafdi, O. Mesalhy, and S. Shaikh, "Experimental study on the influence of foam porosity and pore size on the melting of phase change materials," J. Appl. Phys., vol. 102, no. 8, p. 083549, Oct 2007. DOI: 10.1063/1.2802183.

[10] T. Horbach, A. Schulz, and H.J. Bauer, "Trailing edge film cooling of gas turbine airfoils—external cooling performance of various internal pin fin configurations," J. Turbomach., vol. 133, no. 4, p. 041006, Oct 2011. DOI: 10.1115/1.4002964

[11] J. Zhao, S. Huang, L. Gong, and Z. Huang, "Numerical study and optimizing on micro square pin-fin heat sink for electronic cooling," Appl. Thermal Eng., vol. 93, pp.1347-1359, Jan 2016. DOI: 10.1016/j.applthermaleng.2015.08.105

[12] Z. Zhao, F. Bai, X. Zhang, and Z. Wang, "Experimental study of pin finned receiver tubes for a parabolic trough solar air collector," Solar Energy, vol. 207, pp.91-102, Sept 2020. DOI: 10.1016/j.solener.2020.06.070

[13] X. Gong, F. Wang, H. Wang, J. Tan, Q. Lai, and H. Han, "Heat transfer enhancement analysis of tube receiver for parabolic trough solar collector with pin fin arrays inserting," Solar Energy, vol. 144, pp.185-202, Mar 2017. DOI: 10.1016/j.solener.2017.01.020

[14] M.S. Mahmoud, A.S. Abbas, and A.F. Khudheyer, "Solar parabolic trough collector tube heat transfer analysis with internal conical pin fins," J. Green Eng., vol. 10, no. 10, pp.7422-7436, Oct. 2020.

[15] E. Bellos, C. Tzivanidis, and D. Tsimpoukis, "Optimum number of internal fins in parabolic trough collectors," Appl. Thermal Eng., vol. 137, pp.669-677, June 2018. DOI: 10.1016/j.applthermaleng.2018.04.037

[16] J. Kateshia, and V.J. Lakhera, "Analysis of solar still integrated with phase change material and pin fins as absorbing material," J. Energy Storage, vol. 35, p.102292, Mar 2021. DOI: 10.1016/j.est.2021.102292

[17] D. Dandotiya, and N.D. Banker," Numerical investigation of heat transfer enhancement in a multitube thermal energy storage heat exchanger using fins," Numer. Heat Transfer, Part A: Appl., vol. 72, no. 5, pp. 389-400, Sep 2017. DOI: 10.1080/10407782.2017.1376976.

[18] M.J. Ashraf, H.M. Ali, H. Usman, and A. Arshad, "Experimental passive electronics cooling: parametric investigation of pin-fin geometries and efficient phase change materials," Int. J. Heat Mass Transf., vol. 115, pp.251-263, Dec 2017. DOI: 10.1016/j.ijheatmasstransfer.2017.07.114

[19] B. Kamkari, and H. Shokouhmand, "Experimental investigation of phase change material melting in rectangular enclosures with horizontal partial fins," Int. J. Heat Mass Transf., vol. 78, pp. pp.839-851, Nov 2014.

[20] B. Kamkari, and D. Groulx, "Experimental investigation of melting behaviour of phase change material in finned rectangular enclosures under different inclination angles," Expt. Therm. Fluid Sci., vol. 9797, pp.94-108.

[21] A.M. Abdulateef, S. Mat, J. Abdulateef, K. Sopian, and A.A. Al-Abidi," Thermal performance enhancement of triplex tube latent thermal storage using fins-nano-phase change material technique," Heat Transf. Eng., vol. 39, no. 12, pp. 1067-1080, Jul 2018. DOI: 10.1080/01457632.2017.1358488.

[22] K.Y. Leong, S. Hasbi, and B.A. Gurunathan," State of art review on the solidification and melting characteristics of phase change material in triplex-tube thermal energy storage," J. Energy Storage, vol. 41, p. 102932, Sep 2021. DOI: 10.1016/j.est.2021.102932.

[23] S. Yao and X. Huang," Study on solidification performance of PCM by longitudinal triangular fins in a triplex-tube thermal energy storage system," Energy, vol. 227, p. 120527, Jul 2021, DOI: 10.1016/j.energy.2021.120527.

[24] M.J. Zarei, H. Bazai, M. Sharifpur, O. Mahian, and B. Shabani," The effects of fin parameters on the solidification of PCMs in a fin-enhanced thermal energy storage system," Energies, vol. 13, no. 1, p.198, Jan 2020. DOI: 10.3390/en13010198.

[25] H. Xu, N. Wang, C. Zhang, Z. Qu, and M. Cao," Optimization on the melting performance of triplex-layer PCMs in a horizontal finned shell and tube thermal energy storage unit," Appl. Therm. Eng., vol. 176, p. 115409, Jul 2020. DOI: 10.1016/j.applthermaleng.2020.115409.

[26] H. Eslamnezhad and A.B. Rahimi," Enhance heat transfer for phase-change materials in triplex tube heat exchanger with selected arrangements of fins," Appl. Therm. Eng., vol. 113, pp. 813-821, Feb 2017. DOI: 10.1016/j.applthermaleng.2016.11.067.

[27] A.A. Al-Abidi, S. Mat, K. Sopian, M.Y. Sulaiman, and A.T. Mohammad," Internal and external fin heat transfer enhancement technique for latent heat thermal energy storage in triplex tube heat exchangers," Appl. Therm. Eng., vol. 53, no. 1, pp. 147-156, Apr 2013. DOI: 10.1016/j.applthermaleng.2013.01.011.

[28] Y. Xu, J. Wang, and Z. Yan," Experimental investigation on melting heat transfer characteristics of a phase change material under hypergravity," Int. J. Heat Mass Transf., vol. 181, p. 122004, Dec 2021. DOI: 10.1016/j.ijheatmasstransfer.2021.122004.

[29] C. Ding, C. Zhang, L. Ma, and A. Sharma," Numerical investigation on melting behaviour of phase change materials/metal foam composites under hypergravity conditions," Appl. Therm. Eng., vol. 207, p.118153, May 2022. DOI: 10.1016/j.applthermaleng.2022.118153.

[30] K. Kansara, and V.K. Singh," Effect of heat source direction on the thermal performance of phase change material (PCM) based thermal control module (TCM) under the influence of low gravity environment," Int. Commun. Heat Mass Transf., vol. 128, p. 105615, Nov 2021. DOI: 10.1016/j.icheatmasstransfer.2021.105615.

[31] S. Mat, A.A. Al-Abidi, K. Sopian, M.Y. Sulaiman, and A.T. Mohammad," Enhance heat transfer for PCM melting in triplex tube with internal–external fins," Energy convers. manage., vol. 74, pp. 223-236, Oct 2013. DOI: 10.1016/j.enconman.2013.05.003.

CHAPTER THREE

COMPUTATIONAL STUDIES ON HEAT TRANSFER AUGMENTATION OF PHASE CHANGE MATERIALS IN TRIPLEX TUBE HEAT EXCHANGER WITH NOVEL ANNULAR-FIN CONFIGURATIONS

ABSTRACT

Phase Change Materials have been in use for the passive Thermal Management of Spacecraft avionics ever since the first space mission in the 1960s. However, their reversible cycles of charging and discharging which occur on account of narrow temperature fluctuations, have not been fully leveraged for thermal control applications in the Spacecraft Industry. Computationally investigating the choice of encapsulation geometries for Phase Change Materials remains a major topic of interest and challenge faced by researchers working in this field. Encapsulation geometries influence several thermal characteristics of Phase Change Materials such as their rates of melting and solidification which ultimately prove their worth as vital passive Thermal management components of spacecraft under varying gravity conditions. This study focuses on the role of finetuning the geometrical design of five novel annular Triplex Tube Heat Exchangers (TTHX) towards the optimization of melting rates of PCM. The shape, size, and placement of the constituent fins of the PCM domain are altered, and their effect is observed on the heat transfer characteristics of the PCM. Pockets within the encapsulation geometry wherein a vortex-like melting pattern of PCM can be facilitated, are identified for expedited melting characteristics. This inquiry into the efficacy of various encapsulation geometries for enhanced melting rates also adjudicates their feasibility to endure transition between regions of varying gravity conditions thus establishing the stability of passive thermal control systems. This work also explains the physics behind the melting performance enhancement and maintenance of stability under 0.1g, 1g, and 1.5g gravity conditions.

Keywords: Phase Change Materials, Encapsulation, Triplex Tube Heat Exchangers,

1.INTRODUCTION

Research on energy storage devices is the need of the hour since an efficient energy storage device mitigates the production of more energy and contributes towards energy conservation and sustainability. Moreover, these devices also aid in the thermal management of sophisticated systems such as solar photovoltaics, electronic devices, HVAC etc.[1] [2] [3] In recent times, Phase change materials have been widely recognized as an excellent energy storage technology. PCM can store and release large amounts of thermal energy during the phase change process. The storage or release of latent energy occurs under near isothermal conditions and commences after

the initiation of melting or solidification during the phase change process on account of their high latent heat of fusion.

Since a higher density of energy can be saved during latent heat storage as compared to sensible heat storage, phase change materials have become an increasingly exciting prospect in the spacecraft industry[4]. As the spacecraft avionics transitions towards increased compaction and performance, there is an escalated demand for innovative methods by which phase change materials can be employed in the heat dissipation and storage systems. This presents exciting opportunities for spacecraft industry wherein an advanced thermal management system for avionics can enable the design for reduced payload, thereby providing savings from a techno-economic perspective.

Several recent investigations have been made to evaluate the feasibility of phase change materials for thermal management applications. Notable efforts to feature PCM for spacecraft thermal management include the Hexafly International project[5], Exomars mission[6] and the NASA ISS flight experiment[7]. However, despite their excellent heat storage applications, PCM have low thermal conductivity which necessitates their incorporation with filler material which have appreciable thermal conductivity.

The NASA design handbook for PCM and energy storage devices [8] recommends the usage of filler material for efficient transfer of energy and diminishing the temperature gradient between the PCM and the heated or cooled body. Moreover, the enhanced structural integrity and effective thermal conductivity achieved after this integration is another added advantage of encapsulating PCM. Major PCM fillers usually include honeycomb structures, metallic foams, and fins. Fins can be of longitudinal, straight, annular, or tapered geometries and they are typically welded to the PCM filled casing. This study focusses on the triplex tube heat exchanger (TTHX) (as shown in Fig.3.1) configurations and enhancement of melting rate provided by the latter to the phase change materials on account of accelerated heat transfer rate facilitated by increased surface area for heat transfer between the PCM and casing. Triplex tube Heat Exchangers are an excellent means to encapsulate the PCM wherein three concentric tubes are arranged in such a way a heat transfer fluid flows isothermally through the innermost and outermost tubes whereas the PCM is present in the annulus of the TTHX.

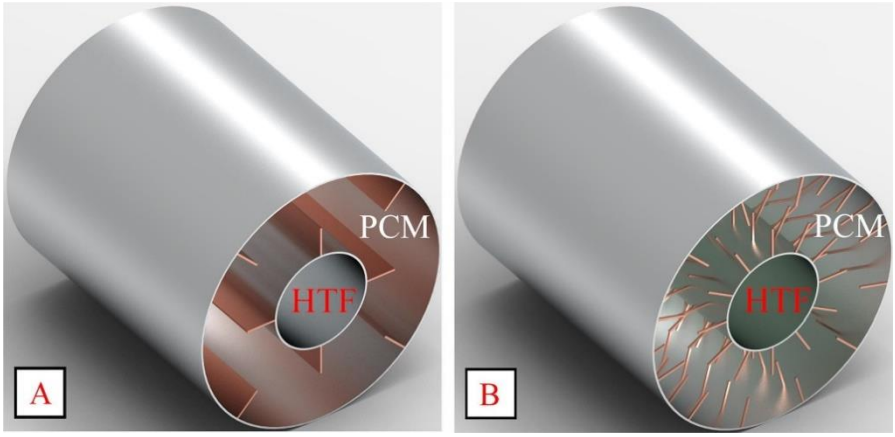

Fig.3.1 Schematic view of Triplex Tube Heat Exchanger with (A) Continuous fins and (B) Discontinuous fins [9]

The significance of encapsulation for the effective utilization of phase change materials for thermal management applications holds instrumental importance since encapsulation protect and contain the PCM, thereby preventing degradation, leakage and loss of performance. Within the scope of PCM research , these encapsulation techniques are classified into 2 broad categories viz. Microencapsulation and Microencapsulation. While the former involves enclosing the PCM within a polymer shell, the latter technique (which is also the point of focus of current research) is mainly concerned with incorporating the PCM within a large tank of container. Other lesser known techniques for encapsulation of PCM are co-precipitation , spray drying and sol-gel method. A deeper understanding of these encapsulation techniques, the importance of fillers and PCM heat convection phenomenon thus becomes a prerequisite for conducting heat transfer research concerned with phase change materials. The literature review by Leong et.al. [10] discusses the studies which focus on triplex tube thermal storage geometries for investigating PCM melting rates. Yao and Huang [11] examined the effect of using triangular fins as compared to traditional rectangular fins on the solidification time of inorganic PCM. Approximately 31% decrement in solidification time was observed while using triangular fins. In their study, it was also observed that the PCM melting in triplex tube configurations occurs in two stages wherein initially the heat transfer interaction takes place between the fins and PCM, however as the time advances, heat transfer occurs between high and low temperature PCM. In another study [12], the resulting effect on the melting rate was investigated by finetuning a of multitude of fin parameters such as the number, dimensions, and angle of attachment of the fins on the triplex tube heat exchanger. Xu et.al. [13] divided the triplex tube geometry into multiple sections and conducted comprehensive storage density evaluation to determine melting performance of the TTHX geometry.

Eslamnezhad and Rahimi [14] tweaked an eccentric model to the triplex tube model proposed by Mat et.al. [15] and bettered the melting time by almost 18% by meticulously analyzing the triplex tube model zone-wise to evaluate the best fin arrangement for accelerated melting. The work presented in this paper focus on multiple geometric configurations of pin-fin arrangements which are welded to the casing of the external and internal tube in different configurations. The angle of attachment of the fins to the tubes, tip angle of pins, placement of fins on the tubes, and number

of fins attached to the tubes are varied to obtain an optimized value of melting time for RT-82 and RT-35.

It is well established from pertinent literature that the melting rates of PCM are inhibited under microgravity and accelerated during hypergravity. However, a deeper physics behind this melting phenomenon is needed to be appreciated to enable the design for PCM melting in suitable geometries and filler configurations, and to obtain optimized melting rates. Earlier published research on gravity assisted melting do not account for natural convection. However, natural convection plays a significant role in PCM melting for constrained geometries. The work by Asako et.al.[16] is a positive step in the direction to comprehensively understand the phenomenon of gravity assisted PCM melting. This study considers the variation of solid and liquid density as the driving force which displace the solid from the center of the geometry towards the wall. It also holds an argument against the negligence of the inertial term within the generated liquid film between the solid phase and heated wall during low gravity conditions, thereby assuming a thick layer between the two under microgravity.

Li et.al. [17] further observed the increased significance in the role of natural convection as the gravity increased from 0g to 1g. Kansara and Singh [18] investigated the effect of heat source direction on the melting performance of PCM under microgravity and observed nearly a fourfold reduction in melting time when the acceleration due to gravity was reduced to g/80. The thermocapillary effects during melting of PCM in a liquid bridge geometry under microgravity was analyzed by Varas et.al. [19]. Another major study to scrutinize the role of hypergravity on the thermal characteristics of a PCM was performed by Xu et.al. [20] wherein an accelerated rate by 20% was observed for the melting of PCM under hypergravity as compared to normal gravity conditions. From the above literature, the importance of the encapsulation of PCM in triplex tube heat exchanger geometry and role of different gravity conditions on the melting performance of PCM has been established. However, there is absence of literature which investigate the effect of different gravity conditions and geometrical parametrs on the melting performance of PCM in triplex tube heat exchanger configurations.

In this work, five distinct novel geometric configurations are evaluated to obtain optimized rates of melting for RT-35 and RT-82 and the best novel configuration amongst them will be evaluated for melting performance under microgravity, terrestrial gravity and hypergravity conditions of 0.1g, 1g and 1.5g respectively. A reference time (T_{ref}) is chosen to present the transient liquid fraction contours. The reference time is the time taken for the complete melting of RT-82 and RT-35 to occur for the best selected novel configuration. The obtained results for melting rates under varying gravity conditions will be compared to the corresponding rates of melting for the baseline and best TTHX configurations proposed by Mat et.al. [21].

2. GEOMETRICAL DETAILS OF THE INVESTIGATED CONFIGURATIONS

The various novel TTHX geometric configurations are shown in Fig.3.2. The configurations 'M1' and 'M2' represent the baseline and finned configuration presented in the study by Mat et.al. [21], where the geometric configurations from C1-C5 are the novel configurations in which the melting of RT-82 and RT-35 is investigated. In general , the PCM filled is filled in the annular region between the inner tube radius (r_i) of 25.4 mm and a middle tube radius (r_m) of 75mm, with the geometrical configuration 'C3' being the only anomaly wherein the middle radius (r_m) is enhanced to 85 mm to accommodate equivalent volume of PCM as that of the best configuration of Mat et.al.[21].

The outer tube radii of the configurations is set to 100mm for all configurations. The thickness of the inner tubes and middle tubes are taken as 1.2 mm and 2 mm respectively. A heat transfer fluid (HTF) flows under isothermal conditions through the inner and outer tubes of all configurations to melt the PCM in the annulus of the TTHX geometry. As it can be observed from Fig.3.2, the number, size, shape, tip angle and angle of attachment of fins are varied within the same annular region of the TTHX to facilitate varying area of contact between the encapsulated PCM and the constraining geometric configurations. The ultimate desired result of this endeavor is to achieve optimized melting rates of PCM for spacecraft thermal control applications and to identify a desired novel geometry among C1-C5 with superior melting performance.

The thermophysical properties of the encapsulated PCM and surrounding tubes (made of copper) are presented in Table 3.1 and the area occupied by the PCM domain in each geometric configuration is shown in Table 3.2.

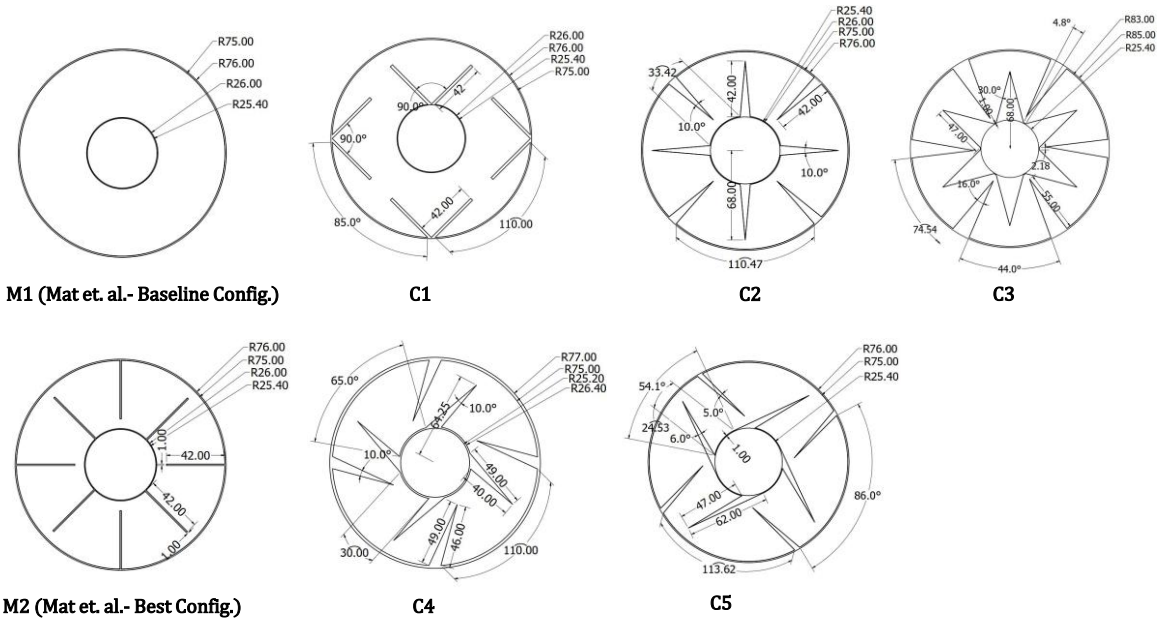

Fig.3.2 All geometric configurations of the TTHX models used in the study

3. GOVERNING EQUATIONS

In the present chapter , it is crucial to recognize the governing equations that lay the foundation of the phase change material's melting process. However, it is imperative to acknowledge that the governing equations pertaining to current chapter have been thoroughly explained in Section 3 of Chapter 2. The fundamental principles and mathematical formulations remain unchanged . In order to ensure conciseness and logical flow in this thesis , the reader is kindly referred to Section 3 of Chapter 2 for a comprehensive analysis of the governing equations.

4. COMPUTATIONAL DOMAIN, NUMERICAL MODELING, MESH GENERATION, INITIAL CONDITIONS, AND BOUNDARY CONDITIONS

The numerical simulations were modelled using the commercially available Finite volume-based solver ANSYS FLUENT (2022 R1). Phase-change was modeled through enthalpy-porosity formulation in which the liquid-solid front is not tracked explicitly but is treated as porous zone with the porosity equal to the liquid fraction. Liquid fraction is the measure of the fraction of the cell volume in liquid form.

The boundary conditions for the wall temperature are same for all configurations. The 2D computational domain of the setup for the configuration 'C3' is shown in Fig.3.3a. The wall thicknesses of 1.2mm and 2mm for the outer and inner tube of the TTHX geometry was taken into consideration for simulating the computational domain. The inner and outer tubes of the geometry are filled with a heat transfer fluid (HTF).

The wall boundary conditions for the outer and inner tube were maintained under isothermal conditions at the exact temperature of the HTF ($T_W = T_{HTF}$). The HTF temperature was suitably chosen to be 363.15K and 325K for simulating the melting of RT-82 and RT-35 respectively and a good convergence was observed for these values of HTF temperatures. The structured mesh generated at the interface between the heated outer walls and PCM domain can be observed from Fig. 3.3b. The melting phenomenon was initiated at 300.15K. Wall slitting of the boundary into

Table 3.1: Thermo-physical properties of PCM and Copper

Property	**RT82**	**RT35**	**Copper**
Density of PCM, solid, ρ_s (kg/m^3)	950	860	8978
Density of PCM, liquid, ρ_l (kg/m^3)	770	770	-
Specific heat capacity, c_{p_l}, c_{p_s} (J/kgK)	2000	2000	381
Latent heat of fusion, L (J/kg)	176000	170000	-
Melting temperature, T_m (K)	343.15 – 355.15	302-309	-
Thermal conductivity, k (W/mK)	0.2	0.2	387.6
Thermal expansion coefficient, β (1/K)	0.001	0.0006	-
Dynamic viscosity, μ (kg/ms)	0.03499	0.023	-

Table 3.2: Area occupied by each geometric configuration

Geometric Configuration	**PCM area (mm^2)**
M1 (Mat et.al. -Baseline Configuration)	15,126
M2 (Mat et.al. -Best Configuration)	15,126
C1	15,218
C2	14,311
C3	15,841
C4	14,613
C5	14,622

distinct zones was done at the interface between the PCM and the walls to establish coupled boundary conditions in which temperature and heat flux continuity was maintained (see Fig. 3.3).

GRID INDEPENDENCE TEST

A grid independence test performed for the melting of RT-82 reported that the results were independent of the adopted grid size and time step when the number of elements were 158,774 and time step was 0.5s. The results of the grid independence study can be shown in Table 3.3. Based on the reported values [23], 158,774 elements and 0.5s time step size was adopted in the present study which provided good agreement with the results reported in [23] as discussed in the next section. The liquidus temperature of 355.15K and 309K was chosen as the operating temperature for Boussinesq equation in case of RT-82 and RT-35 respectively and the density was equal to the liquid density.

The baseline and finned configurations were simulated under varying gravity conditions viz. 0.1g, 1g and 1.5g. The pressure-velocity coupling was solved using the SIMPLE algorithm and PRESTO scheme was used for pressure interpolation. Solution was deemed to be converged when the residuals for continuity, momentum, and energy dropped below 10^{-3}, 10^{-5}, and 10^{-7}, respectively.

5. RESULTS & DISCUSSIONS

In this section, the five novel configurations will be presented and their melting performance can be gauged with respect to the best-chosen configuration by transient liquid fraction contours at specific time intervals for 25%, 50%, 75% and 100% value of reference time. The melting time taken for RT-82 and RT-35 to melt in the best-chosen configuration (C3) is 2444s and 1639s respectively. The fidelity of the present data is already proven when it is validated against Mat et.al. [20] as it has been shown in Section 5 of Chapter 2.

5.1 NOVEL ENCAPSULATION GEOMETRIC CONFIGURATIONS

The geometric configurations used in this study differed on the basis of the arrangement of fins in terms of their orientation, angle of attachment, thickness etc.. These intricate differences facilitate or hinder various melting phenomenon in the encapsulation geometry. It has been observed through extensive computational investigations that the formation of vortex like patterns of

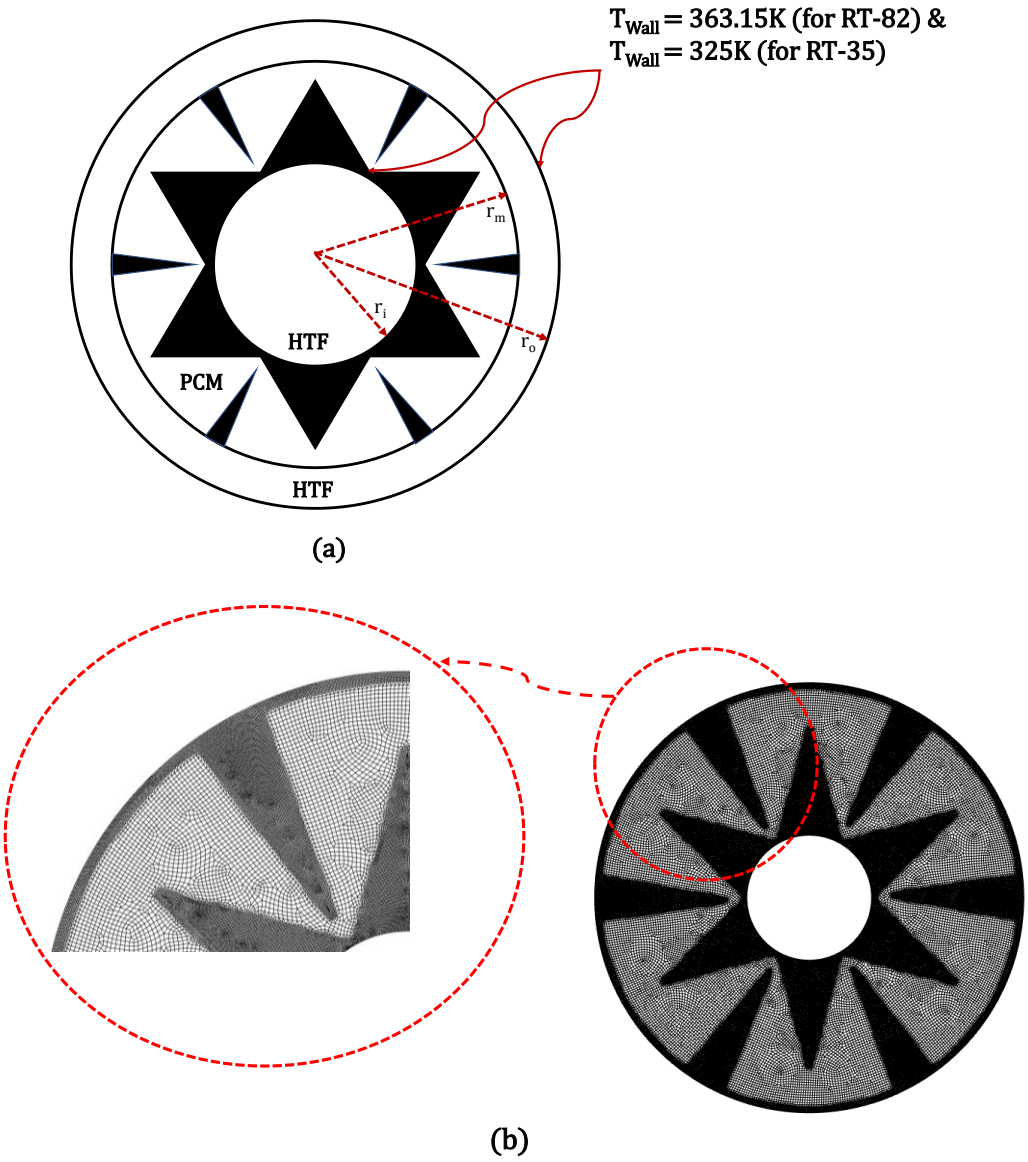

Fig.3.3 (a) Schematic of the 2D computational domain for TTHX configuration simulated in the present study and (b) Structured mesh generated with refinement near the walls

Table 3.3: Grid Independence Test

Mesh type	**No. of Elements**	**Melting time (s)**
Coarse	96,090	2375
Medium	158,774	2444
Fine	204,211	2484

melting within small pockets of the encapsulation geometry expedites the melting of phase change materials. The geometric configuration ‘C1’ was designed to provide an unhindered rise of liquid PCM during the melting process and the fins were attached at the middle section to enhance the area of heat transfer as the liquid PCM rise due to the influence of buoyant forces during melting phenomenon. The melting process in this configuration initiates by conduction heat transfer between the rectangular fins and solid PCM which leads to the formation of a liquid layer at the interface between the fins and solid PCM. This phase is succeeded by the natural convection phase wherein heat transfer occurs between the low and high temperature PCM. The design is also eccentric due to the dissimilar number of fins at the inner and outer tubes of the TTHX geometry. Despite all the careful design considerations, the melting times obtained were 26% and 35% greater than ‘M2’ geometric configuration. Major design flaws associated with this geometric configuration such as entrapment of flow and lack of formation of independent vortices were identified in this geometry.

However, the C2 configuration closely resembles the best configuration of Mat et al. in terms of fin length and placement. However, the fins in this configuration are tapered . This variable length of the fins enables the division of TTHX geometry into smaller independent geometries with stronger vortices formation initiating at the 50% stage wherein the interface at the periphery of each independent geometry is covered by melted PCM for both RT-82 and RT-35. The contours at 75% melting depict intensified convection cell formation at the lower end of the outer tube in case of RT-82. Ultimately, the T/A ratio calculated for the melting of RT-82 was nearly 12% lower than the published configuration ‘M2’ discussed earlier. However, still the T/A for the melting of RT-35 was 11% greater than configuration ‘M2’ . This is a matter of concern since the purpose of this study is to obtain enhanced melting performance for both RT-82 and RT-35 in the novel geometric configurations.

The C3 geometric configuration is a slightly enlarged model compared to other geometric configurations with a 13% larger outer diameter as compared to other geometric configurations. This is done to enable the ‘C3’ configuration to contain an equivalent quantity of PCM as that of the best configuration ‘M2’ of Mat et al. [20]. This configuration also covers 5% more area in the PCM domain and yields 17% and 9% decreased melting times as compared to M2 configuration respectively. Larger vortices (see Fig. 3.4 and 3.5) are formed within the 12 independent unit cell

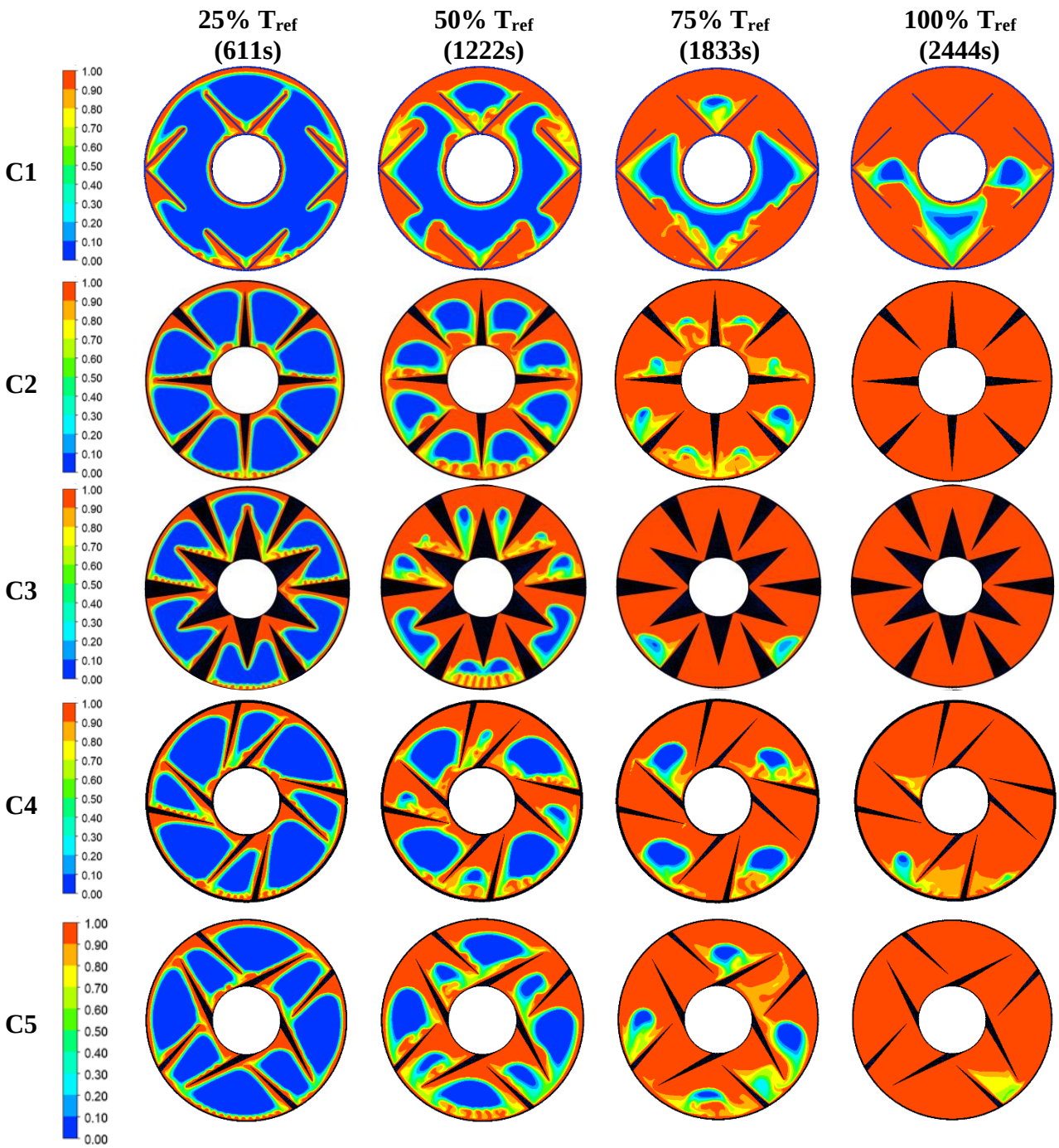

Fig.3.4 Liquid Fraction contours for Novel Configurations C1-C5 at specific time intervals relative to reference time for melting of RT-82

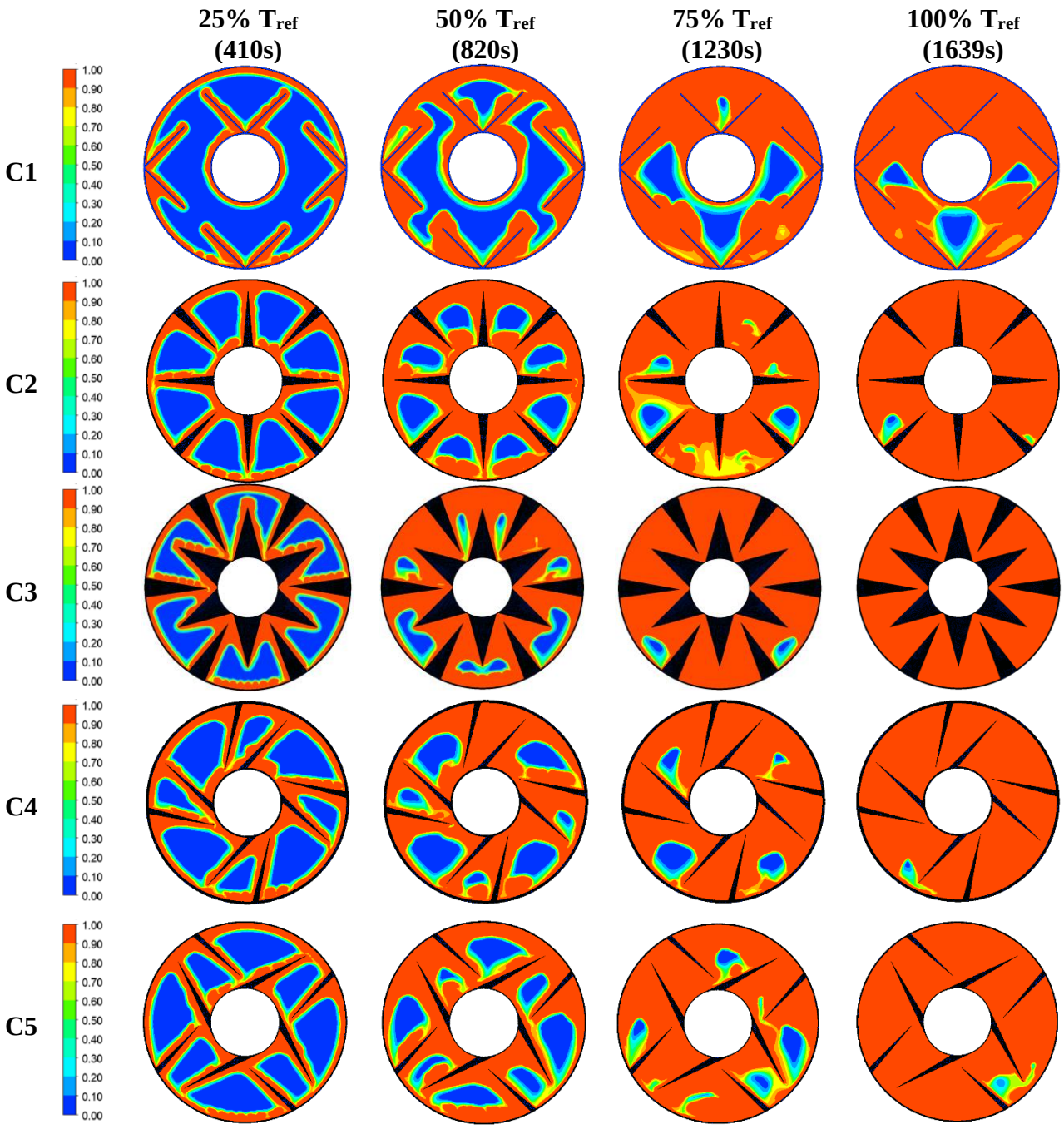

Fig.3.5 Liquid Fraction contours for Novel Configurations C1-C5 at specific time intervals relative to reference time for melting of RT-35

geometries of this configurations and the rise of flow due to natural convection is hindered by the star shaped inner and fins on the outer tube, thereby restricting the flow within the corresponding unit cell area. Another attempt at optimizing the melting characteristics of PCM in triplex tube heat exchange configuration has been done by simulating the melting of RT-82 and RT-35 in geometric configuration-C4. In this configuration, 4 tapered fins (tip angled at 10°), which are inclined at 65° are each placed on the inner and outer tube of the configuration. This design creates alternate regions of small and large unit geometries within which PCM is melted at varying rates. At 90% melting, it is observed that PCM has been melted in the smaller geometries for both the cases of RT-82 and RT-35. This geometry does not provide adequate conditions for intense convection cell formation and therefore the melting times are not optimized in this configuration with respect to the earlier discussed configurations. The T/A ratio for melting in this configuration barely matches the values of the M2 configuration in both the cases for the melting of RT-82 and RT-35. In the C5 configuration, the angle of attachment of the tips has been reduced to 55° and the tip angles have been reduced to 6° and 5° at the inner and outer tube respectively. This creates alternate and distinct triangular and trapezoidal unit cell geometries. The idea is to create unit cell geometries of varying melting rates such that the melting time of alternate unit geometries overlap with each other. This approach ensures that stronger convection cells would be formed within the dissimilar unit cell geometries formed due to the placement of fins in the unit cell sub-geometries on account of enhancement in the heat transfer rate due to increased area for heat transfer. This configuration had a slightly better T/A ratio (nearly 6%) as compared to configuration ‘M2’.

5.2 COMPARISON OF LIQUID FRACTION FOR DIFFERENT GEOMETRIC CONFIGURATIONS

Fig.3.6 represent the liquid fraction evolution trend during the course of time and Fig. 3.7- Fig.3.8 illustrate a comprehensive column chart analysis into the melting times, PCM domain area and the normalized T/A ratios for various configurations. It can be clearly observed from the graph that C3 configuration betters the melting performance of configuration M2 with melting times of 2444s and 1639s for RT-82 and RT-35 respectively. The T/A ratio for configuration ‘C3’ have improved the values obtained by configuration ‘M2’ by 21% and 13% for RT-82 and RT-35 respectively.

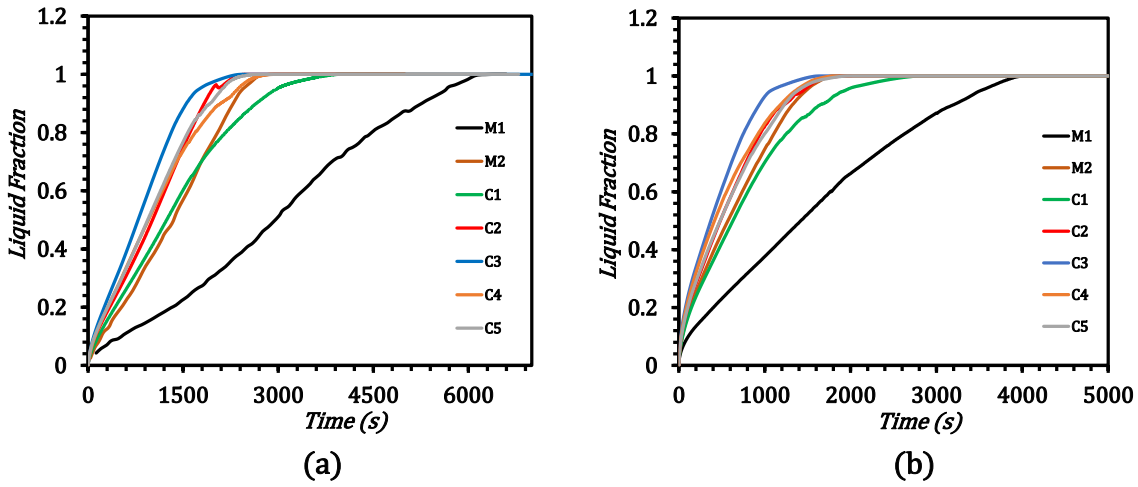

Fig.3.6 Liquid fraction evolution trends for novel configurations C1-C5 for (a) RT-82 and (b) RT-35

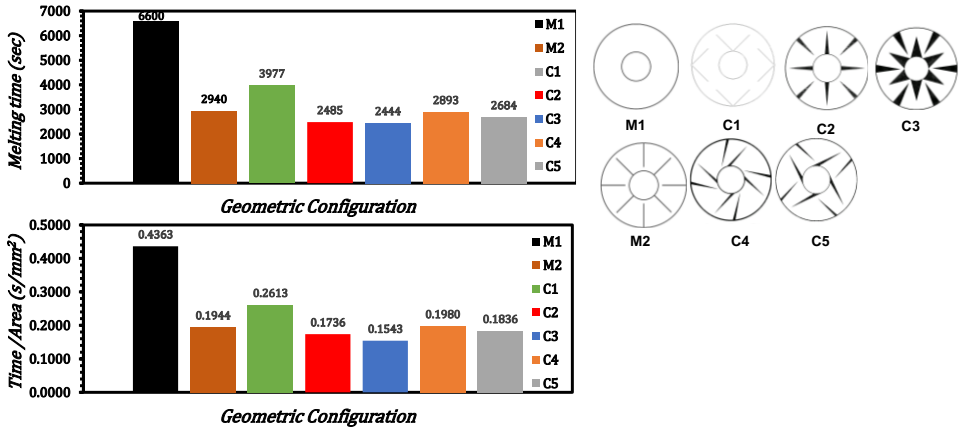

Fig.3.7 Bar chart depicting the comparison of melting time and T/A ratio for configurations C1-C5 during melting of RT-82

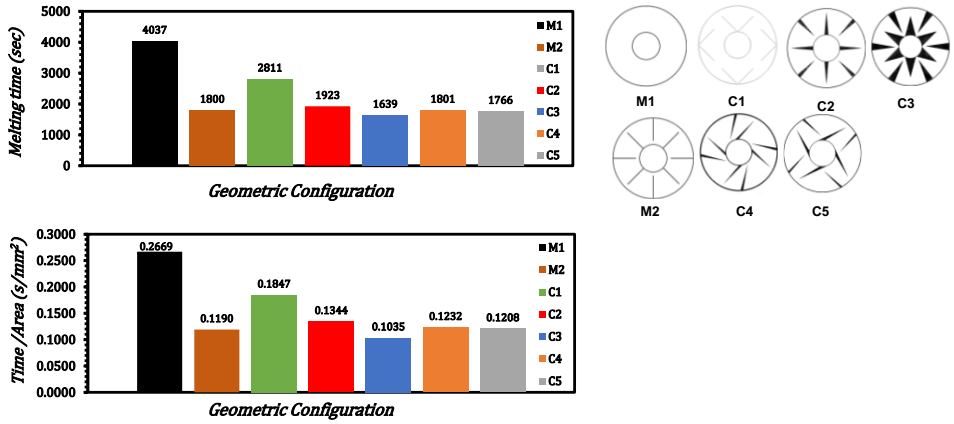

Fig.3.8 Bar chart depicting the comparison of melting time and T/A ratio for configurations C1-C5 during melting of RT-35

The enhanced T/A values are a testimony to configuration ‘C3’ being the better novel configuration with enhanced improved melting performance.

The expedited melting observed in the C3 configuration can be attributed to the formation of conducive triangular unit-cell envelopes within the larger geometry. The melting within these unit-cells ultimately facilitate a vortex-like melting phenomenon which is initiated by the melting of the interfacial layer between the walls and un-melted PCM and this phenomenon is further succeeded by the mixing of the un-melted and melted PCM. The remaining configurations could not achieve a higher rate of melting due to the hindrances provided by certain parameters or orientation of fillers within these geometries such as entrapment of flow within crevices of the unit-cell or unrequired facilitation of un-hindered rise to the melted PCM towards the upper region of the main geometry.

5.3 EFFECT OF GRAVITY

Since the paper focusses on the applicability of phase change materials for spacecraft applications , a major parameter to assess the feasibility of PCM for such applications is its stability and thermal performance under different gravity conditions since a spacecraft maneuver through regions of different gravity conditions . In this section , the liquid fraction contours of the baseline and best configurations of Mat et.al. at microgravity (0.1g) and Hypergravity (1.5g) conditions for RT-82 and RT-35 are investigated and compared with the corresponding liquid fraction contours for the geometric configuration ‘C3’.

As we know Fig.3.8 illustrates the comparison of the best-chosen configuration ‘C3’ with the baseline and best TTHX configurations of Mat et.al. [20]. It is observed that the chosen novel configuration ‘C3’ provides better stability of melting during microgravity and hypergravity conditions providing enhanced maneuverability to the spacecraft. Fig.3.9 and Fig.3.10 illustrates the liquid fraction contours of ‘C3’ configuration under microgravity and hypergravity for RT-82 and RT-35 respectively. It can be observed that the liquid fraction contours of RT-82 is more nucleated about a central core within the unit cell.

Fig. 3.11 represent the liquid fraction progression comparison during the course of melting of RT-82 and RT-35 for the chosen novel configuration ‘C3’ and a comparison was done on the melting performance with respect to the baseline and best (finned) configuration of Mat et.al. [20].

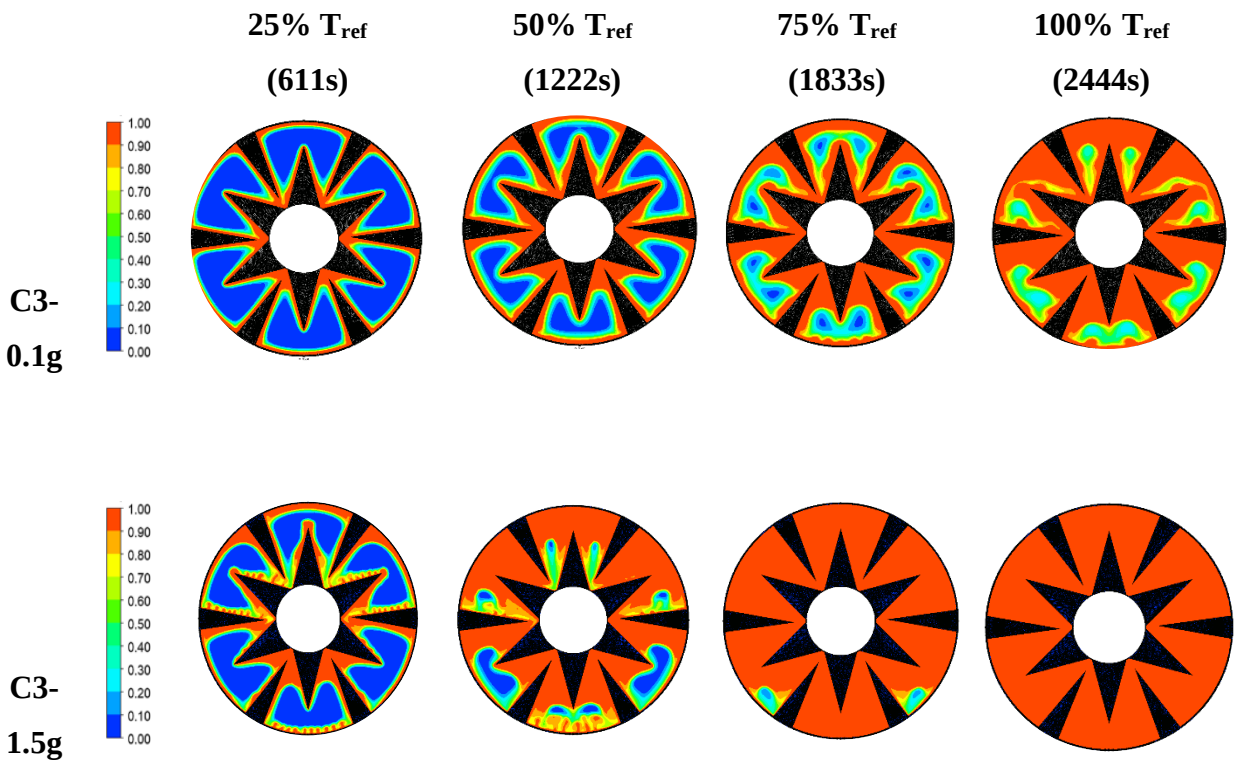

Fig.3.9 Progression of Liquid Fraction contours for 'C3' configuration at Microgravity and Hypergravity condition relative to reference time for melting of RT-82

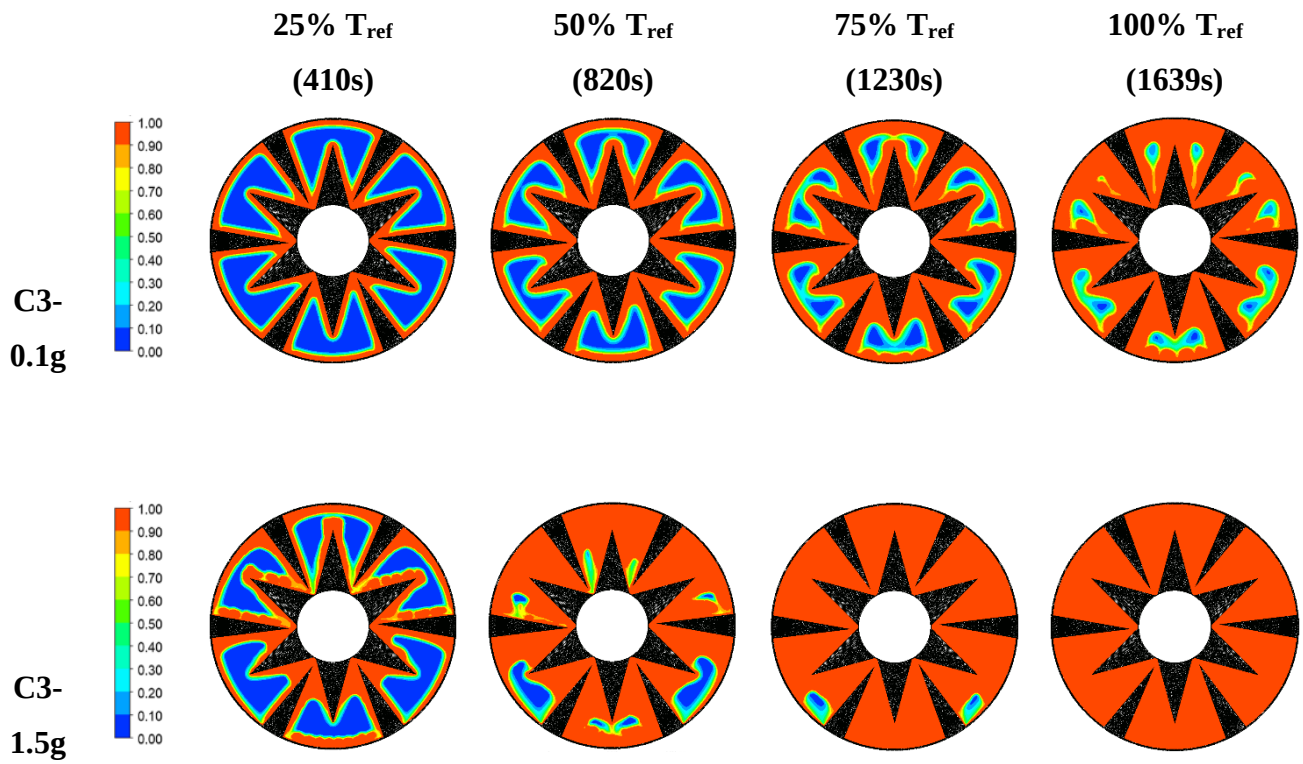

Fig.3.10 Progression of Liquid Fraction contours for 'C3' configuration at Microgravity and Hypergravity condition relative to reference time for melting of RT-35

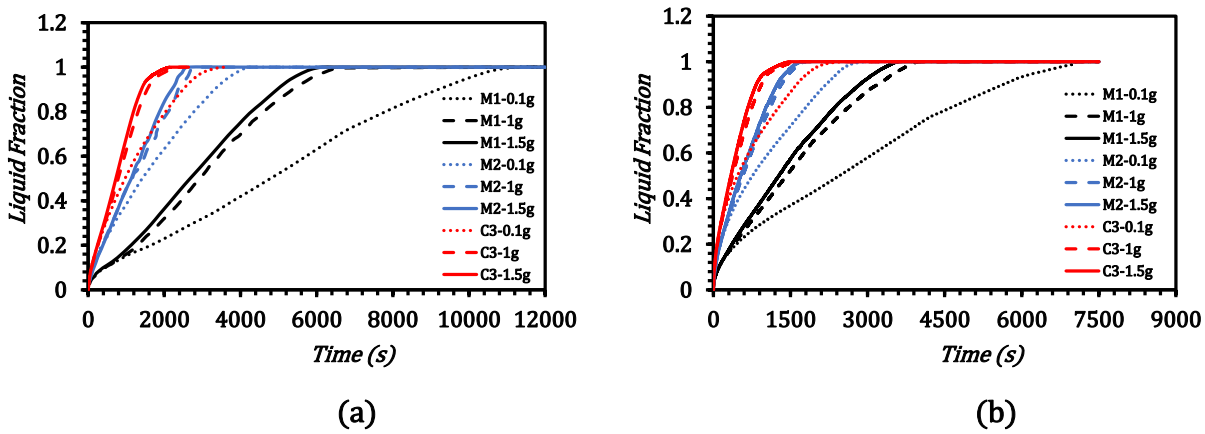

Fig.3.11 Liquid Fraction Comparison v/s time at various gravity conditions for novel configuration ‘C3’ with m1 and m2 for (a) RT82 and (b) RT35

The effect of gravity is investigated on the best-chosen configuration 'C3' and the comparative melting performance with respect to the baseline and best TTHX configuration of Mat et.al. [20] at 0.1g, 1g and 1.5g gravity conditions can be illustrated by the normalized parameter T/A (time per unit area ratio) and represented in the form of a column graph as shown in Fig. 3.12. A low value of T/A ratio is indicative of a superior melting performance and ensures stability of the thermal management capability of the PCM.

The governing aspect of the melting investigations can be zeroed down to one key phenomenon i.e. 'buoyancy -driven flow'. While the melting of PCM in space is impacted by other major factors such as the thermal conductivity of the encapsulation geometry material and surroundings, it is the lack of buoyancy-driven flow in low gravity conditions which gives rise to uneven heat distribution, resulting in the melting process becoming slow and non-uniform. The lack of convection makes the heat transfer process entirely dependent on heat conduction.

A converse of the above described phenomena is true in the case of hypergravity conditions which is experienced by the spacecrafts during launch and re-entry maneuvers wherein an exaggerated physical strain is experienced due to the tremendous g-forces. Heat dissipation provided the PCM greatly aids for effective thermal management during these critical phases of exaggerated convection heat transfer.

6. CONCLUSIONS

A novel configuration for the melting of RT-82 and RT-35 is attempted in this work. The superiority of the novel configuration C3 over the best configuration of Mat et al. lies in the formation of independent vortices within the main geometry which isolates and limits the flow in narrower regime thereby inhibiting the rise of flow towards the upper part of the main geometry. The role of the number of fins and placement of fins on the melting performance has been ascertained in this study.

A normalized parameter named as the Time per unit area ratio, or the T/A ratio is defined which accounts for the efficacy of the geometric configuration model for melting PCM corresponding to the geometric configurations in the archival literature and facilitates effective comparison of melting performance. Favorable results for enhancing the heat transfer of PCM within the best

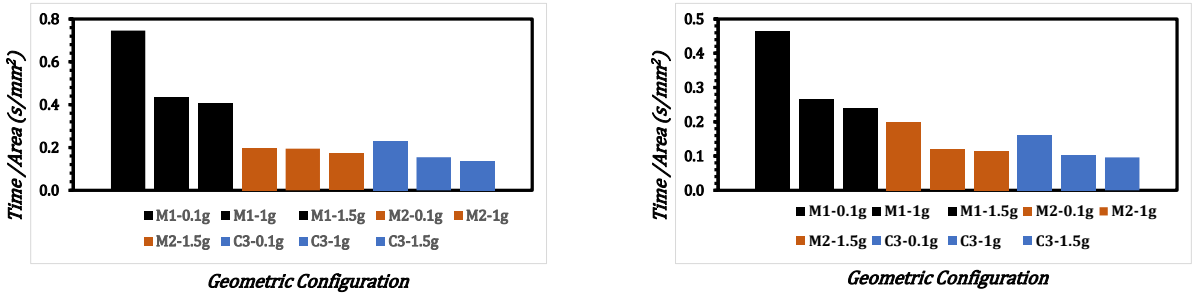

Fig.3.12 Comparison of T/A ratio of C3 configuration with the baseline and best finned TTHX configurations of Mat et al. [20] at 0.1g, 1g and 1.5g gravity conditions.

encapsulation geometry was observed due to the cumulative enhanced melting phenomenon observed within individual unit-cells resulting in overall expedited melting performance of the main geometry.

As a conclusion, these endeavors pursued in this research aims to inspire the current researchers working with phase change materials to devise further innovative methods and encapsulation geometries which establishes the application PCM as the ultimate thermal management tool for spacecrafts to combat through varied gravity conditions.

References

[1] J. Shao, J. Darkwa, and G. Kokogiannakis, “Review of phase change emulsions (PCMEs) and their applications in HVAC systems,” Energy Build., vol. 94, pp. 200–217, May 2015, doi: 10.1016/j.enbuild.2015.03.003.

[2] R. Kandasamy, X.-Q. Wang, and A. S. Mujumdar, “Application of phase change materials in thermal management of electronics,” Appl. Therm. Eng., vol. 27, no. 17–18, pp. 2822–2832, Dec. 2007, doi: 10.1016/j.applthermaleng.2006.12.013.

[3] M. C. Browne, B. Norton, and S. J. McCormack, “Phase change materials for photovoltaic thermal management,” Renew. Sustain. Energy Rev., vol. 47, pp. 762–782, Jul. 2015, doi: 10.1016/j.rser.2015.03.050.

[4] M. BUSBY and S. MERTESDORF, “The benefit of phase change thermal storage for spacecraft thermal management,” in 22nd Thermophysics Conference, American Institute of Aeronautics and Astronautics. doi: 10.2514/6.1987-1482.

[5] J.-P. Collette et al., “Phase Change Material Heat Accumulator for the HEXAFLY-INT Hypersonic glider,” in 49th International Conference on Environmental Systems, BOSTON, United States, Jul. 2019. Accessed: Feb. 01, 2022. [Online]. Available: https://hal.archives-ouvertes.fr/hal-02335121

[6] M. Gottero, V. Perotto, R. Martino, B. Leyda, and B. Ozmat, Phase-change thermal capacitors for ExoMars 2016 mission. 44th International Conference on Environmental Systems, 2014. Accessed: Jan. 14, 2022. [Online]. Available: https://ttu-ir.tdl.org/handle/2346/59519

[7] G. Quinn, J. J. Stieber, R. B. Sheth, and T. Ahlstrom, “Phase Change Material Heat Sink for an International Space Station Flight Experiment,” undefined, 2015, Accessed: Jan. 13, 2022. [Online]. Available: https://www.semanticscholar.org/paper/Phase-Change-Material-Heat-Sink-for-an-Space-Flight-Quinn-Stieber/b496376d9b84e5d2ce69e3ee10d2feea5b2efe8a

[8] “NASA - NSSDCA - Spacecraft - Details.” https://nssdc.gsfc.nasa.gov/nmc/spacecraft/display.action?id=1972-021A (accessed Feb. 22, 2022).

[9] “Numerical investigation of an innovative discontinuous distribution of fins for solidification rate enhancement in PCM with and without nanoparticles | Elsevier Enhanced Reader.” https://reader.elsevier.com/reader/sd/pii/S1359431119358107?token=14DE7186E86EBD8862CBDC2DA1CC54ADBE962025F90F68971E2795F2D7563DDB38FF08388B9D99CD4349CF79AD6517BC&originRegion=us-east-1&originCreation=20230310181548 (accessed Mar. 10, 2023).

[10] K. Y. Leong, S. Hasbi, and B. A. Gurunathan, “State of art review on the solidification and melting characteristics of phase change material in triplex-tube thermal energy storage,” J. Energy Storage, vol. 41, p. 102932, Sep. 2021, doi: 10.1016/j.est.2021.102932.

[11] S. Yao and X. Huang, “Study on solidification performance of PCM by longitudinal triangular fins in a triplex-tube thermal energy storage system,” Energy, vol. 227, p. 120527, Jul. 2021, doi: 10.1016/j.energy.2021.120527.

[12] M. J. Zarei, H. Bazai, M. Sharifpur, O. Mahian, and B. Shabani, “The Effects of Fin Parameters on the Solidification of PCMs in a Fin-Enhanced Thermal Energy Storage System,” Energies, vol. 13, no. 1, Art. no. 1, Jan. 2020, doi: 10.3390/en13010198.

[13] H. Xu, N. Wang, C. Zhang, Z. Qu, and M. Cao, “Optimization on the melting performance of triplex-layer PCMs in a horizontal finned shell and tube thermal energy storage unit,” Appl. Therm. Eng., vol. 176, p. 115409, Jul. 2020, doi: 10.1016/j.applthermaleng.2020.115409.

[14] H. Eslamnezhad and A. B. Rahimi, “Enhance heat transfer for phase-change materials in triplex tube heat exchanger with selected arrangements of fins,” Appl. Therm. Eng., vol. 113, pp. 813–821, Feb. 2017, doi: 10.1016/j.applthermaleng.2016.11.067.

[15] A. A. Al-Abidi, S. Mat, K. Sopian, M. Y. Sulaiman, and A. Th. Mohammad, “Internal and external fin heat transfer enhancement technique for latent heat thermal energy storage in triplex tube heat exchangers,” Appl. Therm. Eng., vol. 53, no. 1, pp. 147–156, Apr. 2013, doi: 10.1016/j.applthermaleng.2013.01.011.

[16] Y. Asako, E. Gonçalves, M. Faghri, and M. Charmchi, “Numerical Solution of Melting Processes for Fixed and Unfixed Phase Change Material in the Presence of Magnetic Field–Simulation of Low-Gravity Environment,” Numer. Heat Transf. Part Appl., vol. 42, no. 6, pp. 565–583, Nov. 2002, doi: 10.1080/10407780290059701.

[17] W. Li, S.-G. Li, S. Guan, Y. Wang, X. Zhang, and X. Liu, “Numerical study on melt fraction during melting of phase change material inside a sphere,” Int. J. Hydrog. Energy, vol. 42, no. 29, pp. 18232–18239, Jul. 2017, doi: 10.1016/j.ijhydene.2017.04.136.

[18] K. Kansara, V. K. Singh, R. Patel, R. R. Bhavsar, and A. P. Vora, “Numerical investigations of phase change material (PCM) based thermal control module (TCM) under the influence of low gravity environment,” Int. J. Heat Mass Transf., vol. 167, p. 120811, Mar. 2021, doi: 10.1016/j.ijheatmasstransfer.2020.120811.

[19] R. Varas, P. S. Sánchez, J. Porter, J. Ezquerro, and V. Lapuerta, “Thermocapillary effects during the melting in microgravity of phase change materials with a liquid bridge geometry,” Int. J. Heat Mass Transf., vol. 178, p. 121586, 2021.

[20] Y. Xu, J. Wang, and Z. Yan, “Experimental investigation on melting heat transfer characteristics of a phase change material under hypergravity,” Int. J. Heat Mass Transf., vol. 181, p. 122004, Dec. 2021, doi: 10.1016/j.ijheatmasstransfer.2021.122004.

[21] S. Mat, A. A. Al-Abidi, K. Sopian, M. Y. Sulaiman, and A. T. Mohammad, “Enhance heat transfer for PCM melting in triplex tube with internal–external fins,” Energy Convers. Manag., vol. 74, pp. 223–236, Oct. 2013, doi: 10.1016/j.enconman.2013.05.003.

[22] A. D. Brent, V. R. Voller, and K. J. Reid, “Enthalpy-Porosity Technique for Modeling Convection-Diffusion Phase Change: Application to the Melting of a Pure Metal,” Numer. Heat Transf., vol. 13, no. 3, pp. 297–318, Apr. 1988, doi: 10.1080/10407788808913615.

[23] S. Mat, A. A. Al-Abidi, K. Sopian, M. Y. Sulaiman, and A. T. Mohammad, “Enhance heat transfer for PCM melting in triplex tube with internal–external fins,” Energy Convers. Manag., vol. 74, pp. 223–236, Oct. 2013, doi: 10.1016/j.enconman.2013.05.003.

VITA

Junaid Khan is a Graduate Research and Teaching Assistant at the University of Tennessee. He had earlier served as a Graduate Research Assistant at Mississippi State University. He obtained his undergraduate degree from Jamia Millia Islamia (Central University), New Delhi, India and master's degree in mechanical engineering from the Aligarh Muslim University, India. He has published a few journal papers, book chapters a patent.